NANO-BASED DRUG DELIVERY SYSTEMS: TARGETING TO CORTICOSPINAL TRACT NEURONS FOR CONTROLLED RELEASE OF THERAPEUTICS

A DISSERTATION

SUBMITTED IN PARTIAL FULFILLMENT OF THE REQUIREMENTS

FOR THE DEGREE OF DOCTOR OF PHILOSOPHY

IN THE GRADUATE SCHOOL OF THE

TEXAS WOMAN'S UNIVERSITY

SCHOOL OF THE SCIENCE

COLLEGE OF ARTS AND SCIENCES

BY

MENGJIE CAO, B.S., M.S.

DENTON, TEXAS

MAY 2023

DEDICATION

To my mom, Qian Rao

Thank you for your unconditional love and belief in me and for inspiring and encouraging me to pursue my dreams.

To my mentor, DiAnna Hynds

For being patient and for carrying me through my difficult moments.

ACKNOWLEDGEMENTS

I would like to gratefully acknowledge the many individuals who have directly or indirectly supported me during this journey. First and foremost, I wish to express my sincere gratitude to my advisor, Dr. DiAnna Hynds, for giving me the chance to join her laboratory. I appreciate her support, guidance in this project, advice, opportunities she has offered, encouragement, kindness, and generosity which were all important to accomplish this work. I would not have been able to complete my dissertation without her quiet support. I am thankful to Dr. Santaneel Ghosh for introducing me to TWU and providing nanoparticles as a collaborator in my project and for guiding me throughout my project as a committee member. I would like to thank Dr. Mills, Dr. Averitt, and Dr. Brower for being on my Ph.D. committee and for their insights, guidance, time, effort, and support in the completion of this dissertation. Thanks to Dr. Shazia Ahmed for all the help in teaching labs and for being a great lab coordinator. I would also like to thank the faculty and staff at the Department of Biology, my colleagues, and friends for all the help and support. Lastly, I would like to thank my family for their continuous love and encouragement.

ABSTRACT

MENGJIE CAO

NANO-BASED DRUG DELIVERY SYSTEMS: TARGETING TO CORTICOSPINAL TRACT NEURONS FOR CONTROLLED RELEASE OF THERAPEUTICS

MAY 2023

Central nervous system (CNS) damage leads to persistent loss of cognition, sensation, and motor control, and affecting approximately millions of patients. Retention or regain of function could be improved by therapies encouraging axon regeneration. However, therapeutic effectiveness is challenged by limited CNS axon regeneration, limited CNS accessibility due to the blood–brain barrier (BBB), and inefficient targeting to specific neurons due to CNS cellular diversity. We suggest using surface functionalized nanoparticles (SFNPs) to specifically target particular neurons and deliver regeneration-encouraging drugs in a remotely actuation-able and controlled manner. We have developed fluorescently labeled polyethylene glycol (PEG) copolymer nanoparticles surface functionalized with amino (N150, 150 nm diameter) or carboxyl (C150 and C750, 150 nm and 750 nm diameters, respectively) functional groups. Here, we attached brain-derived neurotrophic factor (BDNF) using peptide bonding to the surface functional groups and assessed the amount and stability of BDNF derivatization, targeting to corticospinal tract (CST) upper motor neurons, and promotion of outgrowth of neuronal processes from release of the outgrowth promoting therapeutic, C3 transferase. Each SFNP construct stably bound between 68.2 and 74.7% of the initial amount of BDNF. About 40.7% of the N150 and 42% of C150 SFNPs either not derivatized or derivatized with BDNF traversed a continuous monolayer of brain microvascular endothelial cells (BBMVECs, an *in-vitro* BBB model) within 4 hours, while fewer C750 (24%) crossed the barrier in the same time frame. Cell type specific immunolabeling showed that N150 and C150, and to a lesser extent C750, BDNF-

SFNPs were preferentially internalized into CST neurons compared to astrocytes, oligodendrocytes, or microglia. BDNF-SFNP released C3 transferase increased several measures of neurite outgrowth in CST neurons compared to SFNPs without BDNF derivatization. We conclude that the N150 and C150 BDNF-SFNPs efficiently cross a BBB model, are preferentially endocytosed by CST neurons, and release imbibed C3 transferase to increase process outgrowth. The C750 construct less efficiently crossed the *in-vitro* BBB, but their greater BDNF binding and C3 transferase carrying capacity may support comparable axon regeneration compared to the smaller constructs. Thus, collectively, all three BDNF-SFNP constructs hold promise for clinical use in treating neurotraumatic and neurodegenerative conditions.

TABLE OF CONTENTS

DEDICATION ii

ACKNOWLEDGEMENTS iii

ABSTRACT iv

LIST OF TABLES ix

LIST OF FIGURES x

ABBREVIATIONS xii

I. INTRODUCTION 1

CNS Disorders Are a Largely Untreated Significant Health Issue 1

Rho GTPases and Control of Axon Regeneration 2

BBB and Transport Mechanisms 6

Advantages of Nanomaterial-Based Drug Delivery 8

A Nanomaterial-Based Drug Delivery System To Encourage Axon Regeneration Following CNS Damage 10

Specific Aims 13

Specific Aim 1 13

Specific Aim 2 14

Specific Aim 3 14

II. BIOACTIVE BRAIN-DERIVED NEUROTROPHIC FACTOR DERIVATIZED SURFACE FUNCTIONALIZED NANOPARTICLES CROSS A BLOOD–BRAIN BARRIER MODEL *IN VITRO* 16

Abstract 16

Introduction 17

Materials and Methods 19

Synthesis of Surface Functionalized Nanoparticles (SFNPs) 19

Derivatization of SFNPs with Brain-derived Neurotropic Factor 20

BDNF Binding Efficiency and Stabilization by Enzyme-Linked Immunoabsorbance Assay (ELISA) 21

Cell Culture 22

Blood–Brain Barrier Models and Treatments 23

Statistical Analyses 24

Results 25

BDNF Binding Efficiency 25

BDNF Binding Stabilization 27

BDNF-Derivatized SFNPs Cross Through a BBB Model *In Vitro* 28

Discussion 33

Acknowledgements 36

References 37

III. CORTICOSPINAL TRACT NEURONS PREFERENTIALLY INTERNALIZE BRAIN-DERIVED NEUROTROPHIC FACTOR DERIVATIZED SURFACE FUNCTIONALIZED NANOPARTICLES 42

Abstract 42

Introduction 43

Materials and Methods 44

Rat Cortical Cell Culture and Treatment 44

Immunocytochemistry 45

Microscopy and Analysis 46

Statistical Analysis 47

Results 47

Discussion 56

Acknowledgements 58

References 59

IV. OUTGROWTH OF NEURITES FROM CORTICAL NEURONS IS INCREASED FROM EXPOSURE TO SURFACE FUNCTIONALIZED NANOPARTICLES IMBIBED WITH C3 TRANSFERASE 62

Abstract 62

Introduction 63

Materials and Methods 64

C3 Transferase-Imbibed Drug Delivery System 64

Rat Cortical Cell Culture 65

Cell Treatment and Immunocytochemistry 66

Microscopy and Analysis 67

Statistical Analysis 68

Results 68

BDNF-SFNP Delivery of C3 Transferase Increases Neurite Initiation 73

BDNF-SFNP Delivery of C3 transferase Increases Neurite Elongation 79

Discussion 81

Acknowledgements 82

References 82

V. CONCLUSIONS 86

Future Studies 92

REFERENCES 94

LIST OF TABLES

1.1. Functionalized Nanoparticles (SFNPs) With Size and Charge 12

LIST OF FIGURES

1.1. A Structural Illustration of The Blood–Brain Barrier 7

1.2. Nano-Based Drug Delivery System 11

2.1. Co-Culture BBB Model *In Vitro* 24

2.2. BDNF to SFNPs Binding Efficiency 26

2.3. BDNF Binding Stabilization. 27

2.4. FITC-Dextran Permeability Assay 29

2.5. Efficiency of N150 Transport Across BBMVEC Monolayers at Different Time Points 31

2.6. Efficiency of C150 Transport Across BBMVEC Monolayers at Different Time Points. 32

2.7. Efficiency of C750 Transport Across BBMVEC Monolayers at Different Time Points 33

3.1. Confocal Images of BDNF-Derivatized SFNPs in Different Cells in Cortical Culture 49

3.2. Quantification of BDNF-Derivatized N150 in Cortical Culture 51

3.3. Quantification of BDNF-Derivatized C150 in Cortical Culture 52

3.4. Quantification of BDNF-Derivatized C750 in Cortical Culture 53

3.5. BDNF-SFNPs are Internalized at Higher Concentrations than Non-Derivatized SFNPs in CST Neurons 54

3.6. Quantification of Fluorescence Intensity in CST Neurons Treated with Underivatized or BDNF-Derivatized SFNPs 55

4.1. Confocal Images of Cortical Neurons After Exposure to Outgrowth Promoting Substances or N150 SFNPs 70

4.2. Confocal Images of Cortical Neurons After Exposure to Outgrowth Promoting Substances or C150 SFNPs 71

4.3. Confocal Images of Cortical Neurons After Exposure to Outgrowth Promoting Substances or C750 SFNPs 72

4.4. Quantification of Neurite Outgrowth in Cortical Neurons After Exposure to Neurite Outgrowth Promoting Substances of SFNPs Constructs.....74

4.5. Quantification of Neurites Per Cell in Cortical Neurons After Exposure to Outgrowth Promoting Substances or SFNPs.....76

4.6. Quantification of The Percent of Neurite-Bearing Cells in Cortical Neurons After Exposure to Outgrowth Promoting Substances or SFNPs. 78

4.7. Quantification of The Total Neurite Length/Neuron in Cortical Neurons After Exposure to Outgrowth Promoting Substances or SFNPs. 80

ABBREVIATIONS

ANOVA	Analysis of variance
APS	Ammonium persulfate
AU	Arbitrary units
BBB	Blood–brain barrier
BBMVEC	Bovine brain microvascular endothelial cells
BDNF	Brain-derived neurotrophic factor
C150	Anionic nanoparticles surface functionalized with carboxyl group – size 150 nm
C3	C3 transferase
C750	Anionic nanoparticles surface functionalized with carboxyl group – size 750 nm
Cdc42	Cell division cycle 42
CME	Clathrin-mediated endocytosis
CNS	Central nervous system
CSPGs	Chondroitin sulfate proteoglycans
CST	Corticospinal tract
Ctip2	COUP-TF1 interacting protein 2
Cy5	Cyanine 5
DAPI	4’,6-diamidino-2-phenylindole
DMEM-F12	Dulbecco’s modified Eagle’s medium-F12 nutrient mixture
ELISA	Enzyme-linked immunosorbent assay
FBS	Fetal bovine serum
FDA	Food and Drug Administration
FITC	Fluorescein isothiocyanate

GDP	Guanosine diphosphate
GFAP	Glial fibrillary acidic protein
GTP.	Guanosine triphosphate
GTPase	Guanosine triphosphatase
Iba1	Ionizing calcium binding adaptor-1
LIMK	LIN-11, Isl-1, and MEC-3 protein kinase
MAG	Myelin-associated glycoprotein
N150	Cationic nanoparticles surface functionalized with amino group – size150 nm
Oligo	Oligodendrocytes
OMgp	Oligodendrocyte myelin glycoprotein
PBS	Phosphate buffered saline
PDL	Poly-D-lysine
PEG	Poly ethylene glycol
PEGEEMA	Poly (ethylene glycol) ethyl ether methacrylate
PEGMEMA	Poly (ethylene glycol) methyl ether methacrylate
PSA	Penicillin/Streptomycin/Amphotericin B
Rac1	Ras-related C3 botulinum toxin substrate 1
RCNs	Rat cortical neurons
RhoA	Ras homolog family member A
ROCK	Rho kinase; Rho-associated coiled-coil forming protein kinase
ROI	Region of interest
SCI	Spinal cord injury
SCM	Serum containing media

SDS	Sodium dodecyl sulfate
SEM	Standard error of the mean
SFM	Serum free media
SFNPs	Surface functionalized nanoparticles
TE	Tris EDTA
TJs	Tight junctions
TrkB	Tropomyosin receptor kinase B
UV	Ultraviolet

CHAPTER I

INTRODUCTION

Some of the most devastating human disorders come from dysfunction of the central nervous system (CNS), a site that is largely inaccessible to traditional water-soluble drugs and is composed of a multitude of cell types.[1,2] The CNS is protected by the blood–brain barrier (BBB), a series of tissue layers that protect the brain parenchyma from potentially harmful substances traveling through blood vessels and facilitate the transfer of oxygen and nutrients to brain and spinal cord neurons.[3,4]. Therapeutics effective for treating CNS disorders, particularly neuronal dysfunction, need to be able to cross the BBB and selectively affect specific cell species.[5-7] Nanomaterial-based drug delivery systems hold great promise for addressing these challenges as they can be formulated to cross biological barriers, derivatized to target specific cell types, and induced to release therapeutics on demand once they have been endocytosed into the targeted cells. [8,9] In the introduction to this dissertation, we summarize the significant burden of CNS disorders, identify a potential target strategy to encourage CNS regeneration, and provide the rationale leading to our overall hypothesis and the specific aims we designed to address it.

CNS DISORDERS ARE A LARGELY UNTREATED SIGNIFICANT HEALTH ISSUE

Traumatic or degenerative damage to the brain or spinal cord often leads to permanent loss of cognition, sensation, or control over movement. [10,11] Furthermore, neurotraumatic and neurodegenerative conditions constitute a significant health burden. [12] Degeneration and damage to the brain or spinal cord are regarded as the highly lethal diseases having the fourth highest mortality, following tumors, stroke, and cardiovascular and cerebrovascular diseases making the prevention and therapy crucial and urgent. [13] In fact, the leading causes of mortality (tumors, stroke, and cardiovascular/cerebrovascular disease) also significantly impact the CNS. [14] Thus,

addressing CNS disorders in general, and targeting neurotraumatic and neurodegenerative conditions that might be mitigated with therapies encouraging axon regeneration. [15]

Neurotraumatic disorders constitute a significant disease burden. In the United States, approximately 5.3 million and 285,000 patients suffer from pathology related to brain injury or spinal cord injury, respectively. [10] A recent report from the National Spinal Cord Injury Statistical Center reported that the annual incidence of spinal cord injury (SCI) is approximately 17,810 new cases each year in the United States. [16] SCI induced alterations in structure and function of motor and sensory tracts lead to somatosensory, motor, and autonomic dysfunction including cardiovascular conditions and lack of control of bowel, bladder, and sexual function. [14] Patients with traumatic SCI have a higher lethality than uninjured persons. [7] Moreover, SCI leads to substantial individual and societal costs. The annual cost of treatment and care for SCI will exceed $200 billion/year in the US.[17] Currently, there is no effective way to cure or control the disease progression.[18] SCI is a major concern since it impacts a patient's physical and mental health, as well as that of their family, the larger community, and the economy.[15]

RHO GTPASES AND CONTROL OF AXON REGENERATION

There are several mechanisms known to encourage the regeneration of axons and reconnection to appropriate targets.[12,15,19] Small guanosine triphosphatases (GTPases) of the Rho subfamily regulate many essential cellular functions such as apoptosis, proliferation, dendritic spine maintenance, and neuronal growth cone navigation.[20] Importantly, Rho GTPases are major regulators of the molecular events mediating the cytoskeletal rearrangements that lead to axon extension/retraction and synaptic plasticity.[21-22] The superfamily of small GTPases function as molecular switches that cycle between an inactive guanosine diphosphate (GDP)-bound and an active guanosine triphosphate (GTP)-bound conformation.[23] In the GTP-bound state, the proteins

interact with their downstream effectors and transmit cellular signals.[21,24,25] Activation of small GTPases is regulated by guanine nucleotide exchange factors (GEFs) that facilitate the exchange of GTP for GDP, GTPase-activating proteins (GAPs) that stimulate the hydrolysis of GTP, and guanosine dissociation inhibitors (GDIs) that sequester GDP-bound GTPases and prevent their activation.[26]

The biochemical mechanisms through which Rho GTPase subfamily members regulate actin cytoskeletal dynamics and control axon growth and synaptic plasticity are well defined.[6,27] Ras homolog family member A (RhoA), Ras-related C3 botulinum toxin substrate 1 (Rac1), and Cell division cycle 42 (Cdc42) are the Rho GTPases that have drawn the most attention and have well-defined roles in axon growth.[28] Actin polymerization at axonal growth cones is required for axon extension.[20] RhoA activation leads to growth cone collapse and process retraction, whereas Rac1 or Cdc42 activation results in enhanced process extension.[23,29,30] Specifically, activation of Rac1 promotes advance of sheet-like membranous lamellipodial extensions, while Cdc42 activity increases growth of finger-like filopodia that sample the environment and directs the trajectory of extending growth cones.[31-33] Therapeutic strategies that inhibit RhoA and/or promote Rac1/Cdc42 activation are theorized to promote axon extension.[20]

Treatments that inhibit RhoA signaling are attractive therapeutic strategies as they would both decrease growth cone retraction and increase the activity of Rac1 and Cdc42 relative to the activity of RhoA.[30] There is abundant evidence that RhoA activation is involved in the inhibition of axon growth.[33] Many outgrowth inhibitors, including chondroitin sulfate proteoglycans (CSPGs), myelin-associated glycoprotein (MAG), oligodendrocyte myelin glycoprotein (OMgp), and Nogo activate receptors that lead to activation of RhoA.[34] RhoA effectors include Rho-associated kinase, or Rho kinase (ROCK), and LIN-11, Isl-1, and MEC-3 protein kinase (LIMK).

ROCK activation leads to phosphorylation and inactivation of myosin light chain phosphatase and direct phosphorylation of the myosin light chain, both of which activate myosin and increase actin-myosin contractility and growth cone retraction.[35] LIMK phosphorylates and inactivates the actin depolymerizing factor, cofilin, thus stabilizing growth cone actin filaments.[35,36]

Inhibiting RhoA or ROCK reverses the inhibitory effects of these molecules on axon outgrowth and promotes axonal sprouting. Hence, targeting RhoA to inhibit its activation or signaling is a promising strategy for axon regeneration and functional recovery.[37] The downstream effector of RhoA, ROCK, can be inhibited by the small molecule Y27632.[35] This molecule is an attractive therapeutic because it can cross the BBB and is readily endocytosed into neurons. However, Y27632 does not inhibit all the functionally of RhoA that direct inhibition would, and delivery of effective amount of Y27632 to the CNS is difficult and cost-prohibitive.[37] Thus, targeting C3 transferase is a more attractive strategy.

RhoA is directly inhibited by C3 transferase (C3), a 24 kDa single-chain protein derived from *Clostridium botulinum*.[38] C3 transferase belongs to the family of ADP- ribosyltransferases and inhibits RhoA isoforms by preventing GEF-mediated Rho activation or fostering GAP-mediated inactivation and sequestering of GDP-bound Rho.[39,40] A previous study demonstrated that the outgrowth of PC12 cells, retinal neurons, and cortical neurons is enhanced on myelin with C3 transferase treatment.[41]

RhoA promoted growth cone collapse and neurite inhibition in primary neurons is attenuated by the inactivation of Rho with C3 transferase and either full length or bioactive peptides of C3 promote axon outgrowth from primary murine hippocampal neurons, and regeneration of axon *in vitro* and after experimental SCI.[27,42] However, a specific cell entry machinery for C3 transferase has not been identified, and there does not appear to be any

mechanism to transport C3 transferases across cell membranes.[43] Modified versions (e.g., addition of the HIV-tat promoter) that facilitate C3 entry into neurons have been constructed and do promote axon regeneration in experimental SCI.[40,44,45] However, a clinical trial with a modified cell permeable C3 construct has failed, likely due to an inability of targeting effective concentrations to specific neurons.[46] Therefore, a different method of delivering C3 to target neurons to encourage them to regenerate axons is needed. In prior work, we have used a nanomaterial-based delivery system carrying Y27632 and found that these nanospheres can cross a model of the BBB and increase outgrowth of neuronal processes. In this dissertation, we assess the ability of a similar nanoparticle construct in crossing a BBB model and in delivering C3 transferase to corticospinal tract (CST) neurons.

Demonstrating the ability to transport a hydrophilic therapeutic across the BBB would be a major advancement toward treating CNS disorders.[12] However, Rho GTPases are ubiquitous and it is likely that therapeutic benefits to neurons would be diluted by actions on other cell types in the CNS.[42] Therefore, a delivery system would also need to direct treatment to specific subclasses of neurons and avoid effects on glia, like astrocytes, oligodendrocytes, and microglia.[47] Developing effective treatments to encourage axon regeneration is largely challenged by: (a) inaccessibility of the CNS to conventional water-soluble drugs due to difficulties crossing lipid membranes like the BBB;[48] (b) potential off-target therapeutic effects since specifically targeting damaged neurons is challenging;[49] (c) toxicity and poor stability of drugs that are systemically administered;[6] and (d) lack of an effective modality for treatment monitoring.[50] Based on these conditions, specific delivery, enhanced uptake by the brain, and improved neuron regeneration therapeutic efficacy with minimal toxicological side effects are now considered to be the most challenging problem in modern medicine and research.[18]

Accordingly, nanomaterial-based drug delivery systems might be an ideal way to address these concerns.

BBB AND TRANSPORT MECHANISMS

The BBB plays a critical role in protecting and maintaining the microenvironment of the CNS.[48] The BBB is composed of capillary endothelial cells connected by tight junctions, endothelial-derived basement membranes, and cellular layers provided by astrocyte end feet and pericytes (see Figure 1.1).[50] While the other BBB constituents likely decrease BBB permeability, it is thought that the main deterrent is due to the tight junctions. These connections between the endothelial cells of the BBB have high electrical resistance and low paracellular permeability. In fact, 98% of all potent medications that could enhance treatment for CNS diseases are not in use in clinics because they are unable to cross the BBB.[49] Only lipophilic drugs with a molecular weight of less than 400 Da at a sufficient dosage can easily cross the BBB.[51] Nonspecific transcellular trafficking across the BBB is also inhibited by intracellular and extracellular enzymes that can inactivate therapeutic compounds, and efflux transporters actively transport substances entering the endothelium back into the blood supply.[5] Therefore, a lot of research is focused on creating new methods that can successfully cross the BBB and deliver therapeutics to the CNS. Many investigations are being attempted to alter the drug physicochemical properties to improve their permeability across the BBB, enabling CNS brain targeting.[52]

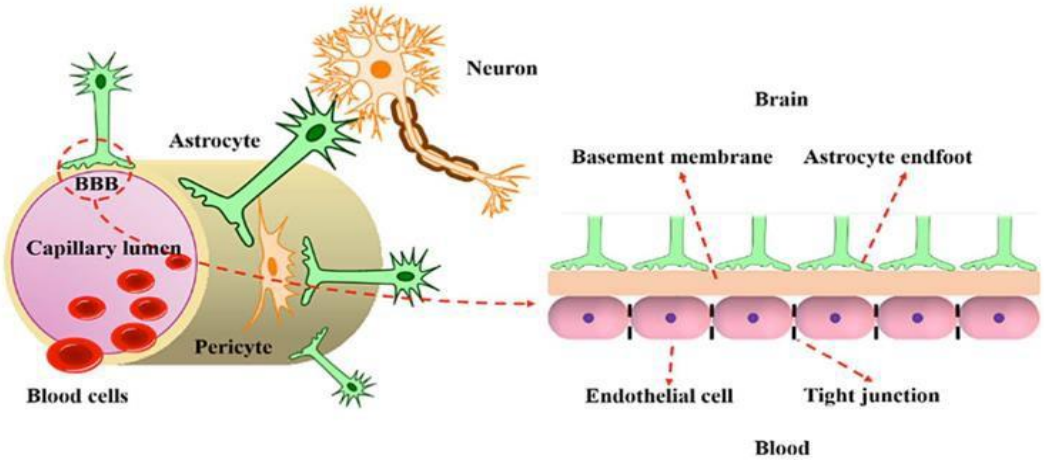

Figure 1.1. A Structural Illustration of the Blood–Brain Barrier. The BBB is composed of four constituent parts, namely the pericytes, astrocytes, basement membrane, and endothelial junctional complexes (tight junctions).

The various mechanistic routes that allow transport across the BBB include: (a) the paracellular aqueous pathway; (b) the transcellular lipophilic pathway; (c) carrier-mediated transport; (d) receptor-mediated transcytosis; and (e) adsorptive-mediated transcytosis.[53] The possible strategies for the reengineering of drugs to enable BBB transport include carrier-mediated transport, receptor-mediated transport, or absorptive-mediated transport.[50] Small molecules are moved by carrier-mediated and active efflux transporters, while large molecules are mostly moved by receptor-mediated transporters.[54] Most existing and theorized drugs for CNS conditions do not meet these requirements.[55] Strategies are being studied for delivering drugs *in vivo* to the CNS by direct injection into the brain.[53] However, until now, these methods failed as clinic therapy and the transport of drugs across the BBB remains a challenge. Currently, nanoparticles are being explored for their drug delivery potential across the BBB due to their excellent biocompatibility, functional versatility and unique surface electrostatics properties.[51] Nanomaterial-based drug delivery systems can be designed to: (a) cross biological membranes,

like those that compose the BBB; (b) target specific subsets of cells, including neurons; (c) be minimally toxic to CNS cells and tissues; and (d) carry therapeutics designed to treat the specific CNS condition, such as encouraging axon regeneration.[56]

ADVANTAGES OF NANOMATERIAL-BASED DRUG DELIVERY

Various strategies for delivering therapeutic agents into the brain have been explored, including viral vectors, nanoparticles, exosomes, and brain permeability enhancers.[57-59] Viral vectors have a natural ability to infect cells with nucleic acids have been developed to treat various brain diseases. However, direct injection into the brain causes a safety concern for this therapy.[59] Exosomes, secreted by cells, deliver small molecules, proteins, and nucleic acids across the BBB. However, the exosome donor cells, *in vivo* toxicity, and pharmacokinetics become critical issues that limit the potential as a therapy in the clinic.[58] Brain permeability enhancers transiently open the BBB and allow high concentrations of drugs to be transported into the brain. Unfortunately, a mismatch between findings in rodents and humans exists for this therapy.[57]

In recent years, nanoparticles have become more widely used in neuroscience in an attempt to cross the BBB and reverse neurodegeneration.[60] Nanoparticles are particles with a nanometer size range, from a few nanometers to hundreds of nanometers. Nanoparticles exhibit size-related properties that significantly differ from bulk materials, including a larger surface area and increased persistence in system circulation, both of which have shown remarkable potential for the use of nanomaterials as novel drug carriers.[61] Nanomaterial properties like biocompatibility, surface charge, and hydrophobicity are among the fundamental considerations for the selection of a nanoparticle for medical applications. Nanoparticle drug delivery systems have been developed to be therapeutically effective, safe, and to allow specific targeting and

controllable drug delivery.[18,62,63] Nanoparticles and their smart surfaces carry excellent therapy potential for clinical solutions since they are able to be modified for specific target cells. For instance, nanomaterial systems could be designed to specifically target CST neurons to facilitate regaining motor function after nervous system damage.[9] Although the initial use of nanoparticles was for their physical, mechanical, electrical, and magnetic applications, current attention is focused on pharmaceutical applications, especially drug delivery.

Nanoparticles have many advantages over other drug delivery agents for targeting CNS cells and treating neurotraumatic or neurodegenerative conditions: (a) nanoparticles may reach well inside biomolecules, a situation not possible for larger particles;[55] (b) nanoparticles can serve as an agent to deliver drugs to the target organ or tissue across the biological barriers like the BBB, a feature of nanoparticles that can solve problems dealing with the insolubility of drug formulations and drug delivery;[64] (c) nanoparticles may recover the function of neuron cells by enhancing neurite regeneration;[65] (d) some nanomaterial constructs are remotely controllable by alternating magnetic fields (eg, constructs containing iron oxide nanocrystals) or pH and temperature-dependent swelling and shrinking properties (eg, polyethylene glycol copolymers) and can be used to precisely control temperature or release drugs inside intracellular environments;[65-67] (e) nanoparticles show remarked biocompatibility with low cellular toxicity at effective concentrations; (f) nanoparticles can be conjugated with proteins, nucleic acids, or other cellular components to enhance therapeutic potential;[68] (g) nanoparticles with amino or carboxyl functional groups can be covalently attached to a peptide ligands to achieve the targeted delivery to a particular cell types;[61,69] and (h) nano-N_2Py nanoparticles can inhibit the formation of beta-amyloid aggregates to protect human cortical neurons from amyloid-beta-associated oxidative damage.[70,71] Together, these qualities make nanomaterial drug or drug delivery systems highly

attractive alternatives to conventional drug administration methods for treating neurological conditions.

A NANOMATERIAL-BASED DRUG DELIVERY SYSTEM TO ENCOURAGE AXON REGENERATION FOLLOWING CNS DAMAGE

In addition to the complexity of brain diseases, the lack of efficient technologies to deliver drugs across the BBB hinders CNS drug development. Besides the poor ability of the drug to cross BBB, delivering drugs to the target cells is challenging because of the great cellular diversity in the CNS. A nanomaterial-based drug delivery system to encourage axon regeneration following CNS damage has been designed and is described and tested in this study.

We collaborated with Santaneel Ghosh (Southeast Missouri State University) to design a nanomaterial system to address issues of efficient targeting, enhanced intracellular uptake, and reduced toxicity for treating CNS disorders. To enhance axon regeneration following CNS damage, we designed a thermoresponsive nanomaterial system surface functionalized to allow derivatization with targeting molecules, and having the ability to be remotely actuated to release therapeutic (see Figure 1.2). The constructed nanoscale system is fluorescently labeled to allow tracking of the nanomaterials in neurons and neuronal cell lines and *in vivo*. The original system is composed of polymer-encapsulated magnetic nanoparticles that can be guided to target regions using an external magnetic field and the polymer coat allows a volumetric transition when temperatures are increased or when nanoparticles are exposed to an oscillating magnetic field. This allows release of drug molecules imbibed in the polymer matrix. The surface functionalized nanoparticles (SFNPs) used in this system are essentially the designed system without the iron oxide nanocrystals. These SFNPs retain thermoresponsive volumetric transitions to allow on demand release of imbibed drug. The copolymer shell is further modified by derivatization with

surface –COOH or –NH_2 functional groups, which is used to bind brain-derived neurotrophic factor (BDNF) peptides to their surfaces (see Figure 1.2).

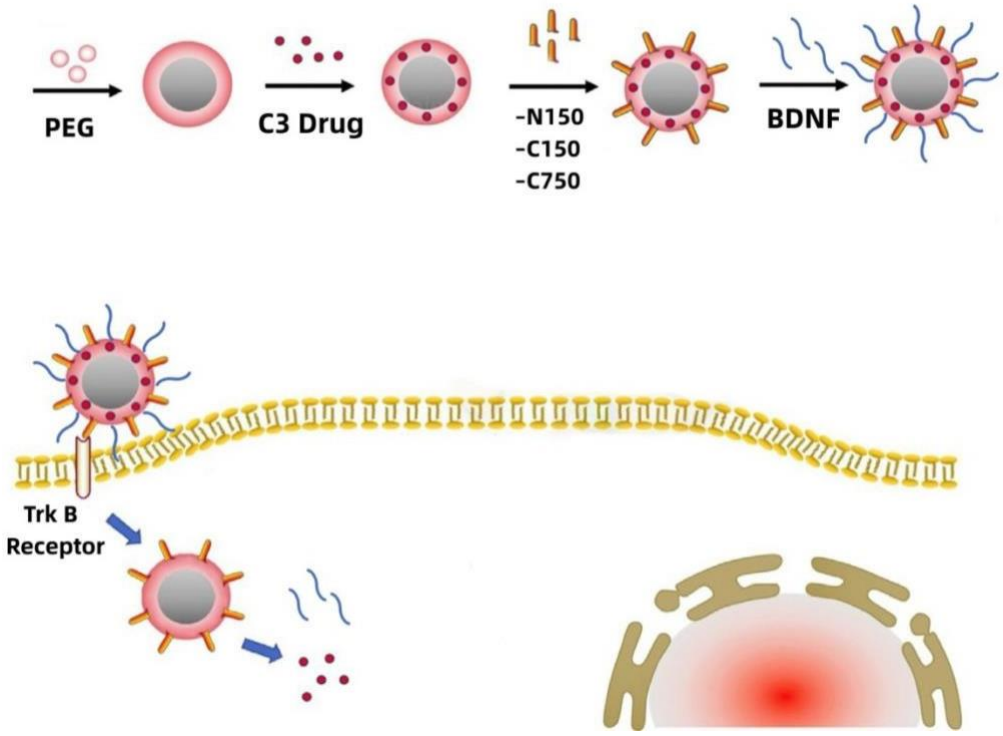

Figure 1.2. Nano-Based Drug Delivery System. The PEG shell of the nanoparticles imbibed with the drugs that facilitate axon growth, C3 transferase. Further, the SFNPs (N150, C150, C750) attached on the surface of nanoparticles and derivatized with BDNF. Attached BDNF will recognized by it high affinity receptor, TrkB, which will internalize the nanospheres.Drug release will be initiated by increasing the temperature briefly to 37°C. This increase in temperature will shrink the size of nanoparticles then embedded drug released within cells.

We constructed several versions of this basic system to test specific functionality in neurons and *in vivo*. In the current work, we tested three species of fluorescently labeled polyethylene glycol (PEG) copolymer SFNPs that do not contain iron oxide nanocrystals (see Table 1.1). The SFNPs retain the ability to be derivatized with targeting molecules and thermoresponsive volumetric transition to allow on demand release of loaded therapeutic. We

tested SFNPs with amino functional groups that are ~150 nm in diameter (N150) and SFNPs with carboxyl functional groups that are either ~150 nm in diameter (C150) or ~750 nm in diameter (C750). The nanospheres are composed of materials that are approved by the Federal Drug Administration (FDA) for human use. The PEG coating provides an external surface that is highly amenable to biochemical modification. Previous toxicity studies showed that the SFNPs are non-toxic to PC12 and B35 cells and promote outgrowth from these cell lines and primary cultures of cortical neurons.[72,73]

Table 1.1. Surface Functionalized Nanoparticles (SFNPs) With Size and Charge

Nanocarriers	Size (nm)	Charge
N150	~150	Cation (NH^{3+})
C150	~150	Anion ($COOH^{-}$)
C750	~750	Anion ($COOH^{-}$)

In the current work, we further modified the SFNPs by derivatizing them with BDNF peptides covalently bonded to the functional groups. BDNF derivatization allows SFNPs to be recognized by the tropomyosin receptor kinase B (TrkB) receptor, which is expressed on the surface of neurons and other cells. We chose BDNF to test the preferential uptake by target neurons, especially CST neurons, which are the major neuron type that leads to lack of voluntary motor control following damage.[74,75] Importantly, CST axons are damaged in SCI and assessments from the current study will allow testing of SFNP constructs in experimental SCI models. We have further determined whether BDNF derivatization affects the intrinsic ability of the SFNPs to cross lipid barriers like the BBB and allows target uptake by TrkB expressing neurons. Finally, we tested whether C3 transferase imbibed within the copolymer shell

overcomes its poor permeability and deliver C3 cross BBB to increase outgrowth in CST neurons.

SPECIFIC AIMS

We suggest an approach that loads drugs into the surface functional nanoparticles and examines targeting and controlled release of BDNF-derivatized SFNPs. This study focuses on the nano-based systems that have the potential to deliver the regeneration drugs to the specific sites of action and respond to external stimulation. From previous studies, we know that SFNPs composed of PEG copolymer coats and surface functionalized with amino or carboxyl functional groups can cross a BBB model *in vitro*, be readily and preferentially endocytosed into cortical neurons, and release imbibed Y27632 to increase neurite outgrowth in cultured neurons.[62,65,72,73] However, we intend to increase the efficacy of the SFNPs by derivatizing them with BDNF, a neurotrophic factor that activates the TrkB receptor.[76] We hypothesize that derivatizing PEG copolymer SFNPs with BDNF will maximize targeting to CST neurons without affecting the ability of SFNPs to cross the BBB and that on demand release of imbibed C3 transferase from BDNF-SFNPs will greatly increase outgrowth of processes from CST neurons. In this study, the SFNP drug-delivery systems are used to investigate the efficiency of crossing the BBB, target CST neurons, and the efficacy of on-demand release of C3 transferase for promoting process extension from CST neurons. To test the hypothesis, we performed the following Specific Aims:

Specific Aim 1

We hypothesize that by binding to the SFNPs, the impermeability of BBB to free BDNF can be overcome. To determine whether attaching BDNF to SFNPs affects their ability to cross the BBB *in vitro*, we attached BDNF to SFNPs surface functionalized with –COOH and $–NH_2$. We have confirmed the efficient attachment of BDNF using enzyme-link immunoabsorbant

assays (ELISA) and assessed the ability of BDNF-SFNPs to cross a monolayer of bovine brain microvascular endothelial cells (BBMVEC) compared to non-derivatized SFNPs.

Specific Aim 2

We hypothesize that these BDNF derivatized nanoparticles with –COOH and $–NH_2$ surface functionalized groups would be internalized by neurons, especially CST neurons, compared to glia in a mixed cortical culture. To determine whether CST neurons preferentially take up SFNPs derivatized with BDNF, we have used immunocytochemistry and image analysis to assess the extent and timing of uptake by CST neurons and glia in cultures of neonatal rat cortices enriched for neurons.

Specific Aim 3

We hypothesize that increased temperature will release the C3 transferase imbibed in SFNPs within the neurons to promote process outgrowth from CST neurons. To determine whether the release of C3 transferase from BDNF-derivatized SFNPs increases axon growth in CST neurons, we have assessed the extent of neurite initiation and elongation from cultured neurons exposed to BDNF-SFNPs induced to release C3 transferase, compared to non-derivatized SFNPs and bath application of BDNF or C3.

The results from these experiments are organized into 3 chapters (Chapter 2 - 4), which will be submitted for publication in peer-reviewed scholarly journals. Specific Aim 1 is addressed in Chapter 2, which is a study to determine whether attaching BDNF to SFNPs affects their ability to cross the BBB *in vitro*. Chapter 3 describes the ability of SFNPs derivatized with BDNF to target and be preferentially taken up by CST neurons, and Specific Aim 3 is relayed in Chapter 4, which assesses the efficacy of C3 released from BDNF derivatized SFNPs to increase neurite outgrowth in CST neurons. We close this work in Chapter 5 where we present a

comprehensive discussion, describe ongoing and future investigations, and provide concluding remarks. Together, these investigations provide a comprehensive analysis of a BDNF-derivatized nano-based drug delivery system designed to release a RhoA inhibitor as a potential therapeutic approach for the future treatment of SCI and other traumatic and degenerative CNS disorders.

CHAPTER II

BIOACTIVE BRAIN-DERIVED NEUROTROPHIC FACTOR DERIVATIZED SURFACE FUNCTIONALIZED NANOPARTICLES CROSS A BLOOD–BRAIN BARRIER MODEL *IN VITRO*

A Manuscript to be Submitted for Publication Consideration in

Biomaterials

Mengjie Cao, Santaneel Ghosh, Ph.D., DiAnna L. Hynds, Ph.D.

ABSTRACT

Delivering therapeutics to corticospinal tract (CST) neurons to enhance motor recovery after spinal cord injury (SCI) is limited by the blood–brain barrier (BBB). Thermoresponsive surface-functionalized nanoparticles (SFNPs) derivatized with brain- derived neurotrophic factor (BDNF) would be preferentially endocytosed by CST neurons expressing high levels of the high affinity BDNF receptor TrkB. Here, we test the efficiency and stabilization of BDNF peptide binding to three SFNPs and determine their ability to cross a monolayer of bovine brain microvascular endothelial cells (BBMVECs), an *in-vitro* BBB model. Over 4 hours, saturating maxima of 70.34%, and 68.2% applied BDNF bound to 150 nm diameter amino (N150) or carboxyl (C150) group SFNPs, respectively. Carboxyl group SFNPs of approximately 750 nm diameter (C750) bound 74.7% of applied BDNF in 4 hours without saturating binding sites. BDNF binding to each SFNP was stable for at least 96 hours and 40.7% BDNF-N150, 42% BDNF-C150, and 24% BDNF-C750 SFNPs crossed a BBMVEC monolayer within 4 hours, similar to the amount of crossing seen with SFNPs not derivatized with BDNF. These data indicate that BDNF efficiently binds SFNPs and does not hinder crossing of an *in-vitro* BBB, suggesting promise for their application in treating SCI.

INTRODUCTION

Damage to corticospinal tract (CST) axons is prevalent in spinal cord injuries (SCIs) and leads to permanent loss of voluntary movement (Martin, 2022). This is a significant medical issue as there are about 294,000 cases of people living with SCI in the United State (NSCISC, 2020). The development of therapies for SCI disorders has grown rapidly in recent years as the population of patients is increasing (NSCISC, 2020). However, drug development for reversing neuron damage has the poorest success rates compared to other therapeutic areas (Hurlbert *et al*., 2013). The design of effective CNS drugs is challenging because of the cellular complexity of the brain and inability to target specific subtypes of neurons and deliver effective concentrations of therapeutics, off target effects of drugs, and the impermeability of the blood–brain barrier (BBB) to water soluble therapeutics (Bellettato & Scarpa, 2018; Pandey *et al*., 2015). The delivery of drugs to specific targets across the BBB could be enhanced by tunable nanomaterial-based drug delivery systems (GhoshMitra *et al*., 2011).

In recent years, nano-scale materials have become more widely used for neuroscience applications (Kim *et al*., 2019; Tyler *et al*., 2013). Such nanoparticles have many advantages over other drug delivery agents *(*Anselmo & Mitragotri, 2016; Nguyen, 2017; Patra *et al*., 2018). Nanoparticles, of a few nm in size, may reach well inside biomolecules, a situation not possible for larger particles (Albanese *et al*., 2012; Khan *et al*., 2019). Nanoparticles can serve as agents to deliver drugs to target organs or tissues across biological barriers, like the BBB (Ahlawat *et al*., 2020). The nanoparticles can be optimized to cross the BBB by exploiting receptor-mediated and adsorptive-mediated transcytosis pathways (Lombardo *et al*., 2020; Tashima, 2020). This feature of nanoparticles can solve problems dealing with the insolubility of drug formulations and drug delivery. Nanoparticles that are remotely controllable allow less invasive treatment

strategies (Zhou *et al.*, 2018). The magnetic and temperature-dependent size properties of these nanoparticles can be used to precisely control the release of therapeutics. Nanoparticles also show marked biocompatibility and the ability to conjugate with proteins, nucleic acids, and cellular components (Biroudian *et al.*, 2019). Thus, nanoparticles can be covalently derivatized (e.g., with amino or carboxyl functional groups) to achieve the targeted delivery to a particular cell type.

The nano-based drug delivery system used in this study is biocompatible, can be remotely actuated to deliver imbibed therapeutic (Alam *et al.*, 2018). The nanoparticles consist of a thermoresponsive polyethylene glycol (PEG) matrix surface modified with either carboxyl (–COOH) or amino ($–NH_2$) functional groups to allow the attachment of peptide ligands, where peptide bonding of proteins can facilitate delivery to cells expressing receptors specific for the attached proteins. These surface-functionalized nanoparticles (SFNPs) and their unmodified forms are minimally toxic to neuron-like PC12 pheochromocytoma cells, B35 neuroblastoma cells, and neonatal rat cortical neurons (Veettil, 2017; Sebastian, 2019). Furthermore, the SFNPs are readily endocytosed into neurons and do not inhibit to outgrowth of neuronal processes(GhoshMitra, 2011; Veettil, 2017).

A major goal in the treatment of SCI is the recovery of voluntary motor function, which is compromised by damage to axons of CST neurons (Zhang *et al.*, 2021). Since CST neurons express the full length tropomyosin receptor kinase B (TrkB) receptor, the high-affinity receptor for brain-derived neurotrophic factor (BDNF), derivitizing SFNPs with BDNF should allow their preferential internalization into CST neurons by receptor-mediated endocytosis (Pilakka-Kanthikeel *et al.*, 2013). BDNF is a neurotrophic factor that promotes the extension of neuronal

processes, which could be further enhanced if the SFNP also carried additional axon regeneration promoting substances (Jiang *et al*., 2018).

In this work, we construct and characterized two sizes of SFNP (approximately 150 nm or 750 nm in diameter) composed of PEG surface functionalized with either amino (150 nm, N150) or carboxyl (150 nm, C150; 750 nm, C750) groups that are bound to BDNF as the first steps toward assessing their efficacy in promoting axon regeneration after SCI. We first evaluate the binding efficiency and stabilization between BDNF and each type of SFNP using a BDNF enzyme-linked immunosorbent assay (ELISA). We then assess the ability of each type of BDNF derivatized SFNP to cross an *in-vitro* BBB model composed of bovine brain microvasculature endothelial cell (BBMVEC) monolayers (Duck *et al*., 2017). Our results indicate that BDNF can be efficiently bound by each type of SFNP and that the addition of BDNF does not significantly affect the ability of SFNPs to across a BBB model. Thus, BDNF-derived SFNP nanoparticles drug delivery system are promising therapeutic strategies for targeting regeneration from CST upper motor neurons to facilitate recovery of motor function following SCI.

MATERIALS AND METHODS

Synthesis of Surface Functionalized Nanoparticles (SFNPs)

Unless noted otherwise, all chemicals were obtained from Sigma (St. Louis, MO). Fluorescent surface functionalized, thermoresponsive nanospheres were synthesized by fluorescently labeling thermoresponsive hydrogels that were surface functionalized with amino or carboxyl functional groups (Ghosh *et al*., 2009; GhoshMitra *et al*., 2011). Three nanosphere constructs were made by altering the size and surface functionalization: (1) nanoparticles of approximately 150 nm in diameter surface functionalized with amino ($–NH_2$) groups (N150); (2) nanoparticles of approximately 150 nm in diameter surface functionalized with carboxyl (–

COOH) groups (C150); and (3) nanoparticles of approximately 750 nm in diameter surface functionalized with carboxyl (–COOH) groups (C750). Fluorescent labeling was accomplished by incorporating methacryloxyethyl thiocarbamoyl rhodamine B fluorescent monomers (Polysciences, Inc., emission: 570 nm) into PEG shells modified by surface functionalization with either - COOH or $–NH_2$ groups. N150 and C150 were synthesized in deionized water using 14.0 mg/ml $PEGETH_2MA$ (Mn ~246 g/mol), 4.6 mg/ml PEGMA (Mn ~300 g/mol), 0.13 mg/ml ethylene glycol dimethacrylate (EGDMA, 97%, Fluka, Buchs, Switzerland; crosslinker), 0.13 g/ml sodium dodecyl sulfate (SDS, surfactant), 3.1 µg/ml methacryloxyethyl thiocarbamoyl rhodamine B fluorescent monomers (Em: 570 nm; Polysciences, Warrington, PA; for fluorescent labeling), and 1.5 mg/ml methacryloyl L-lysine (Polysciences, Warrington, PA; for N150 synthesis) or 0.33 mg/ml polyacrylic acid (PAA, 99%; for C150 synthesis). For C750 synthesis the amount of each reactant was 28.0 mg/ml of $PEGETH_2MA$, 9.2 mg/ml PEGMA, 0.27 mg/ml EGDMA, 0.09 mg/ml SDS, 6.2 µg/ml methacryloxyethyl thiocarbamoyl rhodamine B fluorescent monomers, and 0.67 mg/ml PAA acid in deionized water. In all cases, the solution was purged with nitrogen gas for 40 min at 70°C, 30 volumes of 14.0 mg/ml ammonium persulfate (APS) were added (to initiate copolymerization) and the reaction was run for 6 hours under nitrogen gas bubbling. Fluorescent nanoparticles were dialyzed (MW cut-off 13,000, Carolina, Burlington, NC) against water for 7 days at room temperature with twice daily deionized water changes. Nanoparticles were collected by ultracentrifugation, freeze-dried, and stored at room temperature until solubilized in deionized water for use.

Derivatization of SFNPs with Brain-derived Neurotropic Factor

SFNPs were derivatized with a bioactive brain-derived neurotrophic factor (BDNF) peptide using peptide bonding (BDNF peptide; AbCam, Boston, MA). Different ratios of SFNPs

to BDNF (1 µg:0.01 µg, 1 µg:0.02 µg, 1 µg:0.03 µg, 1 µg:0.04 µg, 1 µg:0.05 µg) were mixed in Tris EDTA (TE: 10 mM Tris-HCl, pH 8; 1 mM EDTA) buffer and incubated on a shaker (100 rpm) at room temperature for 4 hours. BDNF-derivatized SFNPs were collected by centrifugation for 30 min at 400 × g. The pellet was washed twice with deionized water and resuspended to a concentration of 4 µg/ml in 1X Tris EDTA (TE) buffer and stored at 2 - 8°C until further use.

BDNF Binding Efficiency and Stabilization by Enzyme-Linked Immunoabsorbance Assay (ELISA)

A BDNF ELISA (Rat BDNF ELISA Kit from Boster Biological Technology, Pleasanton, CA) was used according to the manufacturer's instructions to calculate the efficiency and stability of BDNF binding to SFNPs. In brief, 100 µl aliquots of each BDNF standard (supplied with kit) and BDNF-SNFP samples for each of the SFNP/BDNF ratios described above were assayed in triplicate. Binding stability was assessed from the samples collected at 12, 24, 48, 72, and 96 hours after the binding reaction. After incubation in the supplied anti-rat BDNF pre-coated 96-well strip microplate for 120 minutes at room temperature, standard and sample solutions were removed and the plate was exposed to 10 µl/ml of the prepared biotinylated anti-rat BDNF antibody for 90 min at room temperature. Wells were washed 3 X 1 min phosphate-buffered saline (PBS), followed by incubation with 10 µl/ml avidin-biotin-peroxidase complex for 40 minutes at room temperature. Plates were washed 5 X 2 min PBS and developed with 3,3′,5,5′-Tetramethylbenzidine (color developing reagent) in the dark for 30 minutes at room temperature. The reaction was halted and the plate was read at 450 nm using a ELx800 plate reader (BioTek Instruments, Winooski, VT). The amount of BDNF bound to the SFNPs in pg BDNF to ng SFNP was calculated from a standard curve.

Cell Culture

Bovine brain microvascular endothelial cells (BBMVECs). Bovine brain microvascular endothelial cells (BBMVECs) were cultured in BBMVEC growth media containing 10% fetal bovine serum (FBS; Cell Applications, San Diego, CA) as described in Duck *et al*. (2017). BBMVECs were cultured at 10,000/cm^2 and grown until they formed a confluent monolayer on Costar Transwell 12 mm 0.4 μm porous filter inserts (Dot Scientific, Burton, MI) coated with 15 μg/ml fibronectin from bovine plasma (Sigma, St. Louis, MO). Monolayers were washed three times with phosphate buffered saline (PBS) and placed in serum free media containing 138 nM hydrocortisone for 72 hours to promote tight junction formation.

Rat cortical cell culture. All animal procedures conformed to the National Research Council Guide for the Care and Use of Laboratory Animals and were performed under an approved TWU Animal Care and Use protocol. Primary cortical cell cultures were isolated from postnatal day 0-1 rats (Charles River Laboratories, Wilmington, MA). Pups cold anesthetized for 20 min and quickly decapitated. Brains were excised from skulls in DMEM-F12 containing 10% FBS (Atlanta Biologicals, Atlanta, GA). Using a dissecting microscope, cerebral hemispheres were removed from brains by cutting away the brainstem along the medial longitudinal fissure and cortices were removed from subcortical white matter with a sterile scalpel and cleaned of meninges and blood vessels with fine forceps. Cleaned cortices were placed in a new sterile petri dish in serum-free DMEM-F12 media and cortical tissue was cut into fine pieces of approximately 1 mm^3. Tissue pieces were digested in 0.25% papain (Worthington Biochemical, Lakewood, NJ) and 100 U/ml DNase I (New England Biolabs, Ipswitch, MA) at 37˚C, 5% CO_2 in 95% humidity for 15 minutes. Papain was inactivated with FBS and gently triturated using fire-polished Pasteur pipettes until the solution was homogenous (approximately 20-30

triturations). Cell solutions were centrifuged at 200 × *g* for 5 minutes at room temperature. The supernatant was aspirated and the cell pellet was resuspended in 10 ml DMEM-F12 supplemented with 10% FBS and 100 U/ml penicillin, 100 µg/ml streptomycin, and 0.25 µg/ml amphotericin B (PSA antibiotic/antimycotic; Hyclone, Logan, UT). Cortical cells were plated at 8,000 cells/well on ultraviolet (UV) light sterilized poly-D-lysine (PDL; MP Biomedicals, Irvine, CA) coated 18 mm coverslips in 24 well tissue culture plates (ThermoFisher, Waltham, MA) and incubated at 37°C, 5% CO_2 for 4 to 6 hours until cortical cells attached to the coverslips. Media was then changed to Neurobasal Plus (Gibco, CA) containing 10% B27 supplement (ThermoFisher, Waltham, MA) and 10% PSA. Media was refreshed every 2-3 days by removing half the volume of media and replacing it with fresh warmed Neurobasal Plus with B27.

Blood–Brain Barrier Models and Treatments

The co-culture blood–brain barrier (BBB) model consisted of two chambers cell culture chambers (Figure 2.1). BBMVECs were grown on transwell inserts in the apical chamber for 72 hours in 24 well plates prior to transfer to new 24 well plates containing cultured cortical neurons, which were in the basal chamber. The establishment of tight junctions between BBMVEC and the integrity of the BBB model was tested using 1mg/ml fluorescence isothiocyanate (FITC) conjugated 70 kDa dextran (Sigma Aldrich, St. Louis, MO). Each BDNF-derivatized SFNPs construct (N150, C150, C750) was added to the apical chamber of intact BBMVEC barriers for 15, 30, 60, 120, or 240 min. Then, 10 µl aliquots were collected from both the apical and basal chambers. The fluorescence intensity of collected aliquots was determined in triplicate for three experimental repeats to estimate the proportion of SFNPs that passed through the BBB model. Fluorescent intensity was measured using a Synergy H1 Hybrid plate reader with excitation at 555 nm and emission at 570 nm (BioTek Instruments, Winooski, VT).

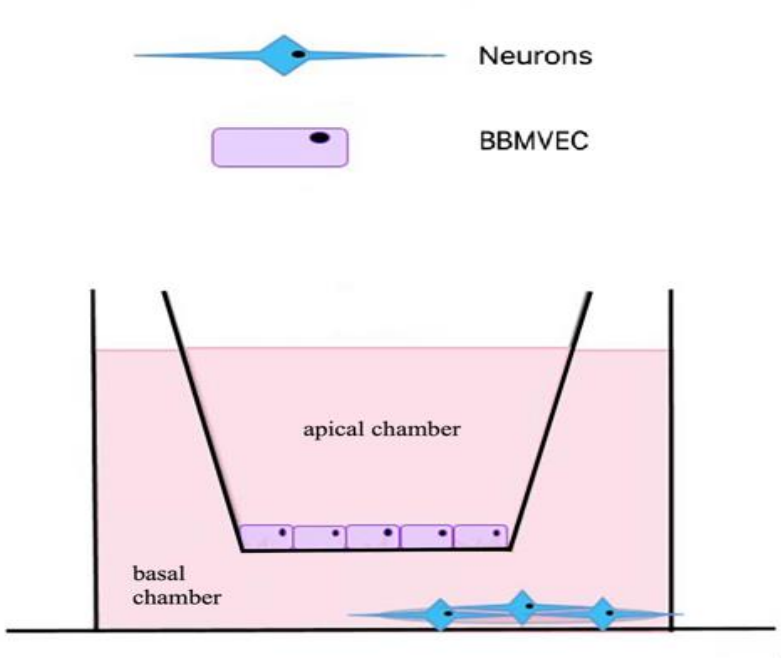

Figure 2.1: *Co-Culture BBB Model In Vitro.* In the blood–brain barrier (BBB) *in vitro* model, bovine brain microvascular endothelial cells (BBMVECs) were grown in a monolayer on the cell insert forming the base for the apical chamber and culture of cortical neurons were cultured on the floor of the well in a 24 well plate, constituting the basal chamber.

Statistical Analyses

Data from three independent experiments were averaged and are expressed as mean ± standard error of the mean (SEM). Means of the fluorescence intensity measured in the BDNF ELISAs, the percent of each type of SFNPs that passed into the basal chamber or remained in the apical chamber were analyzed using one-way Analysis of Variance (ANOVA). Homogeneity was tested using Levene's test, and if ANOVA assumptions were met, pairwise comparisons between experimental groups were assessed using Tukey HSD post-hoc tests. Values of $p \leq 0.05$ were considered significant.

RESULTS

BDNF Binding Efficiency

To confirm that BDNF was efficiently coupled to our surface functionalized nanoparticles (SFNPs), we calculated how much BDNF bound to each SFNPs construct (N150, C150, C750) from the amount of unbound BDNF remaining after binding reactions using different input ratios of BDNF to SFNPs. Subtracting the amount of unbound BDNF from the total BDNF used in each binding reactions indicated that the amount of BDNF bound to each type of SFNPs increased with higher BDNF:SFNPs ratios, reaching saturation for some types of SFNPs (Figure 2.2). N150 SFNPs bound 281.3 pg BDNF/ng N150 by 4 hours, corresponding to binding efficiency of approximately 70.34 ± 0.49 (Figure 2.2A). After 4 hours, BDNF to SFNP binding for C150 was 274 pg/ng, or 68.2 ± 0.4 (Figure 2.2B), and for C750, 301 pg BDNF/ng or 74.7% ± 0.35 (Figure 2.2C). BDNF binding to smaller diameter SFNPs (N150 and C150) reached saturation at ratio of 0.04:1.0 BDNF:SFNP (400 pg of BDNF added) since there was no significant increase ($p > 0.05$) between the 0.04:1 and 0.05:1 BDNF:SFNP input ratios. However, significantly more ($p \leq 0.05$) BDNF bound to C750 at the 0.05:1.0 input ratio (500 pg BDNF added), compared to 0.04:1.0 BDNF:SFNP input ratio (400 pg BDNF added), suggesting that C750 binding of BDNF did not reach saturation likely due to the larger diameter (750 nm) and much larger surface area (1,766.25 μm) of C750 compared to the smaller SFNPs (150 nm diameter, 70.65 μm surface area). In subsequent experiments, the 0.04:1.0 BDNF to SFNPs binding ratio was used for each SFNP construct to allow consistent comparisons between the SFNPs. These results from the measurement BDNF binding to each type of SFNPs indicate that all SFNPs constructs efficiently bound BDNF.

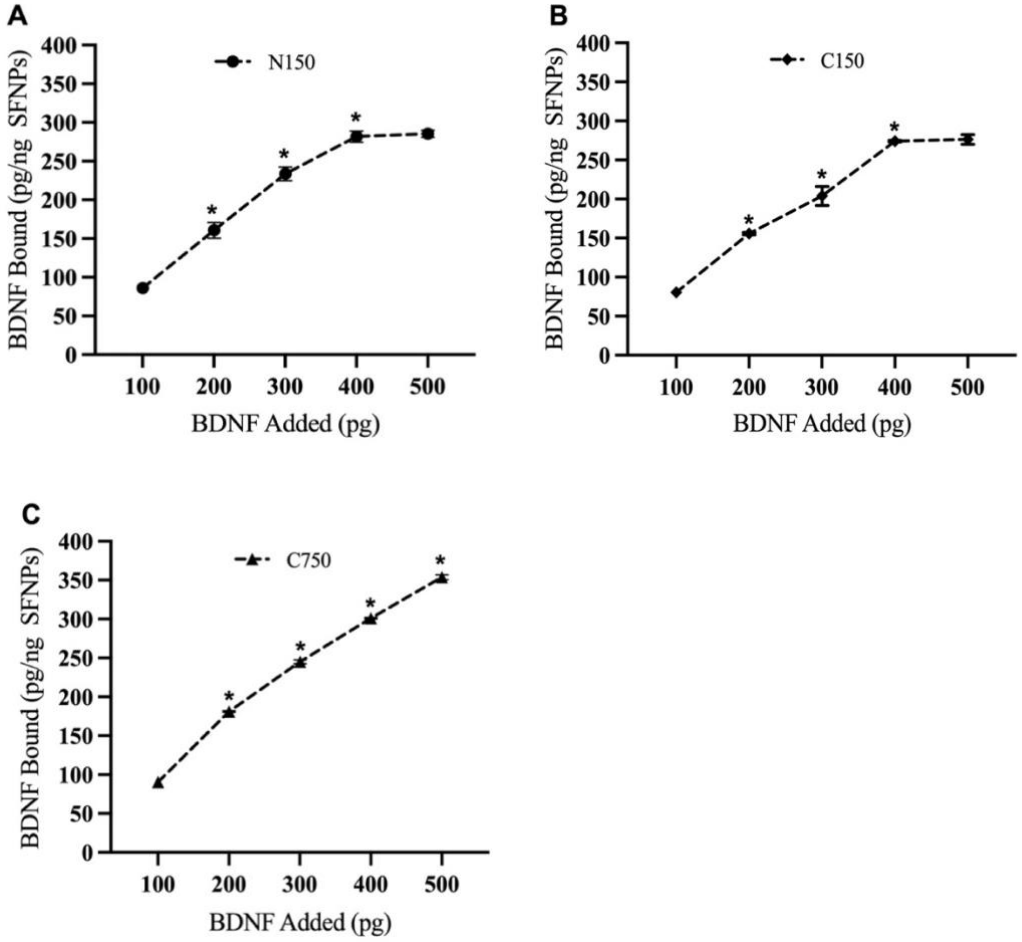

Figure 2.2: *BDNF to SFNPs Binding Efficiency.* Input ratios of 0.01:1.0, 0.02:1.0, 0.03:1.0, 0.04:1.0, and 0.05:1.0 pg BDNF to ng SFNPs were used in peptide bonding reactions performed at room temperature. The amount of BDNF in reaction supernatants collected after 4 hours was measure by ELISA and the BDNF to SFNPs binding efficiencies (pg BDNF/ng SFNPs) for N150 (A), C150 (B), and C750 (C) were calculated by subtracting the supernatant concentration from the input concentration. Data are reported as means ± SEM from three independent experiments, and asterisks indicate statistically significant differences at $p \leq 0.05$ for the amount of BDNF bound to each SFNPs compared to the next lowest input concentration (ANOVA with Tukey HSD post-hoc).

BDNF Binding Stabilization

We next determined the stability of BDNF to SFNPs binding by measuring the release of BDNF from each SFNPs construct using ELISA 12, 24, 48, 72, and 96 hours after the binding reaction. There were no significant differences between each time points ($p > 0.05$) for all three types SFNPs for up to 96 hours (Figure 2.3). These results demonstrate that the covalent peptide bonds between BDNF and the functional groups on the surface of each type of SFNP (N150, C150, C750) are stable, indicating that BDNF is unlikely to leach off of the BDNF-derivatized SFNPs.

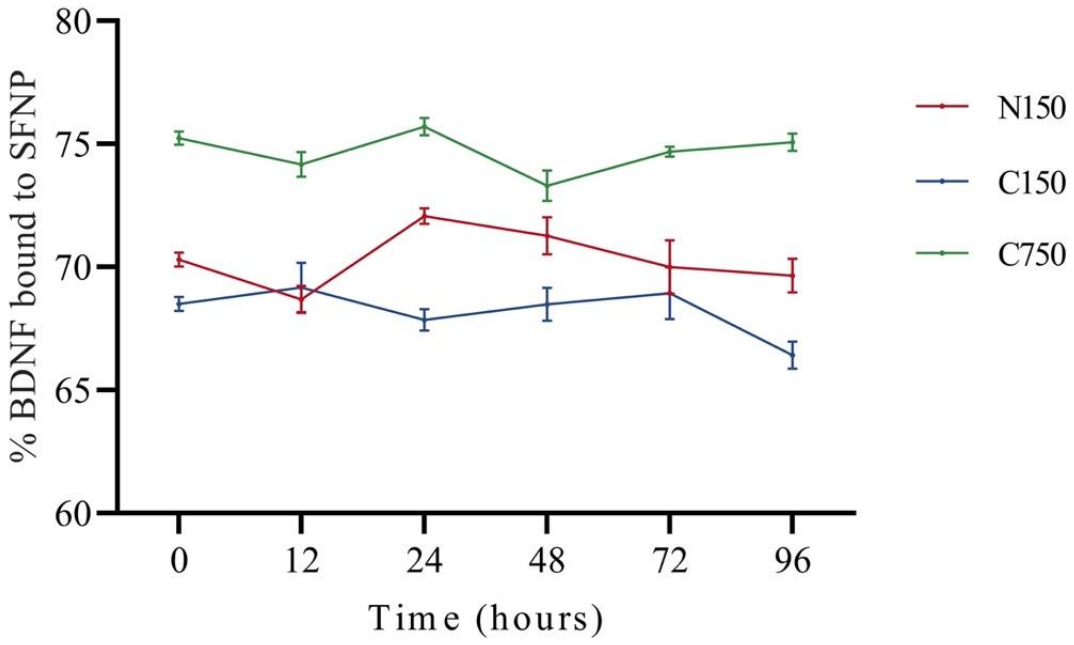

Figure 2.3: *BDNF Binding Stabilization.* Binding stability was assessed from amount of BDNF that remained bound for BDNF-bound N150 (red line), C150 (blue line), and C750 (green line), determined by subtracting BDNF in media samples (measured by ELISA) collected after 12, 24, 48, 72, and 96 hours after the binding reaction from the total amount of bound BDNF bound to each type of SFNP. Data are presented as mean ± SEM at each time point from 3 separate experiments. No significant differences between time points were observed (ANOVA).

BDNF-Derivatized SFNPs Cross Through a BBB Model *In Vitro*

One challenge for effective therapies for central nervous system (CNS) dysfunction is the general inaccessibility of the brain to hydrophilic macromolecules because of the blood–brain barrier (BBB; Lombardo *et al*., 2020). After demonstrating the efficiency and stability of BDNF binding to SFNPs, we next determined whether BDNF derivatized SFNPs can be transported across the BBB and whether traversing the BBB affects their efficacy. For this, we used an established *in-vitro* BBB model of bovine brain microvascular endothelial cells (BBMVECs) as described in Duck *et al*. (2017).

We first determined that an intact barrier of BBMVECs was established by assessing the amount of fluorescein isothiocyanate (FITC) conjugated dextran (FITC-dextran, 70 kDa) that crossed a monolayer of BBMVECs grown on Transwell inserts into the basal chamber at different time points (15, 30, 60, 120, and 240 min) after adding 1 mg/ml FITC-Dextran to the apical chamber. FITC-Dextran readily crossed a Transwell insert without a BBMVEC barrier at time points from 15 to 240 min after addition with 60% of the FITC-dextran passing through the filter by 240 min (Figure 2.4). Significantly less FITC-dextran crossed into the basal chamber when a BBMVEC monolayer was grown on the Transwell filter at each time point (15-240 min, Figure 2.4). These data suggest that the BBMVEC monolayer established tight junctions and functioned as an *in-vitro* BBB model. BBMVEC monolayer integrity was consistently tested in subsequent experiments before and after the addition of SFNPs.

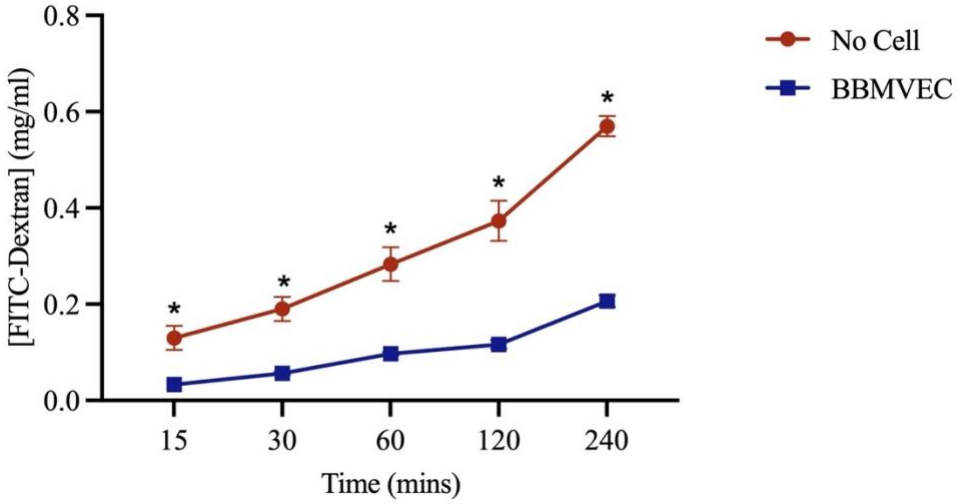

Figure 2.4: *FITC-Dextran Permeability Assay*. Permeability of 0.4 µm pore size transwell inserts with or without a monolayer of BBMVEC cells to 70 Da FITC-dextran was assessed by measuring fluorescence intensity in the basal chamber at 15, 30, 60, 120, and 240 min after addition of FITC-dextran to the apical chamber. Data are means ± SEM from three separate experiments performed in triplicate (n = 3), at $p \leq 0.05$ (ANOVA, Tukey's post-hoc). Asterisk denotes a statistical significance between inserts with a BBMVEC monolayer and inserts without a BBMVEC monolayer at each time points ($p \leq 0.05$).

We next determined the ability for passing through the *in-vitro* BBB for each type of fluorescently labeled SFNP (N150, C150, C750) the ability of the underivatized SFNP (control), BDNF-derivatized SFNPs, and BDNF-derivatized SFNPs loaded either not loaded or loaded with the C3 transferase therapeutic. To do this, we measured the amount of each labeled SFNP that remained in the apical chamber and the amount that passed into the basal chamber at each time point. For N150, the amount of fluorescently labeled underivatized SFNP remaining in the apical chamber was similar at 15 and 30 min with a significant reduction at 60, 120, and 240 min, compared to the initial amount of fluorescence. Similar decreases in apical chamber fluorescence intensity were seen with BDNF-derivatized N150 without or with imbibed C3 transferase (Figure 2.5). When

measuring SFNP passage into the basal chamber for N150, there was not an increase in basal chamber fluoresce during the first 15 min for underivatized N150, BDNF-derivatized N150, or C3 imbibed BDNF-derivatized N150, whereas all three N150 treatments had a steady increase in basal chamber fluorescence from 30 to 240 min (Figure 2.5). When we calculated the percentage of each type of N150 construct that was transported through *in-vitro* BBB model and the potential adsorption to the transwell insert, approximately 58.2% of the underivatized N150, 47% of the BDNF-derivatized N150, and 40.7% of C3 imbibed BDNF-derivatized N150 was transported across the barrier at 240 min. These results indicated that underivatized N150 can readily pass through BBB, but that BDNF derivatization and imbibing N150 SFNPs with C3 transferase each decrease the efficiency of crossing.

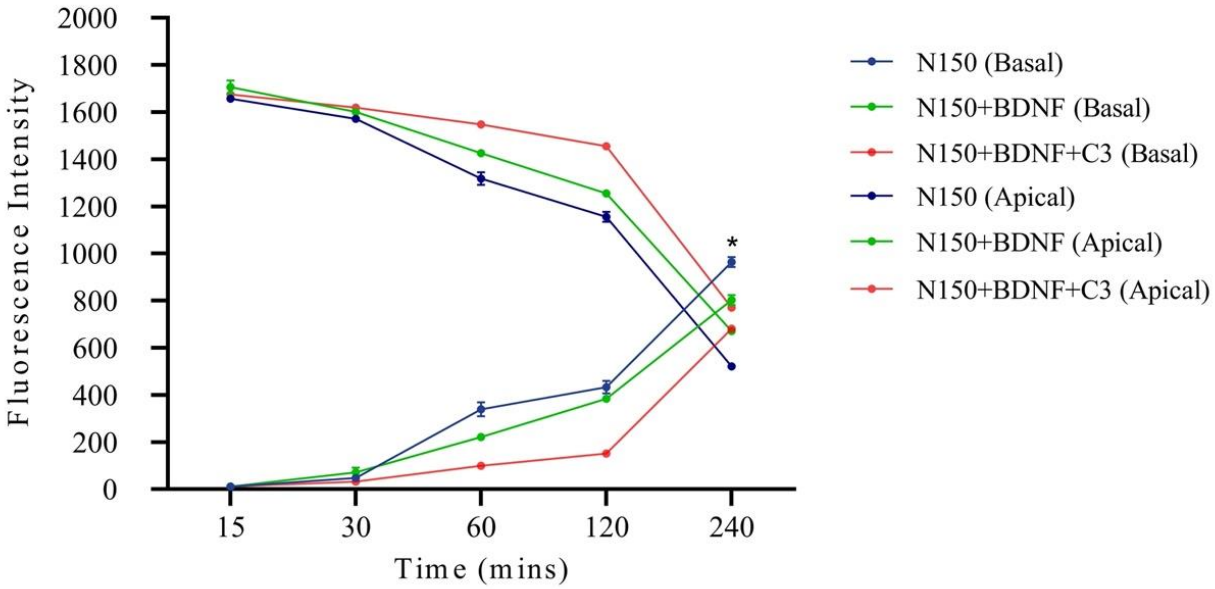

Figure 2.5: *Efficiency of N150 Transport Across BBMVEC Monolayers at Different Time Points*. Measurement of concentration by fluorescence intensity of underivatized N150 (dark blue line), BDNF-N150, and BDNF-N150 (green line) imbibed with C3 transferase (red line) in the apical and basal chambers of 0.4 µm transwell insert with intact monolayers of BBMVECs at different time points. Data shown are means ± SEM from three separate experiments performed in triplicate (n = 3), with asterisks indicating significant difference at $p \leq 0.05$ compared to the 15 min time point (ANOVA, Tukey's post-hoc).

Similar analyses for C150 SFNP constructs indicated that significantly less of each construct remained in the apical chamber and significantly more of each construct passed into the basal chamber at time points greater than 15 min (Figure 2.6). Specifically, approximately 69% of underivatized C150, 58% of BDNF-derivatized C150, and 42% of the C3 imbibed BDNF-derivatized C150 was able to cross through the *in-vitro* BBB model by 240 min. Thus, the efficiency of C150 SFNP constructs for crossing an *in-vitro* BBB was similar to that for N150

constructs with C3 imbibed BDNF-derivatized C150 showed the lowest crossing efficiency compared to the other two groups.

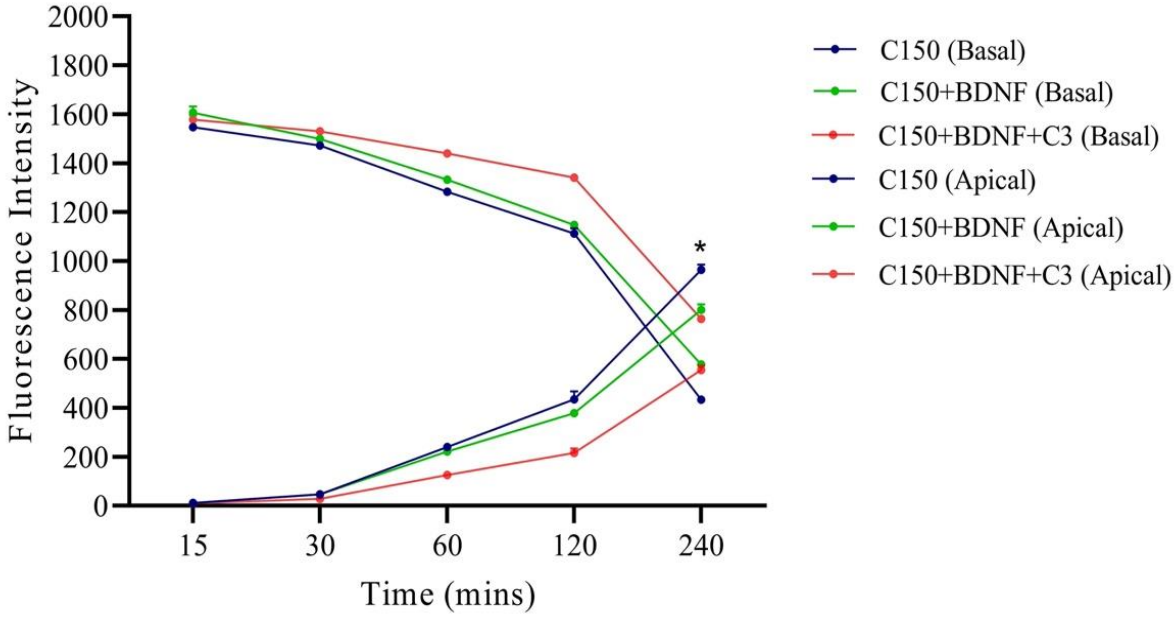

Figure 2.6: *Efficiency of C150 Transport Across BBMVEC Monolayers at Different Time Points*. Measurement of concentration by fluorescence intensity of underivatized C150 (dark blue line), BDNF-C150 (green line), and BDNF-C150 imbibed with C3 transferase (red line) in the apical and basal chambers of 0.4 μm transwell insert with intact monolayers of BBMVECs at different time points. Data shown are means ± SEM from three separate experiments performed in triplicate (n = 3), with asterisks indicating significant difference at $p \leq 0.05$ compared to the 15 min time point (ANOVA, Tukey's post-hoc).

Performing similar analyses on larger C750 SFNPs yielded somewhat different results compared to the smaller N150 and C150 SFNPs. Underivatized C750, BDNF-derivatized C750, and BDNF-C750 imbibed with C3 constructs showed a significant decrease in apical chamber fluorescence, but only after 240 min time point (Figure 2.7). Similarly, a significant increase in basal chamber fluorescence only occurred at 240 min for all three C750 constructs (Figure 2.7). The calculated BBB crossing efficiency indicated that approximately 33.2% of C750, 31% of

BDNF-C750, and 24% of the C3 imbibed BDNF-C750 were able to cross BBB at 240 min. Collectively, these data indicate that BDNF derivatization and imbibing SFNPs with larger molecule therapeutics like C3 transferase somewhat impede transport across biological barriers like the BBB, and that nanoparticle size has a greater influence on the ability of SFNPs to cross biological barriers with crossing being more difficult for larger size nanocarriers.

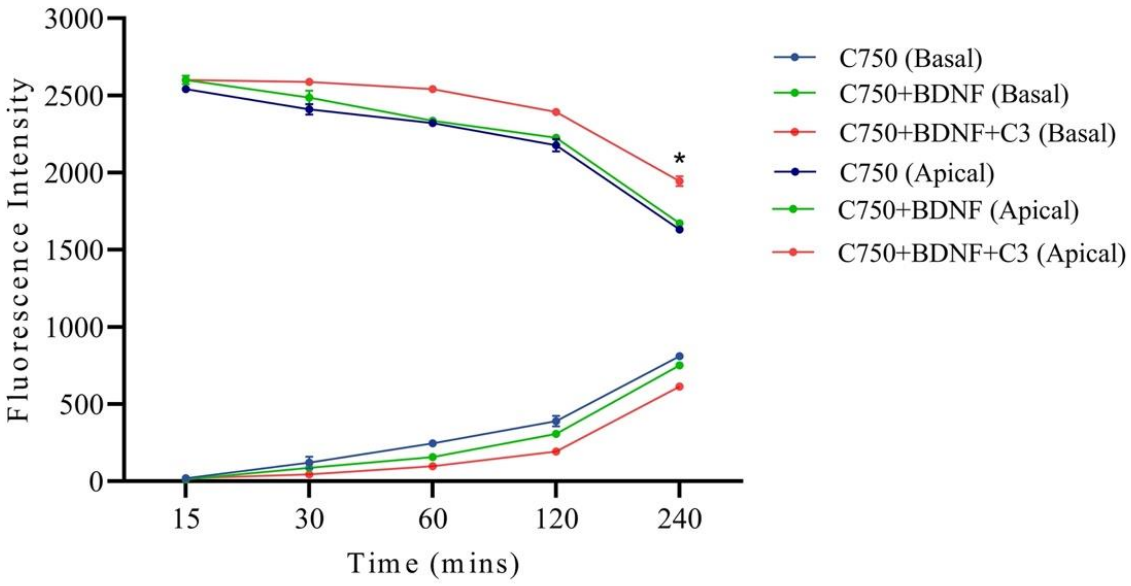

Figure 2.7: *Efficiency of C750 transport across BBMVEC monolayers at different time points*. Measurement of concentration by fluorescence intensity of underivatized C750 (dark blue line), BDNF-C750 (green line), and BDNF-C750 imbibed with C3 transferase (red line) in the apical (A) and basal chambers (B) of 0.4 µm transwell insert with intact monolayers of BBMVECs at different time points. Data shown are means ± SEM from three separate experiments performed in triplicate (n = 3), with asterisks indicating significant difference at $p \leq 0.05$ compared to the 15 min time point (ANOVA, Tukey's post-hoc).

DISCUSSION

Many studies *in vitro* and *in vivo* have been reported that use nanoparticles as drug-targeting agents for treatment (Afzal *et al*., 2022; Yetisgin *et al*., 2020). Nanoparticle drug

delivery systems have been shown to cross the BBB to deliver anticancer drugs to brain tumors (Mitusova *et al*., 2022). The use of magnetic nanoparticles has attracted significant attention for importance in biomedical applications (GhoshMitra *et al*., 2011). However, to our knowledge no attempts have been reported to use nano-based drug delivery systems to overcome BBB and target cortical neurons to treat SCI.

As a first step to assessing our proposed strategy for treating SCI with BDNF derivatized SFNPs to target CST neurons, we bound BDNF to SFNPs and assessed their ability to cross a BBB *in vitro*. We first checked the efficacy of BDNF binding to SFNPs and found that the binding is efficient of all 3 types of SFNPs, with 68.2-74.7% of applied BDNF binding to the SFNPs constructs. After 4 hours, BDNF binding to N150 and C150 SFNPs reached maximal level with 400 pg BDNF/ng SFNP of applied BDNF, while binding to the larger 750 nm SFNPs did not reach a maximum with up to 800 pg BDNF/ng SFNPs applied BDNF. The much larger surface area of the C750 compared to N150 or C150 (1,766.25 μm versus 70.65 μm) likely limits the amount of BDNF binding. A much larger amount of BDNF would need to be applied to reach maximal binding for 750 nm diameter SFNPs. BDNF binding efficiency to our SFNPs is similar to that found by Pilakka-Kanthikeel and colleagues (2013) who reported that approximately 70% BDNF binding to magnetic nanoparticles. In that work, binding was about 177 mg of BDNF bound per mg of magnetic nanoparticles in 3 hours, whereas binding in our SFNP system was 0.281-0.301 mg BDNF to mg SFNP. The lower binding ratio in our systems is not surprising as the system used by Pilakka-Kanthikeel *et al*. consisted of bare iron oxide nanoparticles of 4.6 nm in diameter, and binding was through electrostatic interaction with iron oxide, rather that covalent BDNF binding in our system, which consisted of much larger, lighter nanomaterial constructs.

We have also assessed the stability of BDNF to SFNP binding since the BDNF needs to be stably associated with the SFNPs to avoid off-target drug release. The binding was stable for all three SFNPs for as long as any subsequent assay in which they were used (96 hours), and is likely stable as long as particle integrity is preserved. This also prevents low therapeutic efficacy caused by off-target delivery. All those results suggest that BDNF had efficiently bound to SFNPs and BDNF is stabilized in its bound form.

We evaluated whether our SFNPs can traverse the BBB. For this, we used an established *in-vitro* model of BBB by using bovine brain microvascular endothelial cell (BBMVEC) culture. The validation of functional tightness of BBMVEC monolayers was tested by the efficacy by which a fluorescently labeled tracer (70 kDa FITC-dextran) crossed a BBMVEC monolayer. We observed minimal flux of 70-kDa FITC-dextran from 1 through 4 hours. This is similar to the permeability ratio reported previously with BBMVEC-based *in-vitro* BBB models (Gil and Lowe, 2008). Suggesting that the BBMVEC monolayer model of the BBB is similar in our experiments compared to other groups using the same model.

BDNF-derivatized SFNPs were able to efficiently cross this *in-vitro* model of the BBB. The calculated BBB crossing efficiency of our SFNPs systems with or without BDNF derivatization or loading with C3 transferase (the RhoA inhibitor we proposed using to facilitate extension of CST axons) was, 40.7% - 58.2% of the N150, 42% - 69% of C150, and 24% - 33.2% of C750 at 240 min. The addition of BDNF did not significantly alter the ability of SFNPs to cross BBMVEC monolayers. However, C750 SFNPs had a lower efficiency at crossing a BBMVEC monolayer than did either N150 or C150, indicating that the ability of molecules to cross BBB is size associated with fewer particles of larger size crossing the barrier. Intravenous injection of different sizes of gold nanoparticles in mice showed a 70% decrease in transport

across BBB for bigger particles (200 nm) compared to smaller ones (100 nm) (Sonavane *et al.*, 2008). Similarly, transport of different sizes of silica nanoparticles across an *in-vitro* rat BBB model showed that 30 nm particles readily transported across the membrane, 100 nm particles hardly passed through the membrane and 400 nm particles remained in the apical chamber (Hanada *et al.*, 2014). Our results showing that larger SFNPs do not cross a BBB model as easily as the smaller SFNP constructs follow the same tents as seen in these other studies. It is unlikely that the transport of any of the SFNP constructs across the BBMVEC monolayers was related to a decrease in monolayer integrity as post-experiment analysis showed that 70 kDa dextran transported continued to be inhibited by the barrier. Comparing the ability of differently sized SFNPs with the results for the efficacy of binding BDNF, it seems that larger SFNPs are able to bind more of a peptide for targeting, but fewer will cross biological barriers. Thus, there is a trade-off as to which size of SFNP would be better to use. The biological function of SFNPs that have crossed a barrier will need to be compared in future studies.

We interpret these results to indicate that the SFNP systems we constructed can efficiently cross the BBB as non-BDNF bound forms as well as derivatized with BDNF and C3 drugs. The poor permeability for both BDNF and C3 can be overcome so that can be further used as an agent to target specific receptors.

ACKNOWLEDGEMENTS

This work was supported by the Texas Woman's University (TWU) Department of Biology, the TWU Research Enhancement Program, and the Southeast Missouri State University Department of Physics and Engineering Physics.

REFERENCES

Afzal, O., Altamimi, A. S. A., Nadeem, M. S., Alzarea, S. I., Almalki, W. H., Tariq, A., Mubeen, B., Murtaza, B. N., Iftikhar, S., Riaz, N., & Kazmi, I. (2022). Nanoparticles in drug delivery: from history to therapeutic applications. *Nanomaterials*, *12*(24). https://doi.org/10.3390/nano12244494

Ahlawat, J., Guillama Barroso, G., Masoudi Asil, S., Alvarado, M., Armendariz, I., Bernal, J., Carabaza, X., Chavez, S., Cruz, P., Escalante, V., Estorga, S., Fernandez, D., Lozano, C., Marrufo, M., Ahmad, N., Negrete, S., Olvera, K., Parada, X., Portillo, B., & Narayan, M. (2020). Nanocarriers as potential drug delivery candidates for overcoming the blood–brain barrier: challenges and possibilities. *ACS Omega*, *5*(22), 12583-12595. https://doi.org/10.1021/acsomega.0c01592

Albanese, A., Tang, P. S., & Chan, W. C. (2012). The effect of nanoparticle size, shape, and surface chemistry on biological systems. *Annu Rev Biomed Eng*, *14*, 1-16. https://doi.org/10.1146/annurev-bioeng-071811-150124

Anselmo, A. C., & Mitragotri, S. (2016). Nanoparticles in the clinic. *Bioeng Transl Med*, *1*(1), 10-29. https://doi.org/10.1002/btm2.10003

Bellettato, C. M., & Scarpa, M. (2018). Possible strategies to cross the blood–brain barrier. *Ital J Pediatr*, *44*(Suppl 2), 131. https://doi.org/10.1186/s13052-018-0563-0

Biroudian, S., Abbasi, M., & Kiani, M. (2019). Theoretical and practical principles on nanoethics: A narrative review article. *Iran J Public Health*, *48*(10), 1760-1767.

Duck, K. A., Simpson, I. A., & Connor, J. R. (2017). Regulatory mechanisms for iron transport across the blood–brain barrier. *Biochem Biophys Res Commun*, *494*(1-2), 70-75. https://doi.org/10.1016/j.bbrc.2017.10.083

Ghosh, S., Ghoshmitra, S., Cai, T., Diercks, D. R., Mills, N. C., & Hynds, D. L. (2009). Alternating magnetic field controlled, multifunctional nano-reservoirs: Intracellular uptake and improved biocompatibility. *Nanoscale Res Lett*, *5*(1), 195-204. https://doi.org/10.1007/s11671-009-9465-9

GhoshMitra, S., Cai, T., Diercks, D., Hu, Z., Roberts, J., Dahiya, J., Mills, N., Hynds, D., & Ghosh, S. (2011). Evaluation of the biological effects of externally tunable, hydrogel encapsulated quantum dot nanospheres in *Escherichia coli*. *Polymers*, *3*(3), 1243-1254. https://doi.org/10.3390/polym3031243

Gil, E.S., Lowe, TL. (2008). Invention of polysaccharide-based nanoparticles for enhancing drug permeability across the blood–brain barrier. *Nanotechnology*, *2*, 379-381

Hanada, S., Fujioka, K., Inoue, Y., Kanaya, F., Manome, Y., & Yamamoto, K. (2014). Cell-based *in-vitro* blood–brain barrier model can rapidly evaluate nanoparticles' brain permeability in association with particle size and surface modification. *International Journal of Molecular Sciences*, *15*, 1812 - 1825.

Hurlbert, R. J., Hadley, M. N., Walters, B. C., Aarabi, B., Dhall, S. S., Gelb, D. E., Rozzelle, C. J., Ryken, T. C., & Theodore, N. (2013). Pharmacological therapy for acute spinal cord injury. *Neurosurgery*, *72 Suppl 2*, 93-105. https://doi.org/10.1227/NEU.0b013e31827765c6

Jiang, Y., Fay, J. M., Poon, C. D., Vinod, N., Zhao, Y., Bullock, K., Qin, S., Manickam, D. S., Yi, X., Banks, W. A., & Kabanov, A. V. (2018). Nanoformulation of brain-derived neurotrophic factor with target receptor-triggered-release in the central nervous system. *Adv Funct Mater*, *28*(6). https://doi.org/10.1002/adfm.201703982

Khan, I., Saeed, K., & Khan, I. (2019). Nanoparticles: Properties, applications and toxicities. *Arabian Journal of Chemistry*, *12*(7), 908-931. https://doi.org/https://doi.org/10.1016/j.arabjc.2017.05.011

Kim, J., Ahn, S. I., & Kim, Y. (2019). Nanotherapeutics engineered to cross the blood–brain barrier for advanced drug delivery to the central nervous system. *J Ind Eng Chem*, *73*, 8-18. https://doi.org/10.1016/j.jiec.2019.01.021

Lombardo, S. M., Schneider, M., Türeli, A. E., & Günday Türeli, N. (2020). Key for crossing the BBB with nanoparticles: the rational design. *Beilstein J Nanotechnol*, *11*, 866-883. https://doi.org/10.3762/bjnano.11.72

Martin, J. H. (2022). Chapter 22 - Neuroplasticity of spinal cord injury and repair. In A. Quartarone, M. F. Ghilardi, & F. Boller (Eds.), *Handbook of Clinical Neurology* (Vol. 184, pp. 317-330). Elsevier. https://doi.org/https://doi.org/10.1016/B978-0-12-819410-2.00017-5

Mitusova, K., Peltek, O. O., Karpov, T. E., Muslimov, A. R., Zyuzin, M. V., & Timin, A. S. (2022). Overcoming the blood–brain barrier for the therapy of malignant brain tumor: current status and prospects of drug delivery approaches. *J Nanobiotechnology*, *20*(1), 412. https://doi.org/10.1186/s12951-022-01610-7

National Spinal Cord Injury Statistical Center. (2020). Facts and figures at a glance. https://www.nscisc.uab.edu/Public/Facts%20and%20Figures%202020.pdf

Nguyen, K. T., Pham, M. N., Vo, T. V., Duan, W., Tran, P. H., & Tran, T. T. (2017). Strategies of engineering nanoparticles for treating neurodegenerative disorders. *Curr Drug Metab*, *18*(9), 786-797. https://doi.org/10.2174/1389200218666170125114751

Pandey, P. K., Sharma, A. K., & Gupta, U. (2015). Blood–brain barrier: An overview on strategies in drug delivery, realistic *in-vitro* modeling and *in vivo* live tracking. *Tissue Barriers*, *4*(1), e1129476. https://doi.org/10.1080/21688370.2015.1129476

Patra, J. K., Das, G., Fraceto, L. F., Campos, E. V. R., Rodriguez-Torres, M. d. P., Acosta-Torres, L. S., Diaz-Torres, L. A., Grillo, R., Swamy, M. K., Sharma, S., Habtemariam, S., & Shin, H.-S. (2018). Nano based drug delivery systems: recent developments and future prospects. *Journal of Nanobiotechnology*, *16*(1), 71. https://doi.org/10.1186/s12951-018-0392-8

Pilakka-Kanthikeel, S., Atluri, V. S., Sagar, V., Saxena, S. K., & Nair, M. (2013). Targeted brain derived neurotropic factors (BDNF) delivery across the blood–brain barrier for neuro-protection using magnetic nano carriers: an *in vitro* study. *PLoS One*, *8*(4), e62241. https://doi.org/10.1371/journal.pone.0062241

Sebastian S. (2019). Drug release kinetics and blood–brain barrier crossing efficacy of polymer encapsulated magnetic nanocarriers. *Texas Woman's University*.

Singh, R., & Lillard, J. W., Jr. (2009). Nanoparticle-based targeted drug delivery. *Exp Mol Pathol*, *86*(3), 215-223. https://doi.org/10.1016/j.yexmp.2008.12.004

Sonavane, G., Tomoda, K., & Makino, K. (2008). Biodistribution of colloidal gold nanoparticles after intravenous administration: effect of particle size. *Colloids Surf Biointerfaces*, *66*(2), 274-280. https://doi.org/10.1016/j.colsurfb.2008.07.004

Tashima, T. (2020). Smart strategies for therapeutic agent delivery into brain across the blood–brain barrier using receptor-mediated transcytosis. *Chem Pharm Bull (Tokyo)*, *68*(4), 316-325. https://doi.org/10.1248/cpb.c19-00854

Tyler, J. Y., Xu, X. M., & Cheng, J. X. (2013). Nanomedicine for treating spinal cord injury. *Nanoscale*, *5*(19), 8821-8836. https://doi.org/10.1039/c3nr00957b

Veettil R.A. (2017). Polyethylene glycol copolymer nanocarriers: biocompatibility, uptake and intracellular trafficking in neurons. *Texas Woman's University*.

Yetisgin, A. A., Cetinel, S., Zuvin, M., Kosar, A., & Kutlu, O. (2020). Therapeutic nanoparticles and their targeted delivery applications. *Molecules*, *25*(9). https://doi.org/10.3390/molecules25092193

Zhang, H., Liu, Y., Zhou, K., Wei, W., & Liu, Y. (2021). Restoring sensorimotor function through neuromodulation after spinal cord injury: Progress and remaining challenges. *Frontiers in Neuroscience*, *15*. https://doi.org/10.3389/fnins.2021.749465

Zhou, Y., Peng, Z., Seven, E. S., & Leblanc, R. M. (2018). Crossing the blood–brain barrier with nanoparticles. *J Control Release*, *270*, 290-303. https://doi.org/10.1016/j.jconrel.2017.12.015

CHAPTER III

CORTICOSPINAL TRACT NEURONS PREFERENTIALLY INTERNALIZE BRAIN-DERIVED NEUROTROPHIC FACTOR DERIVATIZED SURFACE FUNCTIONALIZED NANOPARTICLES

A Manuscript to be Submitted for Publication Consideration in

Molecular Pharmacology

Mengjie Cao, Santaneel Ghosh, Ph.D., DiAnna L. Hynds, Ph.D.

ABSTRACT

Current therapy to encourage axon regeneration is challenged by inefficient targeting of specific neurons due to the cellular diversity of the central nervous system (Ronn et al., 2000). Our previous studies using surface functionalized nanoparticles (SFNPs) have shown successful uptake by B35 and PC12 cell lines and cortical neurons. In this work, we used brain-derived neurotrophic factor (BDNF) attached to the SFNPs to study the uptake efficiency by the cells in a rat cortical neuron culture compared to glial cell uptake. BDNF derivatized SFNPs were taken up more efficiently by corticospinal tract (CST) neurons compared to astrocytes, microglia, and oligodendrocytes. Quantification using relative fluorescence intensities from representative images of cells exposed to BDNF derivatized SFNPs through amino or carboxyl group peptide bonding to 150 nm SFNPs (N150, C150) or carboxyl group bonded 750 nm SFNPs show that that CST neurons expressing high levels of the TrkB BDNF receptor incorporate BDNF-derivatized SFNPs better than other cortical cell types. As the uptake discrepancy was larger for BDNF-derivatized SFNPs versus non-derivatized SFNPs, we interpret these results to suggest that BDNF derivatization enhances SFNP internalization into CST neurons, making it an

improved system for encouraging axon regeneration from upper motor neurons for fractionated voluntary movement.

INTRODUCTION

Traumatic SCI leads to permanent loss of sensory and motor control (Papa et al., 2019). Functional recovery would best be accomplished by therapies that promoted the extension of ascending and descending axons across the lesion site and subsequent reconnection to appropriate targets (Tedeschi and Bradke, 2017). For recovery of voluntary movement, axon regeneration of corticospinal tract (CST) neurons located in layer V of the cortex in the precentral gyrus should be targeted (Hu et al., 2017). Unfortunately, delivery of therapeutics to CST neurons is limited by the inaccessibility of the brain to drugs administered through the circulatory system due in part to therapeutic dilution and effects in other neurons or glial cells (Mitusova et al., 2022). Nanomaterial-based drug delivery systems that can be tuned to target specific cells and to offer administration of therapy on demand would address these caveats.

There is still no effective clinical treatment yielding significant functional recovery in SCI patients (Watson et al., 2013). Current therapy for SCI is focused on preventing the secondary injury, stabilizing the spine, or controlling inflammation rather than encouraging axon regeneration (McNeil, 2005). The only drug approved for SCI treatment in the United States, methylprednisolone, shows tissue preservation in only 20% of the patients and does not promote axon regeneration that could lead to functional recovery (Chen et al., 1996). While some axon regeneration occurs in experimental SCI with other inhibitors, the only one that has undergone a clinical trial is a modified cell permeable version of the RhoA inhibitor C3 transferase (Persidsky et al., 2006). This trial failed, likely due to inefficient delivery of C3 to the CNS or primary

effects in glia rather than CST neurons. Nanomaterial-based drug delivery systems have been developed to be able to target specific cell types and limit off target effects.

We have developed PEG copolymer-based, fluorescent, surface-functionalized nanoparticles (SFNPs) system that can undergo a volumetric transition to release imbibed therapeutic and can be used for target delivery drugs in CNS. To begin to assess the latter ability, we choose to initially target CST neurons. CST neurons express the high affinity tropomyosin receptor kinase B (TrkB) brain derived neurotrophic factor (BDNF) receptor (Li *et al*., 2019; Jin, 2020) Our SFNP system that is surface-functionalized with amino or carboxyl functional groups has been derivatized by binding BDNF through peptide bonds. These BDNF-derivatized SFNPs should bind to TrkB and be internalized into TrkB expressing cells to delivery imbibed therapeutic like C3 transferase.

In this study, we assess the ability of BDNF C terminally bound to 150 nm SFNPs surface functionalized amino groups and N terminally bound to carboxyl group functionalized 150 or 750 nm SFNPs to be taken up by CST track neurons or glia in neonatal rat cortical neuron enriched cultures. Uptake is measured using fluorescently labeled SFNPs and differential immunolabeling with cell specific markers. Our results demonstrate that CST neurons take up all three types of BDNF derivatized SFNPs to a much greater extent than glia. This supports the ability to target specific cell types using SFNPs derivatized with peptides to preferentially bind specific receptors on target cells.

MATERIALS AND METHODS

Rat Cortical Cell Culture and Treatment

All animal procedures were performed under a protocol approved TWU Animal Care and Use Committee and conform to the National Research Council Guide for the Care and Use of

Laboratory Animals. Cultures of primary rat cortical neurons (RCNs) were established postnatal day 0-1 rats (Charles River Laboratories, Wilmington, MA). Pups were cold anesthetized and quickly decapitated. Cortices cleaned of meninges and large blood vessels were isolated from excised brains in Dulbecco's Modified Eagle's Medium: F12 Nutrient Mixture (DMEM-F12; ThermoFisher, Waltham, MA) containing 10% fetal bovine serum (FBS; Atlanta Biologicals, Atlanta, GA). Cortical tissue was minced and digested in 0.25% papain (Worthington Biochemical, Lakewood, NJ) and 100 U/ml DNase I (New England Biolabs, Ipswitch, MA) at 37°C, 5% CO_2 for 15 minutes, followed by trituration in fire-polished Pasteur pipettes. After centrifugation (200 × *g*, 5 min,) cells were resuspended and plated at 8,000 cells/well on poly-D-lysine (PDL; MP Biomedicals, Irvine, CA) coated 12 mm coverslips in 10 ml DMEM-F12 containing 10% FBS and supplemented with penicillin, streptomycin, and amphotericin B (Hyclone, Logan, UT) for 4 to 6 hours at 37°C. Media was changed to Neurobasal with B27 (ThermoFisher, Waltham, MA) and cultures were grown for 3-5 days with regular media changes (Sahu et al., 2019). Cultures were treated with 100 µg/ml (PEG concentration) non-derivatized SFNPs (C750/C150/N150) or BDNF-derivatized SFNPs at room temperature (25°C) for 4 hours and then transferred to 37°C. After 24 h, cell cultures were fixed in 4.0% paraformaldehyde for 30 min at room temperature, washed 2 X 5 min in phosphate buffered saline (PBS), and stored in PBS at 4.0°C until immunolabeled.

Immunocytochemistry

Non-specific binding sites for secondary antibodies were blocked using 0.1% Triton-X, 1.5% bovine serum albumin (BSA), and 1.5% preimmune secondary serum in PBS (blocking buffer) for 1 hour. After blocking, the cells were washed 2 X 5 min in PBS and incubated overnight at 4°C with primary antibodies, followed by washing with blocking buffer (3 X 5 min)

and incubation in secondary antibodies for 2 h at room temperature. All antibodies were purchased from AbCam (Boston, MA). CST neurons were labeled using rat anti-COUP-TF1 interacting protein 2 (Ctip2, 1:200) followed by AlexaFluor 647 conjugated donkey anti-rat secondary antibodies (1:500); microglia were labeled using rabbit anti-ionized calcium-binding adapter molecule-1(Iba1, 1:200) followed by AlexaFluor 647 conjugated goat anti-rabbit secondary antibody (1:500); astrocytes were labeled using rabbit anti-glial fibrillary acidic protein (GFAP) primary antibody (1:200) and oligodendrocytes labeled using primary antibody rabbit anti-oligo (1:200) followed by secondary donkey-anti-rabbit antibodies (1:500, AlexaFluor 647). For double staining, the cells were washed 3 X 5 min with PBS and the same immunolabeling protocol was repeated for the second antibody labeling. Cells were double labeled by using mouse anti-tropomyosin receptor kinase B (TrkB) primary antibody (1:250) and goat-anti-mouse secondary antibodies (1:500, AlexaFluor 488). After washing, coverslips were mounted on glass slides using Vectashield mounting medium with 4,6-diamidino-2-phenylindole (DAPI; Vector Laboratories, Newark, CA) and allowed to dry for 48 h. Coverslip edges were sealed with clear nail polish.

Microscopy and Analysis

Slides were observed and analyzed by capturing photomicrographs through a 60X objective on a Nikon AIR- A1 confocal system. Five images per condition were captured, one from each quadrant and one from the center of each coverslip in each experiment using 405 nm (for DAPI labeling), 488 nm (for AlexaFluor 488 labeling of TrkB), 561 nm (for rhodamine B labeled SFNPs), and 640 nm (for Alexafluor 647 labeling of different cell types) lasers and appropriate filter sets. Image capture conditions including exposure time, gain, and laser intensity were held constant in each experiment. The average fluorescence intensities from raw

data for Alexafluor 555 labeling (SFNP uptake) in different cell types (CST neurons, astrocytes, oligodendrocytes, and microglia), identified by cell type-specific immunolabeling were measured from identified regions of interests (ROIs) defined by outlining each measured cell. Obtained values were averaged for each culture in each experiment. Three cultures per condition were measured in three separated experiment (total n = 9). For display purposes, only brightness and contrast of images were adjusted, and the same adjustments were applied to all displayed images.

Statistical Analysis

GraphPad Prism 9 (Boston, MA) was used for all statistical analyses and data graphing. Data from three independent experiments were averaged and are expressed as means ± standard error of the mean (SEM). For experiments where three or more experimental groups were compared, statistical differences between groups were determined using one-way Analysis of Variance (ANOVA) and pairwise comparisons between were assessed using Tukey HSD post-hoc tests. For experiments were two treatment groups were compared to each other Student's t-tests were used to determine statistical differences. A level of significance of $p \leq 0.05$ was considered to be significant in all cases. Triplicate cultures were used for each treatment condition in each experiment and experiments were repeated three times (n = 9/condition).

RESULTS

To allow a comparison of the BDNF-derivatized SFNPs evaluated in this work to prior studies, we used primary cortical cultures to assess the ability of corticospinal tract (CST) neurons and other cell types to internalize BDNF-derivatized SFNPs. In these experiments, internalization of SFNPs was promoted for 4h at 25°C before returning cultures 37°C to ensure SFNP volumetric shrinking and imbibed therapeutic release occurred after SFNP internalization.

After treatment, the cultures were fixed and immunostained for cell-type specific markers—anti-Ctip2 for neurons, anti-GFAP for astrocytes, anti-Iba1 for microglia and anti-oligodendrocyte specific protein (oligo) for oligodendrocytes—followed by morphological and fluorescence intensity analyses. In confocal images (Figure 3.1) of cultures, cells in each panel were identified by DAPI labeling (first column, blue) with cell type identification being accomplished using cell type-specific markers (second column). All cell types identified by their markers had typical morphology for that cell type (Figure 3.1). Expression of TrkB BDNF receptors (column 3, green) and SFNP incorporation (column 4, red) in each of the immunolabeled cell types suggested that CST neurons expressed high levels of TrkB (minimally detected in other cell types) and had higher SFNP fluorescence intensity compared to astrocytes, microglia, and oligodendrocytes. These representative images from cells exposed to BDNF-N150 SFNPs suggest that CST neurons expressing high levels of the TrkB BDNF receptor incorporate BDNF-derivatized SFNPs better than other cortical cell types.

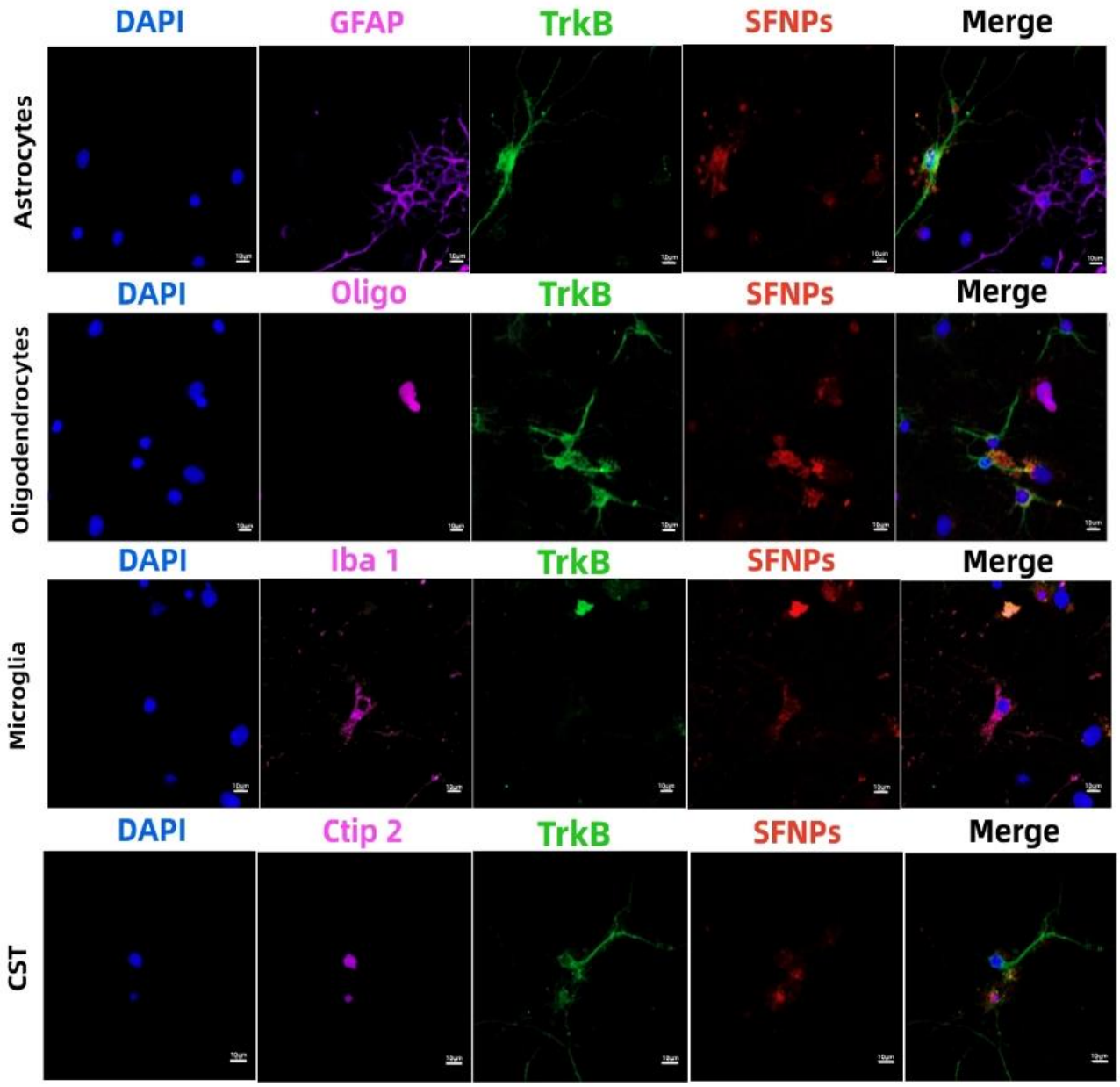

Figure 3.1: *Confocal images of BDNF-derivatized SFNPs in different cells in cortical culture.* Representative images of different cell types identified by their specific markers are indicated in row labels. Cells were identified by DAPI labeling (column 1, blue) and cell type by cell specific markers (column 2). TrkB expression (column 3, green) and SFNP incorporation (column 4, red) demonstrate that high levels of TrkB occur mainly on CST neurons, which also seem to internalize more BDNF-derivatized SFNPs (N150 constructs in these images). Merged images are shown in column 5 and scale bars in each image are 10 μm.

We used average fluorescence intensity measurements in identified ROIs (individual cells) to quantify uptake of each type of BDNF-derivatized SFNP constructs into different cell types (CST neurons, oligodendrocytes, astrocytes, and microglia). All cell types examined showed uptake of BDNF-derivatized SFNPs 24h after exposure (Figures 3.2, 3.3, and 3.4). Previous studies have shown that in a mixed primary culture, our nanoparticles (without modified by BDNF) are internalized by neurons 1.5- to 3-fold more than microglia and astrocytes (Veettil, 2017). However, on testing the uptake on the cell types individually, we found the fluorescence intensity was much higher in CST neurons compared to astrocytes, microglia, and oligodendrocytes across all types of SFNPs. In our study, BDNF-N150 showed a 2.5-fold increase in uptake of BDNF-derivatized N150 compared to astrocytes or microglia and a 5-fold increase compared to oligodendrocytes (Figure 3.2). In addition, the uptake of BDNF-N150 was higher in astrocytes and microglia compared to oligodendrocytes (Figure 3.2).

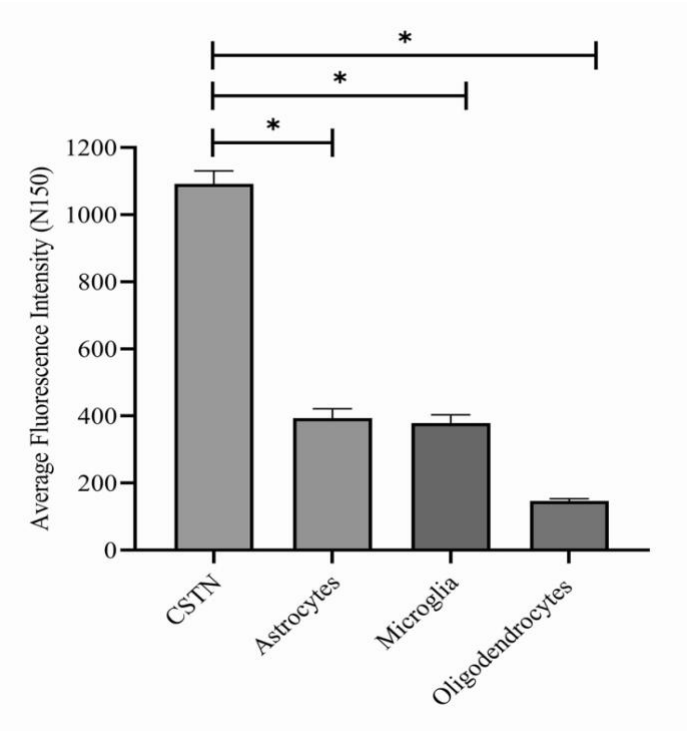

Figure 3.2: *Quantification of BDNF-derivatized N150 in cortical culture.* Primary rat cortical cultures were exposed to 100 µg/mL concentrations of SFNC-N150 for 24 hours. The mean fluorescence intensity of BDNF-N150 in each cell type was measured from defined regions of interest (ROIs, individual cells). Data shown are means ± SEM from three cultures/condition in three separate experiments (n = 9). Asterisks indicate statistically significant differences between the ROI mean intensity of BDNF-N150 in different cell types, at $p \leq 0.05$ (ANOVA and Tukey HSD post-hoc).

For BDNF-derivatized C150 there was a 3-fold increase in SFNP uptake in CST neurons compared to astrocytes or microglia and a 5-fold increase compared to oligodendrocytes (Figure 3.3). The mean fluorescence intensity of BDNF-C150 was also higher in astrocytes and microglia compared to oligodendrocytes (Figure 3.3).

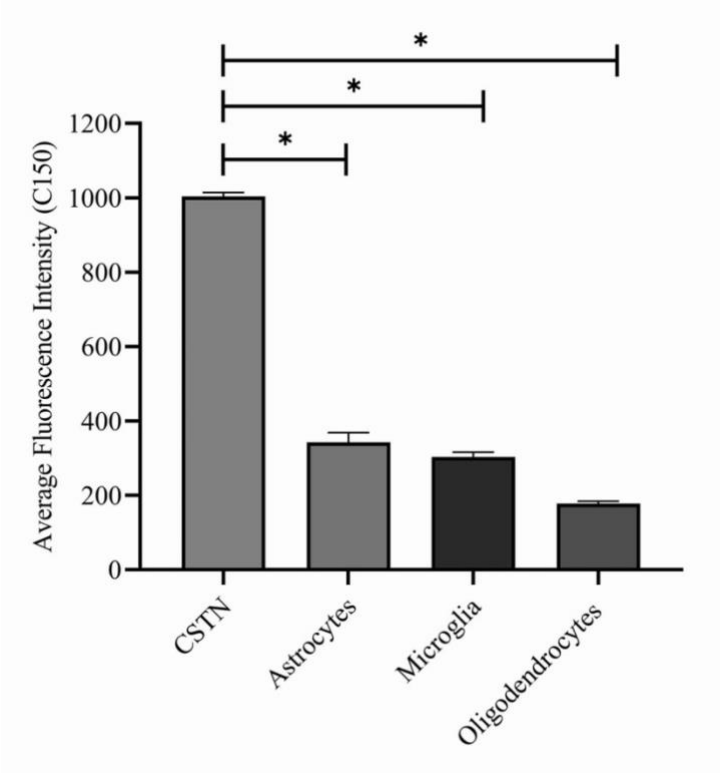

Figure 3.3: *Quantification of BDNF-derivatized C150 in cortical culture.* Primary rat cortical cultures were exposed to 100 μg/ml BDNF-C150 for 24 hours. The mean fluorescence intensity of BDNF-C150 in each cell type was measured from defined regions of interest (ROIs, individual cells). Data shown are means ± SEM from three cultures/condition in three separate experiments (n = 9). Asterisks indicate statistically significant differences between the ROI mean intensity of BDNF-N150 in different cell types, at $p \leq 0.05$ (ANOVA and Tukey HSD post-hoc).

Similar results were seen with BDNF-derivatized C750, which showed uptake by CST neurons that was three times higher fluorescence intensity compared to either astrocytes or microglia, and six times more compared to oligodendrocytes (Figure 3.4). Additionally, the mean fluorescence intensity for BDNF-C750 was higher in astrocytes and microglia compared to oligodendrocytes (Figure 3.4). Moreover, BDNF-C750 has a greater mean fluorescence level than BDNF-N150 or BDNF-C150 (compare Figures 3.2 and 3.3 to Figure 3.4). These results support the idea that SFNPs modified with targeting molecules (BDNF) are internalized to a

greater extent in CST neurons, compared to other cell types and this incorporation is higher than was seen with underivatized SFNPs in previous experiments.

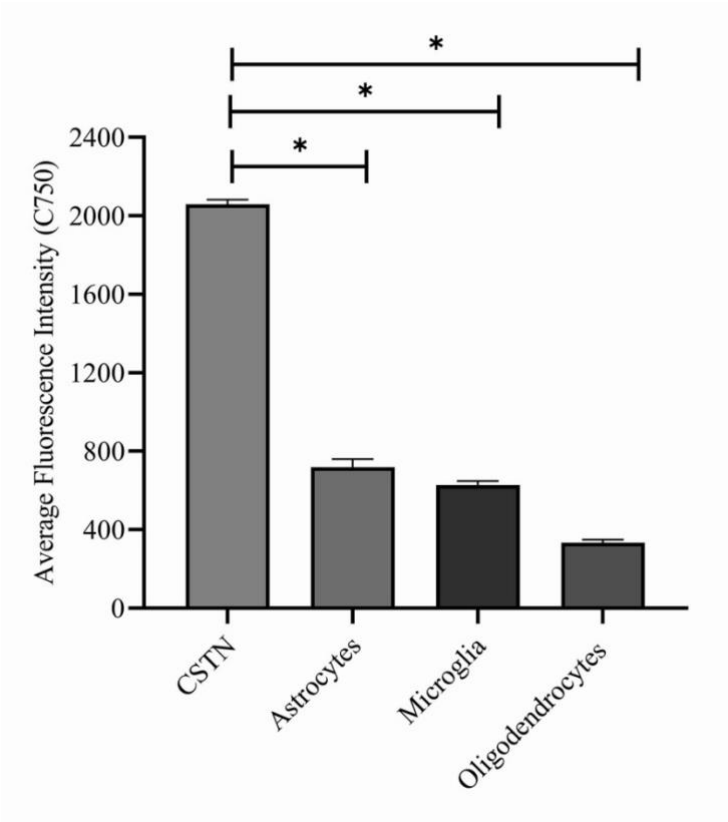

Figure 3.4: *Quantification of BDNF-derivatized C750 in cortical culture.* Primary rat cortical cultures were exposed to 100 µg/mL concentrations of BDNF-C750 for 24 hours. The fluorescence intensity of BDNF-C750 in each cell type was measured from defined regions of interest (ROIs, individual cells). Data shown are means ± SEM from three cultures/condition in three separate experiments (n = 9). Asterisks indicate statistically significant differences between the ROI mean intensity of BDNF-N150 in different cell types, at $p \leq 0.05$ (ANOVA and Tukey HSD post-hoc).

Our current results compared to previous experiments using non-derivatized SFNPs indicate that BDNF-derivatization leads to more SFNP internalization based on the more robust CST neuron uptake compared to uptake in non-neuronal cells. This could be a result of high level of expression of TrkB in CST neurons, which would encourage receptor-mediated

endocytosis of BDNF-SFNPs. To address whether this could be the case, we measured the amount of uptake in CST neurons of BDNF-SFNPs (N150, C150, C750) compared to the uptake of non-derivatized SFNPs. Confocal images of Ctip2 immunoreactive CST neurons (Figure 3.5, second column) exposed to BDNF-N150 (top row) or non-derivatized N150 (bottom row) appeared to have higher levels of SFNPs uptake based on rhodamine fluorescence (Figure 3.5, third column, red) with merged images showing cell nuclei labeled with DAPI (Figure 3.5, right column).

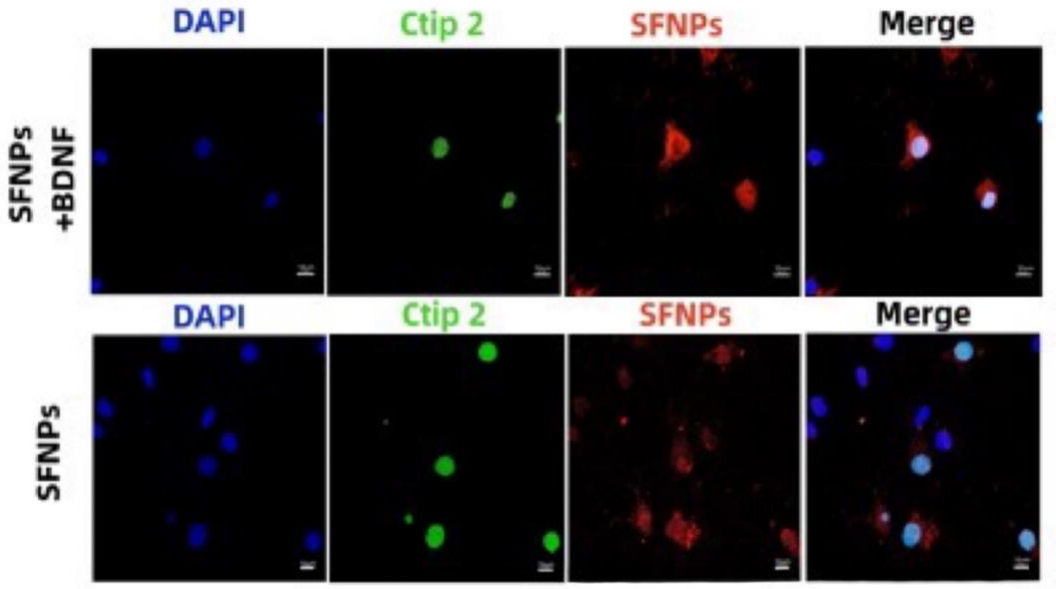

Figure 3.5: *BDNF-SFNPs are internalized at higher concentrations than non-derivatized SFNPs in CST neurons.* Primary rat cortical cultures were exposed to 100 µg/ml underivatized (top row) or BDNF-derivatized SFNPs (bottom row) for 24 hours and SFNP uptake into CST neurons (Ctip2 positive, second column) was assessed by SFNP fluorescence (rhodamine labeled N150 SFNPs, third column). The total number of cells in each field was identified by DAPI nuclear labeling (blue in first column). BDNF-N150 uptake showed higher fluorescence compared to underivatized N150. Scale bars in each panel are 10 µm.

Quantification of the average fluorescence intensity in individual CST neurons (ROIs) showed that neurons treated with BDNF-derivatized SFNPs (N150, C150, C750) had about 1.5-fold higher fluorescence for BDNF-derivatized SFNPs compared to the underivatized SFNPs for each type of SFNP (N150, C150, C750, Figure 3.6).

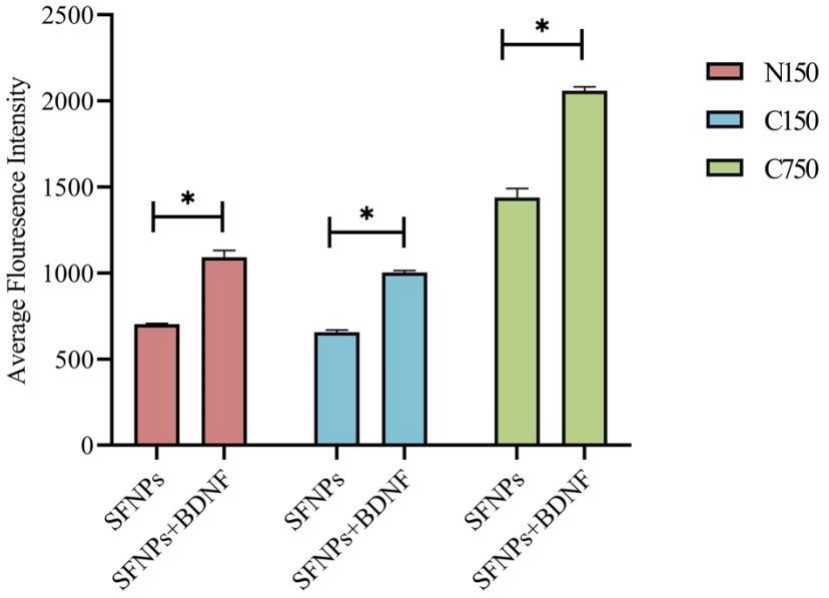

Figure 3.6: *Quantification of fluorescence intensity in CST neurons treated with underivatized or BDNF-derivatized SFNPs*. Primary rat cortical cultures were exposed to 100 μg/ml N150 (red bars), C150 (blue bars), or C750 (green bars) either not derivatized (left bar in each pair) or derivatize with BDNF (right bar in each pair) for 24 hours show that BDNF- derivatization increased SFNPs uptake by approximately 1.5 fold for each type of SFNP. Data shown are means ± SEM from ROIs (individual CST neurons) from three separate experiments with three culture per each condition in each experiment (n = 9/condition). Asterisks indicate statistically significant differences at $p \leq 0.05$ between the ROI mean intensity of underivatized SFNCs compared to BDNF derivatized SFNPs of the same type (Student's t-test).

DISCUSSION

Major challenges to delivering effective therapies to the CNS to treat neurological conditions like SCI exist even if efficacious therapeutics are available (Wen et al., 2015). These include issues of off-target effects due to cellular diversity, delivery of effective concentrations due to solubility in the bloodstream and filtering in the liver and kidney, and limited delivery of water-soluble therapeutics due to the impermeability of the BBB to these substances (Kim et al., 2019). From previous work, techniques for delivering therapeutic agents to the SCI include using silicone reservoirs, polymeric delivery systems, and osmotic pumps (Begley, 2004). However, these systems still require a large amount of each drug and they do not provide for a more controlled delivery profile that targets specific cells (Sahoo & Labhasetwar, 2003). Furthermore, device materials that contact patient tissues should be medical grade with acceptable physicochemical characteristics and biocompatibility profiles (Singh & Lillard, 2009). Selective delivery of pharmaceutical agents to target sites in the body remains a major challenge (Wen et al., 2015). Peptides have recently been reported that may provide target delivery to the damaged neurons, and enhanced performance for the potential therapy of promoting axon regeneration after SCI (Georgieva et al., 2012). Peptides specifically interact with different types of biological systems and cells, which allows them to be applied in a multitude of scenarios for effective results (Jeong et al., 2018). A simple approach to overcoming the problems of the current peptide-based delivery systems is to combine them with nanoparticles (Jeong et al., 2018). The peptide-bound nanoparticles can be served as targeting agents that selectively deliver the drugs to the target neurons while reducing off-target toxicity (Liu et al., 2021).

We have hypothesized that these BDNF derivatized nanoparticles bound to nanoparticles surface functionalized with –COOH and $–NH_2$ groups would be internalized to a greater extent

by neurons, especially CST neurons, compared to the other cells in a mixed cortical culture. To investigate the efficiency of SFNPs taken up by different cell types, we have used mixed cortical cells extracted and cultured from neonatal rat brain (P1) and treated with underivatized SFNPs or BDNF derivatized SFNPs. The mixed cortical cultures are immunolabeled according to different types of cells: CST neurons, astrocytes, oligodendrocytes, and microglia. It is challenging to deliver drugs using nanoparticles specifically to neurons during SCI. It is a possible that nanoparticles could be internalized preferably by glial cells because astrocytes and microglia possess phagocytic properties. Both confocal images and measurements of average fluorescence intensity of SFNPs in different cell types, however, show that this is not the case. This gives us a better understanding on how to optimize SFNPs for *in vivo* targeted delivery to enhance axon regeneration following SCI.

According to results from representative images and quantification of fluorescence intensity of SFNPs, CST neurons uptake more SFNPs compared to astrocytes, microglia, and oligodendrocytes across all types of SFNPs. Also, CST neurons expressing high levels of TrkB, the high affinity BDNF receptor and incorporate BDNF-derivatized SFNPs better than other cortical cell types. To further understand the uptake of SFNPs by different types of cortical cells, our experiments compare treatment with and without BDNF modification. The results show that CST neurons exposed to BDNF-SFNPs (N150, C150, C750) have 1.5-fold higher levels of SFNP uptake than non BDNF-derivatized SFNPs. Further, BDNF-C750 SFNPs have a greater mean fluorescence intensity level than BDNF-N150 or BDNF-C150, This might be expected due to the larger size of BDNF-C750. However, the discrepancy was not as large as would be predicted based on SFNP volume, which may indicate that C750 has similar uptake efficiency compared with the other two types of SFNPs. Together, these results suggest that BDNF targets uptake by

TrkB expressing CST neurons better than any glial cell type and also better than SFNPs without BDNF derivatization.

Our current uptake results compared to previous experiments, using of BDNF-derivatization leads to more SFNP internalization based on the more robust CST neurons uptake compared to uptake in non-neuronal cells. This is because expression of TrkB in CST neurons, which would encourage receptor-mediated endocytosis of BDNF-SFNPs (Glueckert et al., 2015). The potential mechanism of uptake might be because the receptor mediated endocytosis and alternatives like macropinocytosis (Gilleron et al., 2013). Furthermore, according to the results, CST neurons expressed higher levels of TrkB compared to astrocytes, microglia, or oligodendrocytes. This can explain the better uptake in CST neurons even though astrocytes and oligodendrocytes express TrkB.

All above support the hypothesis that SFNPs modified with targeting molecules (BDNF) are internalized to a greater extent in CST neurons, compared to other cell types and this incorporation is higher than that seen with underivatized SFNPs in experiments reported previously (Veettil, 2017). Together, the nano-based drug delivery system derivatized with BDNF allow the poor permeable drug passing though BBB as well as targeting CST neurons. The next challenge is check if C3 be able to release inside the neurons and promote neurites outgrowth.

ACKNOWLEDGEMENTS

This work was supported by the Texas Woman's University (TWU) Department of Biology, the TWU Research Enhancement Program, and the Southeast Missouri State University Department of Physics and Engineering Physics.

REFERENCES

Begley DJ (2004) Delivery of therapeutic agents to the central nervous system: the problems and the possibilities. *Pharmacology & Therapeutics* **104**(1):29-45.

Chen TC, Mackic JB, McComb J, Giannotta SL, Weiss MH, and Zlokovic BV (1996) Cellular uptake and transport of methylprednisolone at the blood–brain barrier. *Neurosurgery* **38**(2): 348-354.

Georgieva JV, Brinkhuis RP, Stojanov K, Weijers, H. Zuilhof FP, Rutjes D, Hoekstra JC, Hest van, and Zuhorn IS (2012) Peptide-mediated blood–brain barrier transport of polymersomes. *Angew Chem Int Ed Engl* **51**(33): 8339-8342.

Gilleron J, Querbes W, Zeigerer A, Borodovsky A, Marsico G, Schubert U, Manygoats K, Seifert S. Andree C, Stöter M, Epstein-Barash H, Zhang L, Koteliansky V, Fitzgerald K, Fava E, Bickle M, Kalaidzidis Y, Akinc A, Maier M, and Zerial M (2013) Image-based analysis of lipid nanoparticle-mediated siRNA delivery, intracellular trafficking and endosomal escape. *Nat Biotechnol* **31**(7): 638-646.

Glueckert R, Pritz CO, Roy S, Dudas J, and Schrott-Fischer A (2015) Nanoparticle mediated drug delivery of rolipram to tyrosine kinase B positive cells in the inner ear with targeting peptides and agonistic antibodies. *Front Aging Neurosci* **7**: 71.

Hu J, Zhang G, Rodemer W, Jin LQ, Shifman M, and Selzer ME (2017) The role of RhoA in retrograde neuronal death and axon regeneration after spinal cord injury. *Neurobiol Dis* **98:** 25-35.

Jeong WJ, Bu J, Kubiatowicz LJ, Chen SS, Kim Y, and Hong S (2018) Peptide-nanoparticle conjugates: a next generation of diagnostic and therapeutic platforms. *Nano Converg* **5**(1):38.

Jin W (2020) Regulation of BDNF-TrkB Signaling and Potential Therapeutic Strategies for Parkinson's Disease. *J Clin Med* **9**(1):257.

Kim J, Ahn SI, Kim Y (2019) Nanotherapeutics engineered to cross the blood–brain barrier for advanced drug delivery to the central nervous system. *J Ind Eng Chem*. **73:**8-18.

Li X, Wu Q, Xie C, Wang C, Wang Q, Dong C, Fang L, Ding J, and Wang T (2019) Blocking of BDNF-TrkB signaling inhibits the promotion effect of neurological function recovery after treadmill training in rats with spinal cord injury. *Spinal Cord* **57**(1): 65-74.

Liu M, Fang X, Yang Y, and Wang C (2021) Peptide-enabled targeted delivery systems for therapeutic applications. *Front Bioeng Biotechnol* **9**:701504.

McNeil SE (2005) Nanotechnology for the biologist. *J Leukoc Biol **78***(3): 585-594.

Mitusova K, Peltek OO, Karpov TE, Muslimov AR, Zyuzin MV, and Timin AS (2022) Overcoming the blood–brain barrier for the therapy of malignant brain tumor: current status and prospects of drug delivery approaches. *J Nanobiotechnology* **20**(1): 412.

Papa S, Rossi F, Vismara I, Forloni G, and Veglianese P (2019) Nanovector-mediated drug delivery in spinal cord injury: A multitarget approach. *ACS Chem Neurosci* **10**(3): 1173-1182.

Persidsky Y, Heilman D, Haorah J, Zelivyanskaya M, Persidsky R, Weber GA, Shimokawa H, Kaibuchi K, and Ikezu T (2006) Rho-mediated regulation of tight junctions during monocyte migration across the blood–brain barrier in HIV-1 encephalitis (HIVE). *Blood* **107**(12): 4770-4780.

Ronn LC, Doherty P, Holm A, Berezin V, and Bock E (2000) Neurite outgrowth induced by a synthetic peptide ligand of neural cell adhesion molecule requires fibroblast growth factor receptor activation. *J Neurochem* **75**(2): 665-671.

Sahoo SK and Labhasetwar V (2003) Nanotech approaches to drug delivery and imaging. *Drug Discov Today* **8**(24):1112-1120.

Sahu MP, Nikkila O, Lagas S, Kolehmainen S, and Castren E (2019) Culturing primary neurons from rat hippocampus and cortex. *Neuronal Signal* **3**(2)

Singh R and Lillard JW, J (2009) Nanoparticle-based targeted drug delivery. *Exp Mol Pathol* **86**(3):215-223.

Tedeschi A and Bradke F (2017) Spatial and temporal arrangement of neuronal intrinsic and extrinsic mechanisms controlling axon regeneration. *Curr Opin Neurobiol* **42:** 118-127.

Veettil RA (2017) Polyethylene glycol copolymer nanocarriers: biocompatibility, uptake and intracellular trafficking in neurons. *Texas Woman's University*.

Watson PM, Paterson JC, Thom G, Ginman U, Lundquist S, and Webster CI (2013) Modelling the endothelial blood-CNS barriers: a method for the production of robust *in-vitro* models of the rat blood–brain barrier and blood-spinal cord barrier. *BMC Neurosci* **14**:59.

Wen H, Jung H, and Li X (2015) Drug delivery approaches in addressing clinical pharmacology-related issues: Opportunities and challenges. *AAPS J* **17**(6):1327-1340.

CHAPTER IV

OUTGROWTH OF NEURITES FROM CORTICAL NEURONS IS INCREASED FROM EXPOSURE TO SURFACE FUNCTIONALIZED NANOPARTICLES IMBIBED WITH C3 TRANSFERASE

A Manuscript to be Submitted for Publication Consideration in

Biomaterials Science

Mengjie Cao, Santaneel Ghosh, Ph.D., DiAnna L. Hynds, Ph.D.

ABSTRACT

Central neurons display a very limited capacity to regrow their axons after injury, successful strategies to improve regeneration are much sought after.[1,2] Nanoparticle drug delivery systems, such as those we have designed and made, provide an excellent means for minimally invasive treatments that can be specifically targeted to particular neurons and remotely activated to release therapeutics.[3] The drugs that facilitate axon growth, C3 transferase is largely limited by the poor permeability of both barrier and target neurons.[4,5] To overcome this issue, C3 incorporated within the PEG shell of the nanoparticles, and further attaching BDNF to the PEG coat will cause them to bind to the corticospinal tract neurons that express TrkB receptor, which will internalize C3 along with SFNPs.[6] Subsequently, heating or exposure to an oscillating magnetic field causes the internalized SFNPs to shrink, simultaneously expelling a drug (C3) that will encourage axon growth.[7] Both confocal images and quantification results suggest that all three types of SFNP (N150, C150, C750), treat with BDNF-SFNPs imbibed with C3 had the greatest increase in neurite outgrowth and elongation than treatment with C3 itself, underivatized SFNP, and BDNF-SFNP. Thus, this study reports an attractive nano-based drug delivery system with great potential to deliver therapeutics to precise locations within the nervous system for axonal outgrowth and guidance.

INTRODUCTION

Axons are cellular processes that extend from neuron cell bodies during development or regeneration and are guided by extracellular cues.[8,9] However, after damage mature axons do not regrow and reestablish contact with their correct targets.[10,11] If this growth could be manipulated externally, it may be possible to develop therapies to treat maladies like spinal cord injury (SCI) and Alzheimer's disease.[12,13] While many chemical substances do direct axon growth, their clinical application is limited because of difficulties in delivering these substances to the CNS.[14,15] One solution to this dilemma mentioned above is to use nano-based drug delivery systems that cross the blood–brain barrier (BBB) and can be constructed to target damaged neurons.[16,17]

The molecular mechanisms directing neurite outgrowth and regeneration involve both stimulatory and inhibitory influences.[18,19] Previous studies have shown that targeting guanosine triphosphatases (GTPases) of the Rho family is an important interventional strategy to circumvent the limited ability of central axons to regenerate after CNS trauma.[20-22] RhoA is an attractive therapeutic target in SCI.[21] RhoA is activated by axon regeneration inhibitors that are increased following SCI, and its activation causes axon and growth cone retraction through a variety of mechanisms [23-25]. Inhibition of RhoA signaling, including treatment with the direct RhoA inhibitor C3 transferase results in accelerated regeneration and enhanced functional recovery after experimental SCI.[26-29] C3 transferase blocks Rho by locking Rho in an inactive state and keeping it bound to the Rho dissociation inhibitor.[30,31] Treatment using C3 transferase, enhances CST neuron axonal regeneration and improves functional recovery following incomplete transection of the spinal cord in rats.[32-34] However, the lack of uptake and

translocation domains of C3 transferase cause poor permeability in crossing the BBB and neuronal plasma membranes.[31,35]

To reduce the amount of therapeutic and to provide the maximal inhibition of RhoA signaling, loading C3 transferase into a nano-based drug delivery system may provide a viable therapeutic strategy. To address these concerns, our surface-functionalized nanoparticles (SFNPs) consisting of polyethylene glycol (PEG) copolymer coats modified with amino or carboxyl functional groups have a large surface that is able to efficiently bind, absorb and/or carry other compounds such as drugs, probes, and proteins.

The amine and carboxyl groups on the surface of nanoparticles would attach with BDNF which can bind to TrkB receptor from CST neurons. Also, the large surface of SFNPs allowed larger doses of drugs loaded which comparable efficacy as free drugs showed poor biodistribution to the brain. Rat cortical cultures either by untreated (baseline control), treated with SFNPs not imbibed with C3, BDNF derivatized SFNPs, or C3 loaded BDNF-SFNPs. Drug release will be initiated by increasing the temperature briefly to 37°C. This increase in temperature will shrink the nanoparticles and cause the release of the embedded drug. Neurite outgrowth of corticospinal tract neurons was measured and quantified. The process of outgrowth from neurons will involve the assessment of several measured of outgrowth, including neurite initiation (percent of neurite-bearing cells, number of neurites/cell), and neurite elongation (total neurite length/cell).

MATERIALS AND METHODS

C3 Transferase-Imbibed Drug Delivery System

Fluorescent nanoparticles were synthesized by conjugating PEGEEMA-co-PEGMEMA with methacryloxyethyl thiocarbamoyl rhodamine B fluorescent monomers (Polysciences, Inc.,

emission: 570 nm). For the synthesis, 1 mg of fluorescent monomer was added per 6 gm of copolymer content. Any unreacted fluorescent monomer was removed by dialysis for 7 days. The fluorescent nanoparticles were of 3 types, having 2 different surface functional structures: –COOH and $–NH_2$ and being two different sizes 150 nm and 750 nm.

SFNPs were derivatized with a bioactive BDNF peptide using peptide bonding with carboxyl –COOH surface groups of nanoparticles of 150 nm (C150) or 750 nm (C750) diameter or with amine $–NH_2$ surface groups of nanoparticles of 150 nm diameter. Different ratios of SFNPs to BDNF (1:0.01, 1:0.02, 1:0.03, 1:0.04, and 1:0.05 µg PEG to pg BDNF) were mixed in 1X Tris EDTA (TE; 10 mM Tris-HCl, pH 8; 1 mM EDTA) buffer and incubated on a shaker (100 rpm) at room temperature for 4 hours. BDNF-derivatized SFNPs were collected by centrifugation for 30 min at 400 × *g*. The pellet was washed twice with deionized (DI) water and resuspended to a concentration of 4 µg PEG/ml in 1X TE buffer. BDNF-SFNPs were stored at 2-8°C until further use.

To imbibe C3 transferase into the drug delivery system, an aqueous solution of 2 µg/ml C3 transferase (Cytoskeleton, Denver, CO) was added to 100 µg PEG/ml BDNF-derivatized SFNPs. The solution was stirred for 8 h at 25°C. Drug-loaded SFNPs were collected by centrifugation at 400 × *g* for 30 min. These nanocarriers were designed to exhibit a volumetric transition at a temperature slight than the physiological temperatures (37°C) that releases drug from the SFNP.

Rat Cortical Cell Culture

Rat cortical cells were isolated from post-natal day 0-1 rats **(**Charles River Laboratories, Wilmington, MA**)**. The Pups were anesthetized on ice for 20 min and decapitated with the small surgical scissors. The skin was cut along the midline towards the nose using curved forceps. The

skull was cut laterally starting from foramen magnum using sterile scissors and pulled back using forceps. The two halves of the separated skull were peeled back and the whole brain was removed from the head cavity using the curved forceps. The brain was scooped using a sterile spatula to a sterile 35 mm petri dish in DMEM-F12 containing 10% fetal bovine serum (FBS; Atlanta Biologicals, GA). Under a dissection microscope, cerebral cortices were dissected out using a sterile scalpel and the blood arteries were removed using fine-tipped forceps. The cleaned cortices were transferred to a new sterile petri dish containing serum-free DMEM-F12 media. The cortical tissue diced into fine pieces of approximately 1 mm length using a sterile scalpels and transferred to a 15 ml conical tube. Mix 0.25% papain (Worthington Biochemical Corp.) and 100 U/mL DNase I were used to dissociate the diced cortices for 10 min at 37 C. To inactivate papain, 1 ml of FBS was added. The tissue was gently triturated with the fire-polished Pasteur pipettes until the solution homogenous (~15-20 times) and then centrifuged for 5 min at 200 × g. The supernatant was aspirated and discarded. Resuspend the cells in 10 ml DMEM-F12 supplemented with 10% FBS and 1% penicillin, streptomycin, amphotericin (PSA) solution. Following cell counting using 1:4 trypan blue staining, the cells counted were seeded on UV sterilized 12 mm coverslips coated with poly-D-lysine (PDL; Sigma-Aldrich, St. Louis, MO) at a density of 8,000 cells/well and incubated for 4-6 h for the cells to attach at 37°C, 5% CO_2. The media was changed to Neurobasal Plus medium (Gibco, CA, United State) containing 10% B27 supplement (ThermoFisher, Waltham, MA) and 10% PSF. The media was refreshed every 2-3 days by exchanging half of the medium with fresh neurobasal medium.

Cell Treatment and Immunocytochemistry

CST cultures were untreated (baseline control), treated with BDNF (4 µg/ml), exoenzyme C3 transferase (2 µg/ml) (Cytoskeleton, INC., CO, United State), SFNPs (C750/ C150/ N150),

BDNF-derivatized SFNPs not imbibed with drug (negative control for therapeutic), and BDNF-derivatized SFNPs imbibed with C3. Release of therapeutic were induced at 4 hours by briefly increasing the temperature. At 24 hours and 72 hours after inducing release of imbibed drug, the cells were fixed in 4% paraformaldehyde for 30 min at room temperature. The solution was then drawn out and cultures were washed twice in 1X PBS. The fixed cells were blocked using blocking buffer (PBS containing 1.5% normal donkey serum, 0.1% BSA, and 0.1% Triton) for 30 min at room temperature. Cells were exposed to appropriate dilution (1:250) of primary antibody (anti beta III tubulin mono mouse) in blocking buffer for 4 hours at room temperature. Cultures were washed twice with 1X PBS for 5 min each and cultures were incubated in 1:500 donkey anti-mouse IgG AlexaFluor 488 in blocking buffer for 2 hours at room temperature, followed by three 5 min washes with 1X PBS. The solution was then drawn out, and mounted on a glass slide in one drop of Vectashield mounting medium with 4,6-diamidino-2-phenylindole (DAPI; Vector laboratories, Burlingame, CA) and allowed to dry for 48 h.

Microscopy and Analysis

The images (2 images per culture, 3 conditions in each experiment) were captured from four quadrants and the center through 60X objectives using a Zeiss Axiovert 200M. The images were obtained using DAPI (laser 405 nm), FITC (laser 488 nm), and TRITC (laser 561 nm) filters, and the fluorescence intensity of Beta III tubulin in the CSTs was measured from each region of interest. Images were also analyzed for several measurements of outgrowth, including numbers of neurites per cell, percent of neurite-bearing cells, and total neurite length per cell. A neurite was defined as a cell extension greater than 10 um and the total neurite length was the sum of all neurites and branches from a single cell. Only non-aggregated cells where the cell and

all its neurites were included in the image were quantified, and imaged fields were systematically selected from each quadrant and the center of each coverslip to ensure a representative sample.

Statistical Analysis

Prism 9 (GraphPad Software) software was used for all statistical analyses and data graphing. Data from three independent replicates were pooled and are expressed as mean ± standard error of the mean. We compared the results among treatment groups as well as to the control using one-way analysis of variance (ANOVA). The significance of pair-wise comparisons was determined by Tukey HSD post-hoc tests. A level of significance of $p \leq 0.05$ was used for all differences evaluated. Triplicate cultures were used for each treatment condition in each experiment and experiments were repeated three times (n=9).

RESULTS

BDNF-SFNPs hold promise as drug delivery systems that can deliver therapeutic inside specific target cells and release imbibed drugs on demand with a simple increase in temperature. An attractive therapeutic for encouraging axon regeneration is the RhoA inhibitor, C3 transferase. Since C3 transferase is a large molecule that is not cell-permeant, delivery and intracellular release into CST neurons might be facilitated by using BDNF-derivatized SFNPs. We assessed the ability of SFNP delivery of C3 transferase to CST neurons to increase CST neuron process outgrowth to address this hypothesis.

Primary rat cortical neuron cultures were treated with left untreated, or treated with BDNF (4 μg/ml), C3 transferase (2 μg/ml), or SFNPs (100 μg/ml N150, C150, C750) that were not derivatized, derivatized with BDNF, or derivatized with BDNF and loaded with C3 transferase at room temperature for 4 hours to allow endocytosis but prevent drug release, followed by transfer to 37°C. Cytoskeletal changes were assessed from confocal microscopic

images for each type of SFNP (Figures 4.1, 4.2, 4.3). In each figure, nuclei are labeled by DAPI (first column, blue), SFNPs uptake is shown up rhodamine fluorescence (second column, red), and neuronal microtubules are labeled for βIII tubulin (third column, green). Beta III tubulin immunoreactivity alone and in merged images (column for in each figure) shows the extent of process extension for N150 (Figure 4.1), C150 (Figure 4.2), and C750 (Figure 4.3). For each SFNPs construct, the highest level of neurite outgrowth from cortical neurons occurred with C3-imbibed BDNF-derivatized SFNPs. Comparable outgrowth was seen in untreated cultures, cultures treated with C3, or exposed to underivatized SFNPs. Treatment with BDNF or BDNF-SFNPs elicit moderate increases in neurite outgrowth compared to control groups, C3, and underivatized treatments.

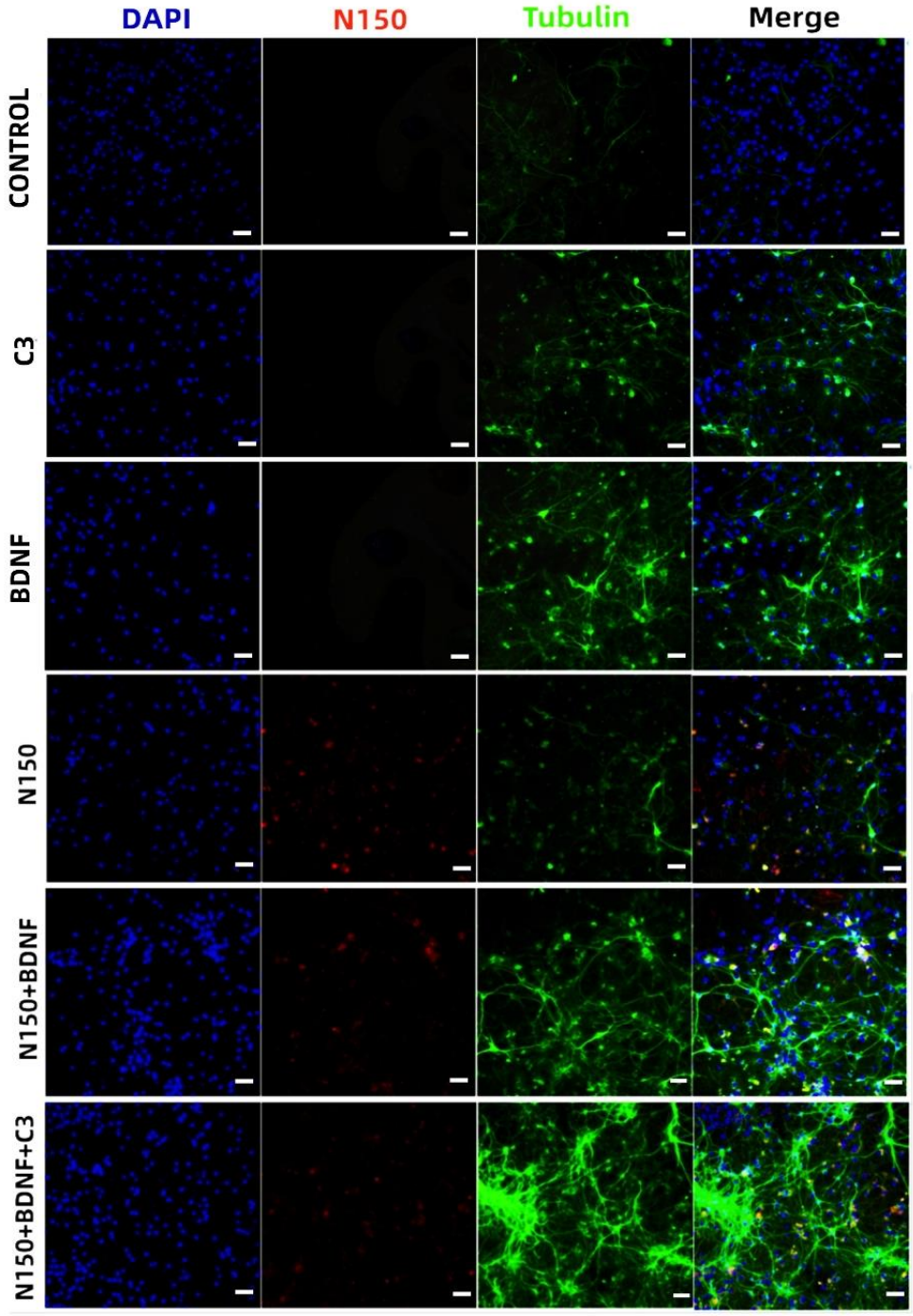

Figure 4.1: *Confocal images of cortical neurons after exposure to outgrowth promoting substances or N150 SFNPs.* Representative photomicrographs of primary cortical neuron cultures either untreated (first row) or treated for 72 hours with 2 µg/ml C3 transferase (second row), 4µg/ml BDNF (third row), 100 µg/ml underivatized N150 (fourth row), 100 µg/ml BDNF-N150 (fifth row), or 100 µg/ml BDNF-N150 imbibed with C3 transferase with DAPI labeled nuclei (first column, blue), rhodamine labeled SFNPs (second column, red), or immunolabeled for Beta III tubulin (third column, green). The last column shows merged images. Scale bars in each panel are 50 µm.

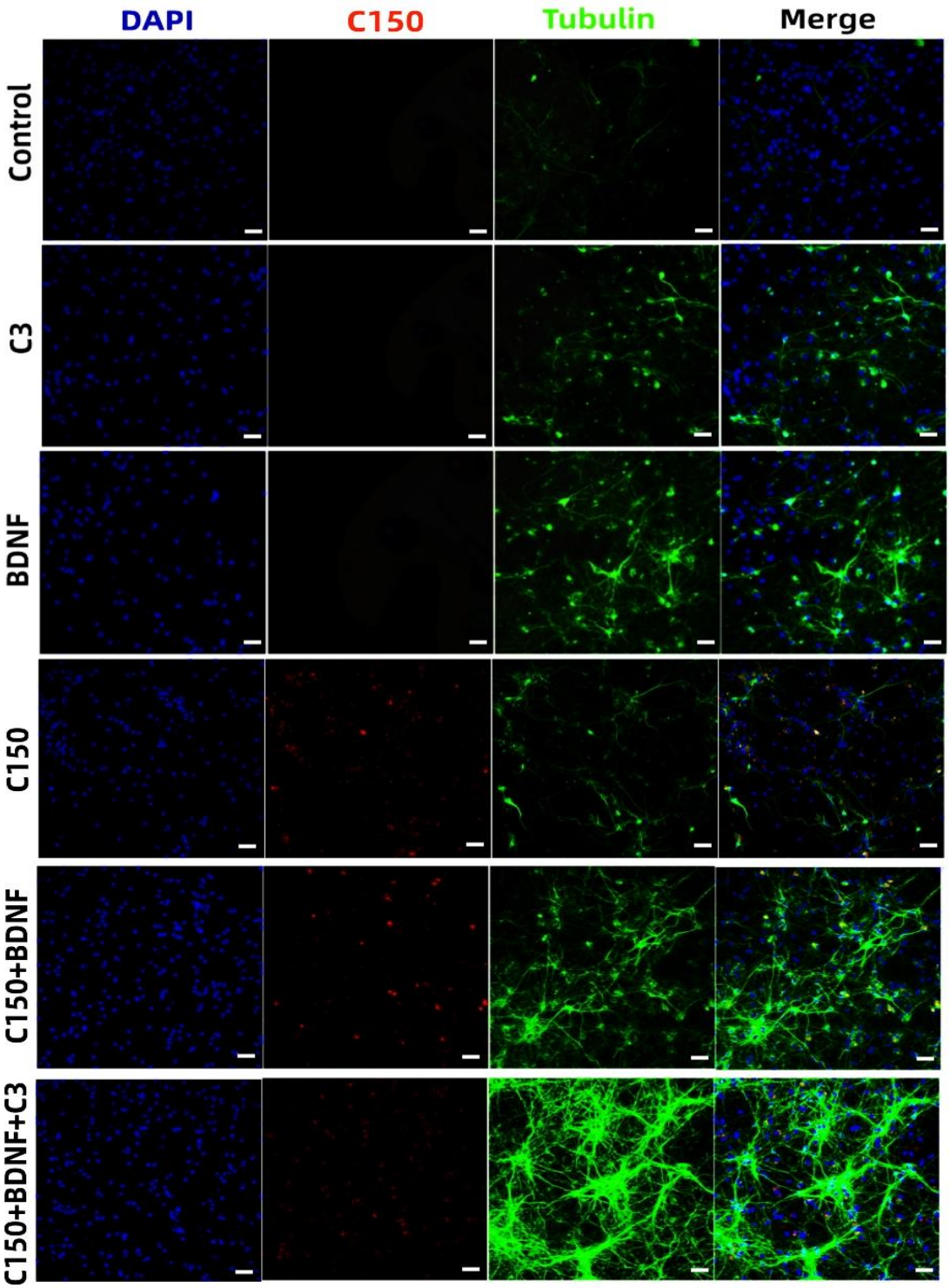

Figure 4.2: *Confocal images of cortical neurons after exposure to outgrowth promoting substances or C150 SFNPs.* Representative photomicrographs of primary cortical neuron cultures either untreated (first row) or treated for 72 hours with 2 µg/ml C3 transferase (second row), 4µg/ml BDNF (third row), 100 µg/ml underivatized C150 (fourth row), 100 µg/ml BDNF-C150 (fifth row), or 100 µg/ml BDNF-C150 imbibed with C3 transferase with DAPI labeled nuclei (first column, blue), rhodamine labeled SFNPs (second column, red), or immunolabeled for Beta III tubulin (third column, green). The last column shows merged images. Scale bars in each panel are 50 µm.

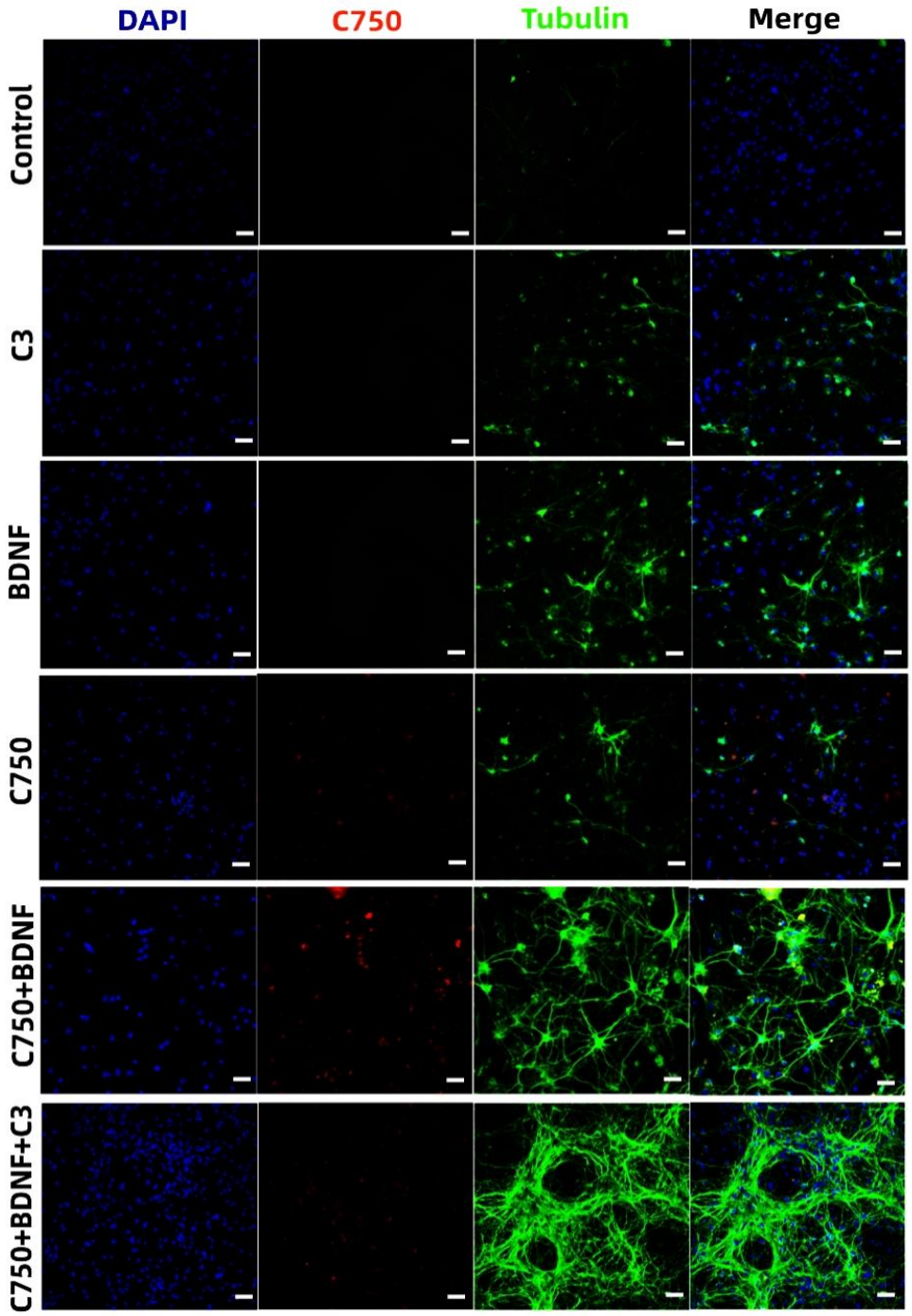

Figure 4.3: *Confocal images of cortical neurons after exposure to outgrowth promoting substances or C750 SFNPs*. Representative photomicrographs of primary cortical neuron cultures either untreated (first row) or treated for 72 hours with 2 µg/ml C3 transferase (second row), 4µg/ml BDNF (third row), 100 µg/ml underivatized C750 (fourth row), 100 µg/ml BDNF-C750 (fifth row), or 100 µg/ml BDNF-C750 imbibed with C3 transferase with DAPI labeled nuclei (first column, blue), rhodamine labeled SFNPs (second column, red), or immunolabeled for Beta III tubulin (third column, green). The last column shows merged images. Scale bars in each panel are 50 µm.

BDNF-SFNP Delivery of C3 Transferase Increases Neurite Initiation

The extent of neurite outgrowth was quantified using beta III tubulin fluorescence intensities across each image. For all three types of SFNP (N150, C150, C750), treatment with BDNF-SFNPs imbibed with C3 had the greatest increase in neurite outgrowth over other conditions being significantly greater than treatment with C3, underivatized SFNP, and BDNF-SFNP (Figure 4.4). Both BDNF and C3 have been reported to increase neurite outgrowth from different types of neurons. The significant difference between BDNF-derivatized SFNPs with and without C3 imbibed. These results show that delivery of C3 to cortical neurons through BDNF-SFNPs dramatically increases neurite outgrowth, supporting their potential role as a therapeutic strategy to increase regeneration after CNS damage.

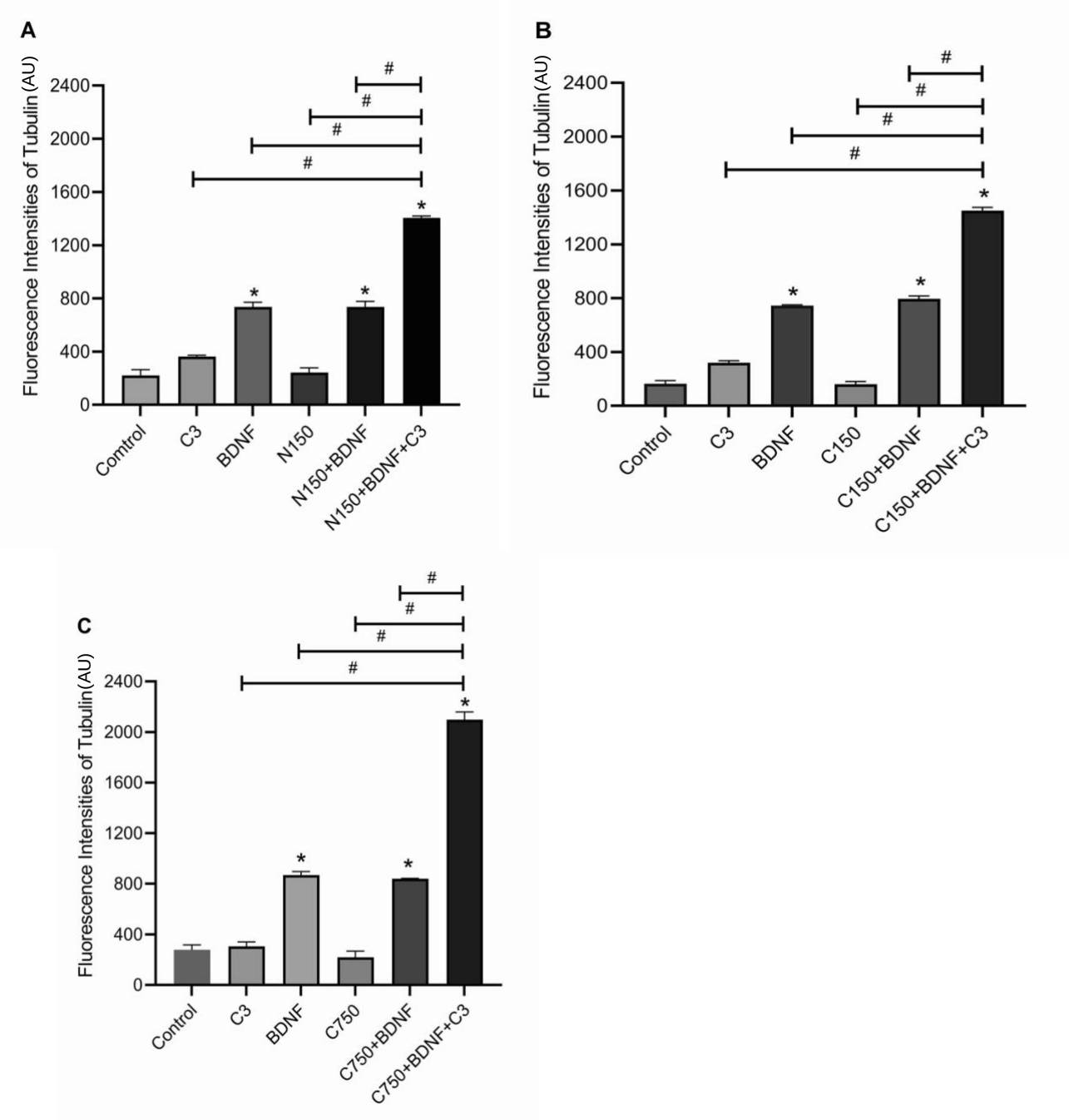

Figure 4.4: *Quantification of neurite outgrowth in cortical neurons after exposure to neurite outgrowth promoting substances of SFNPs constructs.* Cortical neurons were treated for 72 hours with 2 µg/ml C3 transferase, or 100 µg/ml underivatized SFNPs (N150, C150, C750) or derivatized with BDNF and either not loaded or loaded with C3 transferase. Images from fixed cultures were analyzed for total fluorescence intensity of beta III tubulin immunoreactivity across the micrograph. Data shown are means $\pm$ SEM from three separate experiments containing three cultures in each condition (n = 9). Asterisks indicate statistically significant differences between each treatments compare to control and # indicate a significant difference between each treatment ($p \leq 0.05$). (ANOVA and Tukey HSD post-hoc tests).

The elaboration of neuronal processes and arbors is complex, involving several types of cytoskeletal rearrangements leading to different morphological changes.[18,19] To determine how the combination of BDNF-SFNP loaded with C3 transferase affects different aspects of process elaboration, we assessed how experimental treatments affected neurite initiation (Figures 4.5, 4.6) and neurite elongation (Figure 4.7). Quantification of neurite initiation was performed by measuring the number of neurites per cell (Figure 4.5) and the percent of neurite bearing cells (Figure 4.6) 24 and 72 hours after treatment in response to bath application of 2.0 µg/ml C3 transferase, 100 µg PEG/ml SFNPs (N150, C150, C750), 100 µg PEG/ml BDNF-SFNPs, or 100 µg PEG/ml BDNF-SNFPs imbibed with C3 transferase. At 24 hours after treatment, significant differences in the number of neurites/cell were not observed between treatment conditions (data not shown). At 72 hours after treatment, BDNF-SFNPs imbibed with C3 transferase exposure resulted in the highest number of neurites per cell, which was significantly increased compared to untreated control cultures, or cultures treated with bath application of C3 transferase, underivatized SFNPs, or BDNF-SFNPs without imbibed C3 transferase for N150 (Figure 4.5A), C150 (Figure 4.5B), and C750 (Figure 4.5C). There was no significant difference between the untreated control cultures and cultures treated with bath applied C3 transferase, or cultures exposed with any of the underivatized SFNPs for the number of neurites per cell 72 hours after treatment (Figures 4.5). In contrast, treatment with BDNF-SFNPs had significantly higher number of neurites/cell compared to control and BDNF-SFNPs imbibed with C3 transferase had numbers of neurites/cell significantly higher than any other treatment group.

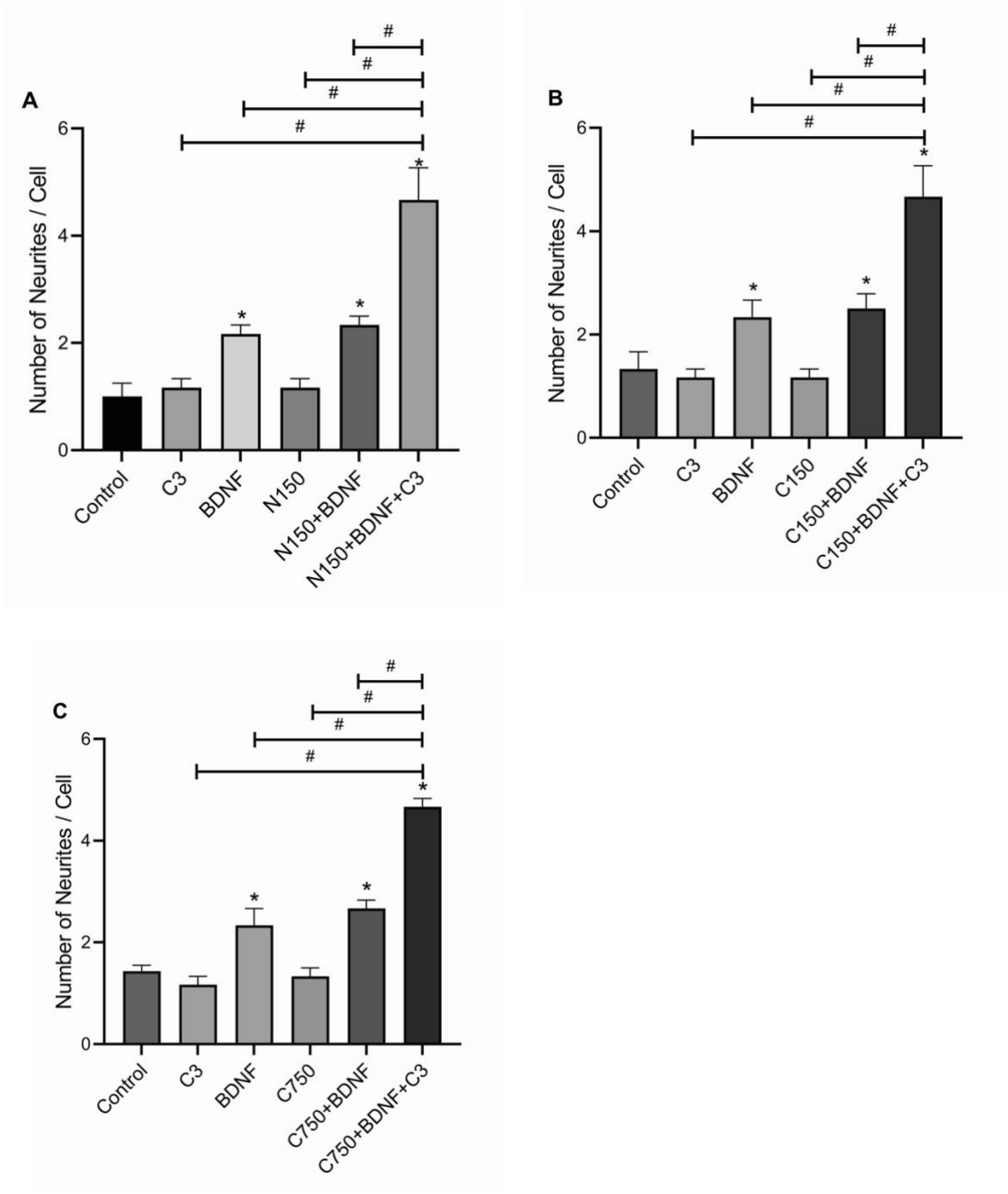

Figure 4.5: *Quantification of neurites per cell in cortical neurons after exposure to outgrowth promoting substances or SFNPs.* Cortical neurons were treated for 72 hours with 2.0 μg/ml C3 or 100 μg/ml underivatized SFNPs, C3, BDNF, BDNF-SFNPs, or BDNF-SFNPs imbibed with C3 for N150 (A), C150 (B), or C750 (C) SFNPs. Images of fixed neuron were analyzed for neurite initiation by counting the number of neurites per cell. Data shown are means $\pm$ SEM from three separate experiments, each with three cultures in each condition (n = 9). Asterisks over the bar indicate the significance of the neurites per neurons of different treatment compared to the negative control. Asterisks indicate statistically significant differences between each treatments compare to control and # indicate a significant difference between each treatment ($p \leq 0.05$; Student's t-test).

We also assessed neurite initiation by measuring the percentage of neurite bearing neurons from cortical neurons after exposure to 100 μg PEG/ml SFNPs for 24 or 72 hours with or without BDNF derivatization or C3 imbibed (Figure 4.6). At 24 hours after treatment, significant differences between treatments in the number of neurites/cell were not observed (data not shown). After 72 hours of treatment, the percentage of neurite bearing cells was significantly increased after the treatment with C3 transferase loaded BDNF-derivatized SFNPs in comparison to untreated controls, bath applied C3 transferase, underivatized SFNPs, or BDNF-SFNPs without imbibed C3 transferase for N150 (Figure 4.6A), C150 (Figure 4.6B), and C750 (Figure 4.6C). The data suggest that neurite initiation is promoted dramatically by BDNF-derivatized SFNPs delivering C3 transferase compared to other SFNP formulation, with there being at least an additive effect if both BDNF and C3 transferase are delivered to cortical neurons.

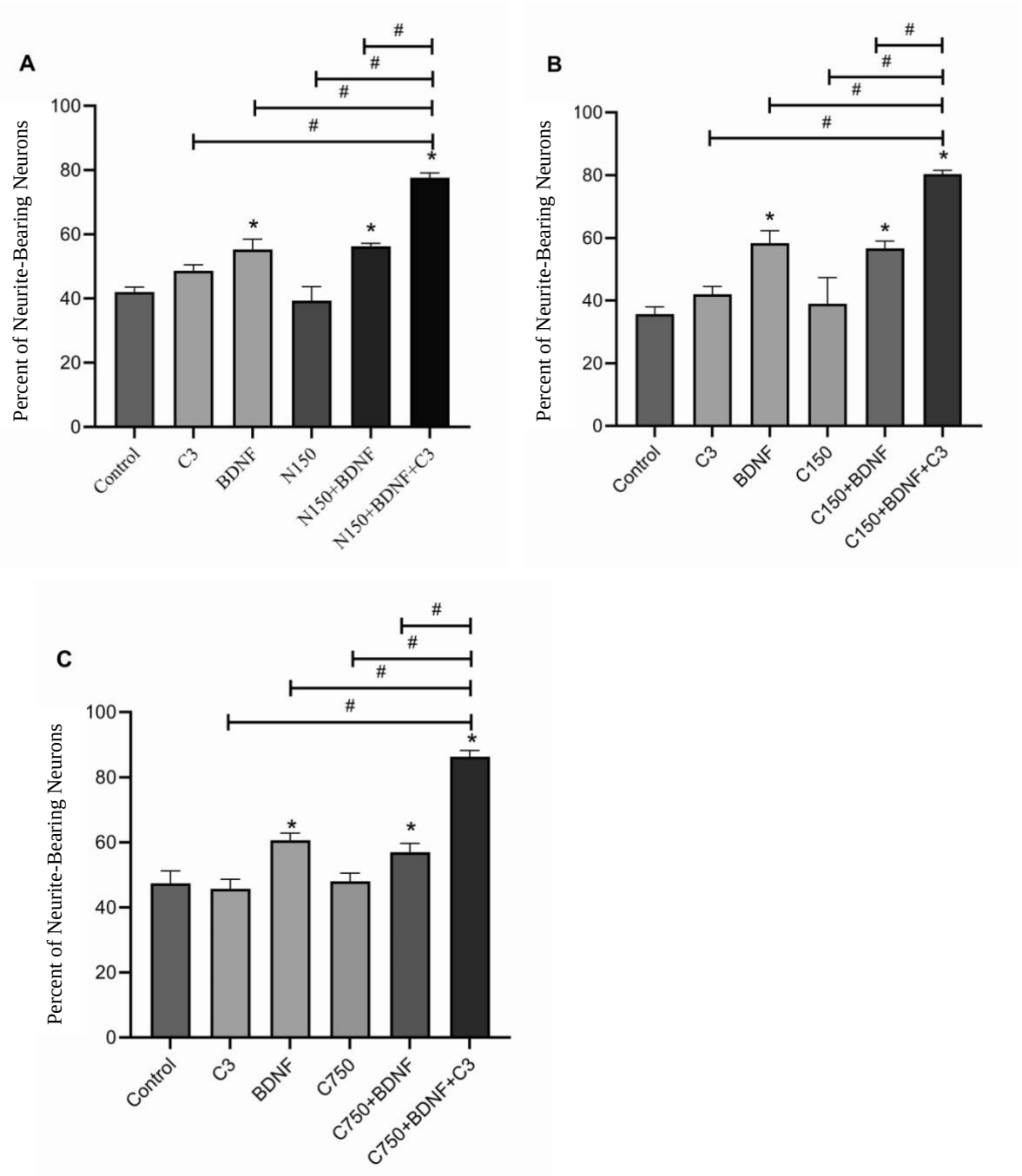

Figure 4.6: *Quantification of the percent of neurite-bearing cells in cortical neurons after exposure to outgrowth promoting substances or SFNPs.* Cortical neurons were treated for 72 hours with 2.0 μg/ml C3 or 100 μg/ml underivatized SFNPs, C3, BDNF, BDNF-SFNPs, or BDNF-SFNPs imbibed with C3 for N150 (A), C150 (B), or C750 (C) SFNPs. Images of fixed neuron were analyzed for neurite initiation by counting the number of neurite-bearing cells. Data shown are means $\pm$ SEM from three separate experiments, each with three cultures in each condition (n = 9). Asterisks over the bar indicate the significance of the percentage of neurites bearing of different treatment compared to the negative control. Asterisks indicate statistically significant differences between each treatments compare to control and # indicate a significant difference between each treatment ($p \leq 0.05$; Student's t-test).

BDNF-SFNP Delivery of C3 transferase Increases Neurite Elongation

To determine if C3 imbided in SFNPs derivatized with BDNF increased measures of neurite elongation, we determined the total neurite length/neuron (Figure 4.7). Quantification was accomplished by measuring summing the length of all primary neurites and their branches for each neuron in the microscopic field for each treatment at 72 h. In all three graphs, C3 and SFNPs groups show no significant difference in the length of the total neurite per neuron compared to the negative control. A significant increase founded in the BDNF-derivatized SFNPs compared with negative control. C3 imbibed BDNF-derivatized SFNPs show an approximately 2-fold increase of total neurite length/cell than BDNF-derivatized SFNPs (without C3).

Totally, the combined treatment with C3 imbibed BDNF-derivatized SFNPs significantly increased the total neurite length/cell compared to all other treatment groups for N150 (Figure 4.7A), C150 (Figure 4.7B), and C750 (Figure 4.7C). This also suggested that C3 is poorly taken up by cortical neurons without SFNPs. Consistent with this, we found that neurite initiation and neurite elongation were not affected by exposure to C3 for up to 72 hours.

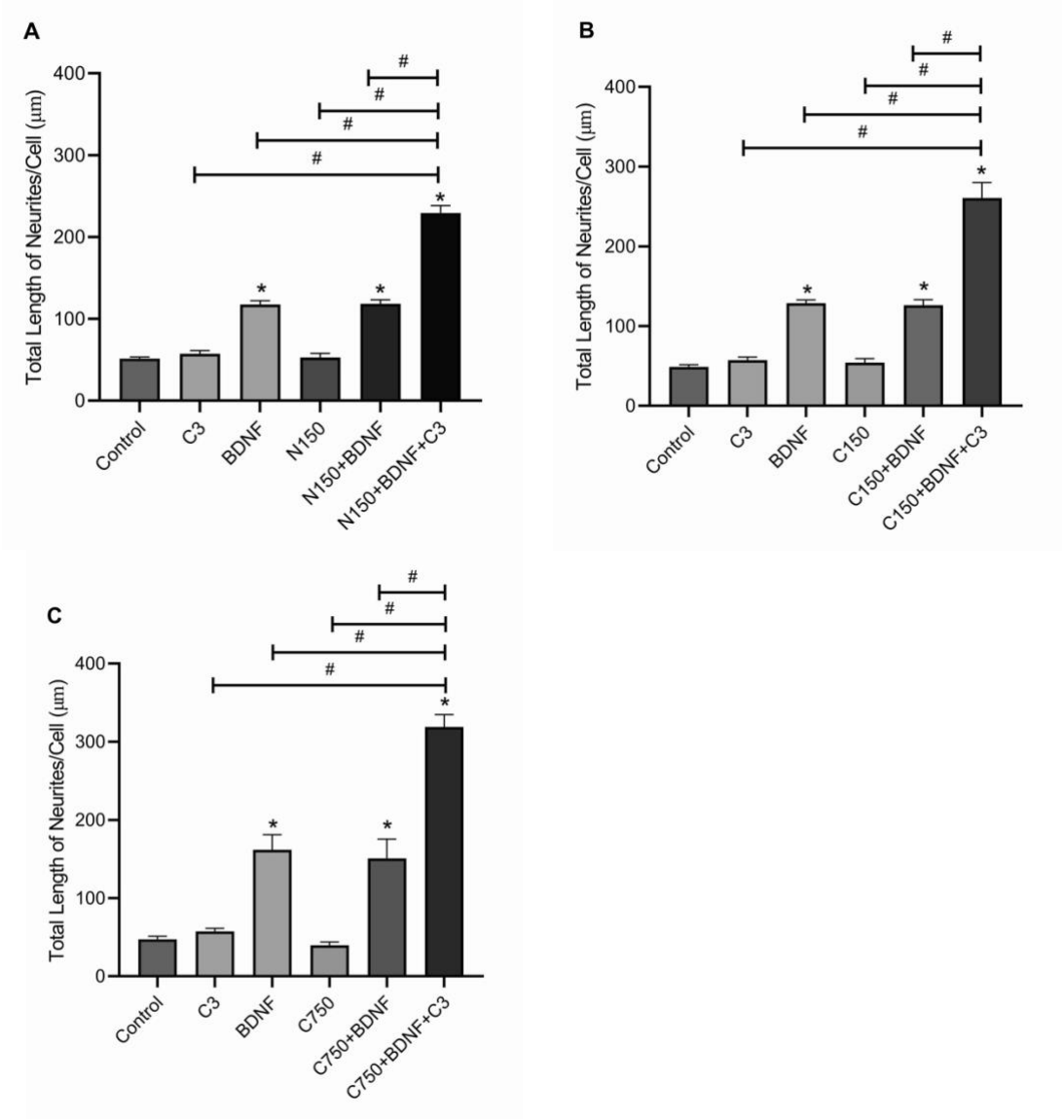

Figure 4.7: *Quantification of the total neurite length/neuron in cortical neurons after exposure to outgrowth promoting substances or SFNPs.* Cortical neurons were treated for 72 hours with 2.0 µg/ml C3 or 100 µg/ml underivatized SFNPs, C3, BDNF, BDNF-SFNPs, or BDNF-SFNPs imbibed with C3 for N150 (A), C150 (B), or C750 (C) SFNPs. Images of fixed neuron were analyzed for neurite elongation by summing the lengths of all primary neurites and their branches for each analyzed neuron. Data shown are means $\pm$ SEM from three separate experiments, each with three cultures in each condition (n = 9). Asterisks over the bar indicate the significance of the total neurites length per neurons of different treatment compared to the negative control. Asterisks indicate statistically significant differences between each treatments compare to control and # indicate a significant difference between each treatment ($p \leq 0.05$; Student's t-test).

DISCUSSION

Primary rat cortical neuron cultures were treated with BDNF, C3 transferase, SFNPs, as well as derivatized BDNF-SFNPs, or derivatized with BDNF and loaded with C3 transferase. Drug release was initiated by increasing the temperature briefly. This increase in temperature shrank the SFNPs and caused the release of the imbibed C3. Neurite outgrowth was detected by using microscopy and image analysis involving several measurements of outgrowth which include neurite initiation (numbers of neurites per cell, percentage of neurites bearing cells), and neurite elongation (length of the longest neurite per cell, total neurite length per cell). The cytoskeletal changes were assessed from confocal microscopic images for each type of SFNP (Figures 4.1, 4.2, 4.3). The highest intensity of beta III tubulin was observed from the treatment with C3 loaded BDNF-SFNPs than other treatments, especially for C3 control. The above results suggest that C3 imbibed with BDNF-SFNPs successfully uptake and released within neurons. Whereas the same outgrowth didn't perform in C3 control. The results from the quantification of neurites initiation and elongation reconfirmed this conclusion. There is no significant difference between the control group, SFNPs, and C3 treatment groups. These results demonstrate two things: first that the SFNPs have no effect on neurites outgrowth, and second, C3 is unable to be uptake by CST neurons, which downstream promote axon growth.

Moreover, both microscopy image and quantification analysis suggest that the neurites outgrowth significantly improved when exposure to the C3 imbibed BDNF-derivatized SFNPs than other treatment groups. The number of neurites per cell with C3 imbibed BDNF-derivatized SFNPs shows about 2-fold more than BDNF-derivatized SFNPs and a 4-fold increase than C3 only. To compare total neurite length/cell, C3 imbibed BDNF-derivatized SFNPs show an approximately 2-fold increase than BDNF-derivatized SFNPs and a 5-fold increase than C3 only.

For each SFNP construct, the highest level of neurite outgrowth from CST neurons occurred with C3-imbibed BDNF-derivatized SFNPs. Comparable outgrowth was seen in untreated cultures, cultures treated with C3, or exposed to underivatized SFNPs. Treatment with BDNF or BDNF-SFNPs elicit moderate increases in neurite outgrowth compared to control groups (bath application of BDNF or C3) and underivatized SFNPs treatments. These results show that delivery of C3 to cortical neurons through BDNF-SFNPs dramatically increases neurite outgrowth, supporting their potential role as a therapeutic strategy to increase regeneration after CNS damage. The combined treatment with C3 imbibed BDNF-derivatized SFNPs significantly promotes neurites outgrowth which is suggested the poor neuron uptake of C3 can be overcome by imbibed with SFNPs. C3 was successfully released from the PEG coat of SFNPs on temperature and location demand. The C3 released is consistently functional and further promotes neurites outgrowth efficiency which suggests a great potential therapy for SCI treatment. Together, our results indicate that a nanomaterial drug delivery system designed to target specific cells in the CNS would offer distinct advantages over conventional treatments for traumatic or degenerative neurological conditions.

ACKNOWLEDGEMENTS

This work was supported by the Texas Woman's University (TWU) Department of Biology, the TWU Research Enhancement Program, and the Southeast Missouri State University Department of Physics and Engineering Physics.

REFERENCES

1. P. Cooke, H. Janowitz and S. E. Dougherty, *Frontiers in Cellular Neuroscience*, 2022, **16**, 872501.

2. E. A. Huebner and S. M. Strittmatter, *Results and Problems in Cell Differentiation*, 2009, **48**, 305–360.

3. J. W. Fawcett, *Neurochemical Research*, 2019, **45**, 144–158.

4. J. Houlton, N. Abumaria, S. F. R. Hinkley and A. N. Clarkson, *Frontiers in Neuroscience*, 2019, **13**, 790.

5. J. Shi, A. R. Votruba, O. C. Farokhzad and R. Langer, *Nano Letters*, 2010, **10**, 3223–3230.

6. S. C. Huelsenbeck, A. Rohrbeck, A. Handreck, G. Hellmich, E. Kiaei, I. Roettinger, C. Grothe, I. Just and K. Haastert-Talini, *Neurotherapeutics*, 2011, **9**, 185–198.

7. Jin, *Journal of Clinical Medicine*, 2020, **9**, 257.

8. S. Meltzer, C. Santiago, N. Sharma and D. D. Ginty, *Neuron*, 2021, **109**, 3736–3757.

9. M. Mahar and V. Cavalli, *Nature Reviews Neuroscience*, 2018, **19**, 323–337.

10. K. Keefe, I. Sheikh and G. Smith, *International Journal of Molecular Sciences*, 2017, **18**, 548.

11. S. A. A. Rizvi and A. M. Saleh, *Saudi Pharmaceutical Journal*, 2018, **26**, 64–70.

12. S. Ning, M. Jorfi, S. R. Patel, D. Y. Kim and R. E. Tanzi, *Frontiers in Neuroscience*, 2022, **16**, 854992.

13. R. Y. Tam, T. Fuehrmann, N. Mitrousis and M. S. Shoichet, *Neuropsychopharmacology*, 2013, **39**, 169–188.

14. S. Naqvi, A. Panghal and S. J. S. Flora, *Frontiers in Neuroscience*, 2020, **14**, 94.

15. W. B. Jacobs and M. G. Fehlings, *Neurosurgery*, 2003, **53**, 943–950.

16. Y.-H. Tsou, X.-Q. Zhang, H. Zhu, S. Syed and X. Xu, *Small*, 2017, **13**, 1701921.

17. T. Patel, J. Zhou, J. M. Piepmeier and W. M. Saltzman, *Advanced Drug Delivery Reviews*, 2012, **64**, 701–705.

18. Y. G. Kim, J. W. Kim, H. J. Pyeon, J. K. Hyun, J.-Y. Hwang, S.-J. Choi, J.-Y. Lee, F. Deák, H.-W. Kim and Y. I. Lee, *Journal of Biomaterials Applications*, 2013, **28**, 790–797.

19. D. A. Kuhn, D. Vanhecke, B. Michen, F. Blank, P. Gehr, A. Petri-Fink and B. Rothen-Rutishauser, *Beilstein Journal of Nanotechnology*, 2014, **5**, 1625–1636.

20. J. M. Reddy, N. G. R. Raut, J. L. Seifert and D. L. Hynds, *Molecular Neurobiology*, 2020, **57**, 2220–2231.

21. J. Hu, G. Zhang, W. Rodemer, L.-Q. Jin, M. Shifman and M. E. Selzer, *Neurobiology of Disease*, 2017, **98**, 25–35.

22. G. Zhang, J. Hu, W. Rodemer, S. Li and M. E. Selzer, *Experimental Neurology*, 2018, **306**, 76–91.

23. A.E. Fournier, B. T. Takizawa and S. M. Strittmatter, *The Journal of Neuroscience*, 2003, **23**, 1416–1423.

24. M. A. Kopp, T. Liebscher, R. Watzlawick, P. Martus, S. Laufer, C. Blex, R. Schindler, G. J. Jungehulsing, S. Knüppel, M. Kreutzträger, A. Ekkernkamp, U. Dirnagl, S. M. Strittmatter, A. Niedeggen and J. M. Schwab, *BMJ Open*, 2016, **6**, 7.

25. S. Stern, B. J. Hilton, E. R. Burnside, S. Dupraz, E. E. Handley, J. M. Gonyer, C. Brakebusch and F. Bradke, *Neuron*, 2021, **109**, 3436-3455.e9.

26. S. Mulherkar and K. F. Tolias, *Cells*, 2020, **9**, 245.

27. C.-A. Gutekunst, J. K. Tung, M. E. McDougal and R. E. Gross, *Neuroscience*, 2016, **339**, 308–318.

28. N. Forgione and M. G. Fehlings, *World Neurosurgery*, 2014, **82**, e535–e539.

29. M. Lehmann, A. Fournier, I. Selles-Navarro, P. Dergham, A. Sebok, N. Leclerc, G. Tigyi and L. McKerracher, *The Journal of Neuroscience*, 1999, **19**, 7537–7547.

30. C. Wilde and K. Aktories, *Toxicon*, 2001, **39**, 1647–1660.

31. A.J. Santiago-Lopez, C.-A. Gutekunst and R. E. Gross, *Methods in Molecular Biology*, 2018, **1821**, 267–281.

32. M. Vogelsgesang, A. Pautsch and K. Aktories, *Naunyn-Schmiedeberg's Archives of Pharmacology*, 2006, **374**, 347–360.

33. J. V. Coumans, T. T.-S. Lin, H. N. Dai, L. MacArthur, M. McAtee, C. Nash and B. S. Bregman, *The Journal of Neuroscience*, 2001, **21**, 9334–9344.

34. W. N. Durán, F. A. Sánchez and J. W. Breslin, *Microcirculation*, 2008, 81–124.

35. M. Auer, I. Allodi, M. Barham, E. Udina, W. F. Neiss, X. Navarro and L. Klimaschewski, *Journal of the Peripheral Nervous System*, 2013, **18**, 30–36.

CHAPTER V

CONCLUSIONS

The major issue to use drugs, like C3 transferase, in clinics is that they do not display binding and affinity with specific neurons and have low efficiency to cross certain barriers (eg, BBB or the blood cerebrospinal fluid barrier).[1] The results from the first aim of this study show that C3 crosses the BBB *in vitro* when imbibed by all three SFNPs. These results are very promising, but the observed effects need to be further validated in a model *in vivo*. The construction of the ligand attached SFNPs drug delivery systems is complex, and several targeting designs must be evaluated. Moreover, their uptake efficiency by target neurons is still unclear. A major reason for designing thermoresponsive drug delivery systems is the ability to load them with therapeutic that can be released on demand by increasing the temperature above the critical transition temperature needed to cause a volumetric transition resulting in the expulsion of imbibed drug.[2] We delivered C3 transferase to corticospinal tract (CST) neurons to inhibit RhoA and increase axon extension.[3] In experiments where we loaded BDNF-derivatized SFNPs with C3 transferase, we found that BDNF/C3 transferase SFNPs had a lower efficiency at crossing a BBMVEC monolayer than SFNPs not carrying C3, regardless of SFNP size. Imbibing SFNPs with C3 may slightly increase nanoparticle size, but the molecular qualities of imbibed drug may also affect the ability to cross the BBB. Additional experiments are needed to determine whether fewer larger SFNPs carrying more therapeutic or smaller SFNPs, each carrying less therapeutic, are more efficacious in promoting axon extension.

Our experiments did not address the mechanism through which the SFNPs traverse the BBMVEC monolayers. Understanding these mechanisms may aid the design of more effective therapeutic drug delivery constructs. Mechanisms through which materials pass through the BBB

include the paracellular aqueous pathway, transcellular lipophilic pathway, carrier-mediated transport, receptor-mediated transcytosis, and adsorptive-mediated transcytosis.[4] Of these, the possible mechanisms used for transporting SFNPs include carrier-mediated transport, receptor-mediated transport, or absorptive-mediated transport.[5] Additional experimentation is required to determine the specific mechanisms for BDNF-SFNPs internalization by neurons.

In clinical trials, about 80% of drug candidates cannot successfully cross the BBB. The two most frequently used tools for testing drugs BBB crossing are animal models and *in-vitro* cell models.[6] Animal models maintain the native matrix architecture and are further capable of forecasting cellular response in a physiological environment.[7] However, there is a discrepancy between animal and human cellular and matrix constitution when it comes to the BBB. *In-vitro* cell models cultivate human cells in a controlled environment to mimic the functioning of tissues and organs.[8] Many human brain endothelial cells, immortalized cell lines, primary cells, induced pluripotent stem cells, and BBMVECs have been employed successfully to mimic the BBB.[9-11] However, a lot of medications that were successfully tested in animal and models *in vitro* fail in clinical trials. The BBB in humans has a distinct cellular structure and physiology, making it difficult to predict the use of any potential drug in the native human brain environment.[12] It is crucial to understand how brain endothelial cells and other components of the human BBB respond to specific paradigm situations, particularly the mechanism(s) of transport across the BBB. Because of the gap between *in-vitro* and *in-vivo* models, studies *in vivo* are necessary to definitively assess whether C3 transferase effectively crosses an intact BBB in a living organism, even though the results we present here using an *in-vitro* BBB model are promising.

Another major concern of treatment is the inability to target specific types of damaged neurons in tissues composed of many types of neurons and other cell types. Our strategy is to

attach peptides to SFNPs that would bind receptors found only on target neurons to prevent the uptake of SFNPs by other cells. The PEG coating provides an external surface that is highly amenable to biochemical modification, making it possible to target nanospheres to particular tissues or cells.[13] For instance, we can attach functional groups (eg, amine or carboxyl) that allow peptide bonding to attach proteins to the PEG coat. Attaching BDNF to the SFNPs allows them to preferentially bind to a subset of neurons, including CST neurons that are often damaged in SCI. SFNPs have been utilized to deliver therapeutic molecules across the BBB for the treatment of SCI. Surface modification of nanoparticles with specific ligands capable of binding to target receptors on specific neurons may lead to engineered nanoparticles loaded with drug cargos, thereby delivering therapeutic molecules into the target neurons.[14]

To determine whether CST neurons preferentially take up SFNPs derivatized with BDNF, we used immunocytochemistry and confocal imaging to assess the extent and timing of endocytosis by CST neurons and glia in cultures of neonatal rat cortices enriched for neurons. The results indicate that CST neurons, identified by immunolabeling for Ctip2, internalize more of the BDNF-derivatized SFNPs than glial cells. Previous work supports this observation that cortical neurons uptake more SFNPs than other types of cells in the CNS. Therefore, using BDNF-derivatized SFNPs to target drugs specifically to the damaged CST neurons can significantly improve the drug effect without affecting other cells. Moreover, the uptake efficiency of cortical neurons is significant higher than glia, for the C750 system. From our BDNF binding efficiency study, we found that C750 allowed more BDNF binding because of its larger surface compared to that of the N150 and C150 constructs. These results support this premise that C750 is taken up more efficiently and likely delivers more loaded drugs than C150 or N150. Also, the fluorescent intensity is higher in neurons treated with BDNF-derivatized

SFNPs compared to those treated with non-derivatized SFNPs, suggesting that internalization mechanisms like receptor-mediated endocytosis may be of paramount importance to consider in designing effective CNS drug delivery systems.

Moreover, this drug delivery system can overcome the challenges in target delivery to avoid potential side effects to off-target cells.[15] This is especially challenging in SCI treatment where the CNS contains different types of cells which might also take up SFNPs, such as glial cells.[16] Our SFNPs have surface-modified ligands as tools in increased local drug concentrations and provide strategies for more specific therapy. The nanoparticles surface modified with BDNF were used to allow C3 drug delivery to the target neurons in this study. To determine if CST neurons preferentially take up SFNPs derivatized with BDNF using immunocytochemistry and real-time imaging, rat cortical cell cultures were treated with C3 loaded BDNF-SFNPs for 24 hrs. The attached BDNF on the surface of SFNPs allows them to preferentially bind to TrkB expressing cells. Results from both confocal images and quantification showed that BDNF-derivatization leads to 3- to 5- fold more SFNPs internalization by CST neurons compared to non-neuronal cells. The study showed that the attachment to TrkB receptors by BDNF derivatized SFNPs enhanced their ability to increase internalization.

TrkB receptor is expressed in different isoforms in the CNS.[17] Full-length Trk tyrosine kinase receptors (TrkB.FL) are highly expressed in neurons, which contains an extracellular ligand binding domain and an intracellular catalytic domain.[17,18] TrkB.FL is the major isoform of TrkB and primary receptor for BDNF.[17,19,20] The truncated isoforms (TrkB.T1) predominantly expressed in astrocytes, lacks the intracellular kinase domain of the full length receptor.[18,21] Also, both type of TrkB isoforms shows less expressed on Microglia cells.[22] The results from our uptake study can explain according to these. First, the BDNF peptide used for derivatized in our

study only contain the partial sequence, which might only be recognized and has more affinity to the TrkB.FL on neurons than TrkB.T1. Second, Astrocytes produce BDNF by itself and downstream transfer to the neurons that nearby, which may cause slightly higher concentration of BDNF surround the astrocytes.[23] The BDNF peptides from BDNF-SFNPs construct has higher chance move towards to the neuron than astrocyte cells. These suggests that the BDNF peptides bound to their high-affinity receptor, TrkB.FL, on the surface of the neuron, which provides the potential of efficiently delivering drug to the target cells. The nano-based drug delivery system presented in this work could be targeted using peptide modified nanoparticles for intracellular delivery, thereby introducing an alternative therapeutic means to payload release and cellular programming.

We further investigated the release of the imbibed C3 transferase from SFNPs which downstream encourage axon outgrowth in cultured rat cortical neurons. The results indicated that increased temperature would release the C3 transferase imbibed in SFNPs within the neurons to promote process outgrowth from CST neurons. We further sought to determine if the induced release of C3 transferase increases neurite outgrowth after BDNF-derivatized SFNPs are taken up by CST neurons. These SFNPs undergo volumetric shrinking when exposed to increased temperature, so that if the nanoparticles are loaded with a therapeutic drug, that drug can be expelled upon SFNP shrinking. The neuronal cultures were kept at room temperature for 4 hours to allow the SFNPs to be uptake as determined from our previous study on SFNP uptake. This was done to prevent the maximum drug release from SFNPs that would occur at 37 °C until after endocytosis. To determine whether the release of C3 transferase from BDNF-derivatized SFNPs increased axon regrowth in CST neurons, we assessed the extent of neurite initiation and elongation from cultured neurons exposed to BDNF-SFNPs induced to release C3 transferase,

compared to non-derivatized SFNPs and bath application of BDNF or C3. The results demonstrate that the C3 released from the SFNPs increased neurite outgrowth compared with SFNPs without drug loading. The data is similar to previous work vitamin B12 can be released from similar nanoparticles using an oscillating magnetic field.[24] Similarly, imbibed cisplatin was released at 37 °C from a similar nanocarrier over a period of 100 hours.[24] The BDNF derivatized nano-based drug delivery systems offer the ability to enhance the efficacy of BBB crossing for poorly permeable drugs, and to deliver these drugs to specific cells. The addition of the targeting molecule, BDNF, did not affect the ability of SFNPs to cross the BBB model, indicating that the addition of targeting peptides is a viable strategy for use of our SFNP systems.

The SFNPs used in this study have different charges and sizes, which might affect their cell or BBB permeability and uptake. Clathrin-mediated endocytosis (CME) is the major endocytic pathway in mammalian cells and plays an important role of internalization of cationic nanoparticles.[25] Previous work with the same nanomaterial constructs studied here shows that N150 can be internalized through CME, but that this mechanism is not involved in the uptake of negatively charged particles.[25,26] Also, larger nanoparticles (up to 500 nm diameter) can be uptake by caveolae-mediated endocytosis.[27,28] Previous uptake studies using anionic magnetic nanoparticles in rat primary mixed cell cultures revealed that anionic SFNPs were preferentially taken up by neurons compare to glia. [29] We see further enhanced preferential neuronal uptake as compared to glial with BDNF derivatization suggesting that other mechanisms of internalization may be involved. Larger SFNPs can be derivatized with more targeting peptides and can carry more imbibed therapeutic drug. However, they are less efficient at crossing a BBB model than smaller SFNPs. While this may result in a similar therapeutic effect between using larger and smaller SFNPs and remains to be determined. Regardless of the details to be worked out, the

current BDNF-SFNP systems hold promise for the efficacious treatment of CNS disorders, including promoting axon regeneration and functional recovery after SCI. Hence, our study suggests that there may be specific circumstances where C750 would be a preferred carrier and when either N150 or C150 would be.

This dissertation has been performed to test whether adding a cell targeting peptide to SFNPs affects their ability to cross the BBB and facilitates uptake in specific target neurons to deliver a combinatorial therapy that efficiently promotes axon regeneration. In brief, we find that the SFNPs could be derivatized with BDNF, a ligand of the TrkB receptor that is expressed on CST neurons. We further find that the addition of BDNF facilitates specific uptake by CST neurons and release of C3 from BDNF derivatized SFNPs and enhances the outgrowth of processes from CST neurons. The SFNPs used here can be also be remotely actuated to release imbibed drugs by simply increasing the ambient temperature. SFNPs derivatized with BDNF can cross the BBB and be endocytosed by specific cells, namely CST neurons. According to the poor membrane permeability of C3 transferase, cell-permeable variants of C3 transferase facilitate its entry into CST neurons as constructed and tested in this work. Together, this nano-based drug delivery system is biocompatible, specifically endocytosed by rat cortical neurons, improves axon outgrowth, and crosses an *in-vitro* BBB, providing a greater potential to deliver therapeutics to precise locations within the CNS to encourage axon regeneration and functional recovery compared to previously constructed systems.

FUTURE STUDIES

Overall, nano-based drug delivery systems can provide exciting opportunities for improved therapeutic management of CNS diseases. The pharmaceutical industry can move forward to develop high molecular weight biotechnology products, which normally cannot cross

the BBB and could substantially benefit from the use of nanoparticles. However, this field is still in its beginning stages. Several issues should be resolved before nano-based drug delivery systems become useful in the clinic. Studies *in vivo* are needed to demonstrate these drug- loaded SFNPs are able to cross a complete intact BBB and target the specifically damaged neurons *in vivo*. Based on the lipiphilic nature of our SFNPs, we expect them to readily cross the BBB and accumulate in cerebral neurons.[30] If nanomaterials do not enter the CNS, directly injecting the constructs into ventricles or the brain parenchyma may be a viable alternative strategy for facilitating their accumulation in neurons. Direct injection of therapeutics into the CNS of humans can be done.[31] It is a possible route of application that most patients suffering from traumatic or neurodegenerative conditions would consider. Controlled release and removable of these SFNPs will also need to be considered to assess the clinical potential of SFNP drug delivery systems as efficient and safe therapeutic agents for neurodegenerative and neurotraumatic CNS disorders.[32]

Although nanotechnology has grown rapidly as a revolutionary therapy, some concerns still need to be addressed such as toxicity. As a therapy *in vivo*, nanoparticles have a tendency to accumulate in the liver or other organs.[33] The mechanisms for removing nanoparticles from the cells and organs of the body need to be further explored and addressed.

Together, future experimentation will test the feasibility of functionalized nanocarriers for targeted drug delivery to enhance axon regrowth following CNS damage. If successful, this nano-based drug delivery system will provide unique therapeutics that may use for the future treatment of brain or SCI or neurodegenerative conditions by allowing precise targeting, high solubility and tunabiliy, low toxicity, and high clearance therapeutics.

REFERENCES

Chapter I

1. Upadhyay RK. Drug delivery systems, CNS protection, and the blood–brain barrier. *Biomed Res Int*. 2014;2014:869269. doi:10.1155/2014/869269
2. Tyler JY, Xu XM, Cheng JX. Nanomedicine for treating spinal cord injury. *Nanoscale*. 2013;5(19):8821-36. doi:10.1039/c3nr00957b
3. Daneman R, Prat A. The blood–brain barrier. *Cold Spring Harb Perspect Biol*. 2015;7(1):a020412. doi:10.1101/cshperspect.a02041
4 Delsing L, Donnes P, Sanchez J, et al. Barrier properties and transcriptome expression in human IPSC-derived models of the blood–brain barrier. *Stem Cells*. 2018;36(12):1816-1827. doi:10.1002/stem.2908
5. Chen Y, Liu L. Modern methods for delivery of drugs across the blood–brain barrier. *Adv Drug Deliv Rev*. 2012;64(7):640-65. doi:10.1016/j.addr.2011.11.010
6. Hurlbert RJ, Hadley MN, Walters BC, et al. Pharmacological therapy for acute spinal cord injury. *Neurosurg*. 2013;72(2):93-105. doi:10.1227/NEU.0b013e31827765c6
7. GhoshMitra S, Diercks DR, Mills NC, Hynds DL, Ghosh S. Role of engineered nanocarriers for axon regeneration and guidance: current status and future trends. *Adv Drug Deliv Rev*. 2012;64(1):110-25. doi:10.1016/j.addr.2011.12.013
8. Albanese A, Tang PS, Chan WC. The effect of nanoparticle size, shape, and surface chemistry on biological systems. *Annu Rev Biomed Eng*. 2012;14:1-16. doi:10.1146/annurev-bioeng-071811-150124
9. Ding G, Guo Y, Lv Y, Liu X, Xu L, Zhang X. A double-targeted magnetic nanocarrier with potential application in hydrophobic drug delivery. *Colloids Surf B Biointerfaces*. 2012;91:68-76. doi:10.1016/j.colsurfb.2011.10.036
10. Gao S, Kumar RG, Wisniewski SR, Fabio A. disparities in health care utilization of adults with traumatic brain injuries are related to insurance, race, and ethnicity: a systematic review. *J Head Trauma Rehabil*. 2018;33(3):e40-e50. doi:10.1097/htr.0000000000000338
11. Nguyen KT, Pham MN, Vo TV, Duan W, Tran PH, Tran TT. Strategies of engineering nanoparticles for treating neurodegenerative disorders. *Curr Drug Metab*. 2017;18(9):786-797. doi:10.2174/1389200218666170125114751
12. Costa G, Ribeiro FF, Sebastião AM, Muir EM, Vaz SH. Bridging the gap of axonal regeneration in the central nervous system: a state of the art review on central axonal regeneration. *Front Neurosci*. 2022;16:1003145. doi:10.3389/fnins.2022.1003145
13. Burke SL, Maramaldi P, Cadet T, Kukull W. Associations between depression, sleep disturbance, and apolipoprotein E in the development of Alzheimer's disease: dementia. *Int Psychogeriatr*. 2016;28(9):1409-24. doi:10.1017/s1041610216000405
14. Egawa N, Lok J, Washida K, Arai K. Mechanisms of axonal damage and repair after central nervous system injury. *Transl Stroke Res.* 2017;8(1):14-21. doi:10.1007/s12975-016-0495-1
15. Bradke F. Mechanisms of axon growth and regeneration: moving between development and disease. *J Neurosci.* 2022;42(45):8393-8405. doi:10.1523/jneurosci.1131-22.2022
16. National Spinal Cord Injury Statistical Center. Spinal cord injury facts and figures at a glance. Updated 2020. Accessed January 9, 2023. https://www.nscisc.uab.edu/Public/Facts%20and%20Figures%202020.pdf

17. Yılmaz T, Turan Y, Keleş A. Pathophysiology of the spinal cord injury. *JCEI*. 2014;5(1). doi:10.5799/ahinjs.01.2014.01.0378
18. Anselmo AC, Mitragotri S. Nanoparticles in the clinic. *Bioeng Transl Med*. 2016;1(1):10-29. doi:10.1002/btm2.10003
19. Al-Ali H, Beckerman SR, Bixby JL, Lemmon VP. *In-vitro* models of axon regeneration. *Exp Neurol*. 2017;287(3):423-434. doi:10.1016/j.expneurol.2016.01.020
20. Dupraz S, Hilton BJ, Husch A, et al. RhoA controls axon extension independent of specification in the developing brain. *Curr Biol*. 18 2019;29(22):3874-3886. doi:10.1016/j.cub.2019.09.040
21. Hall A, Lalli G. Rho and Ras GTPases in axon growth, guidance, and branching. *Cold Spring Harb Perspect Biol*. 2010;2(2):a001818. doi:10.1101/cshperspect.a001818
22. Gomez TM, Letourneau PC. Actin dynamics in growth cone motility and navigation. *J Neurochem*. 2014;129(2):221-34. doi:10.1111/jnc.12506
23. Samuel F, Hynds DL. RHO GTPase signaling for axon extension: is prenylation important? *Mol Neurobiol*. 2010;42(2):133-42. doi:10.1007/s12035-010-8144-2
24. Schmandke A, Schmandke A, Strittmatter SM. ROCK and Rho: biochemistry and neuronal functions of Rho-associated protein kinases. *Neuroscientist*. 2007;13(5):454-69. doi:10.1177/1073858407303611
25. Zhang Z, Guiley KZ, Shokat KM. Chemical acylation of an acquired serine suppresses oncogenic signaling of K-Ras(G12S). *Nat Chem Biol*. 2022;18(11):1177-1183. doi:10.1038/s41589-022-01065-9
26. Tolias KF, Duman JG, Um K. Control of synapse development and plasticity by Rho GTPase regulatory proteins. *Prog Neurobiol*. 2011;94(2):133-48. doi:10.1016/j.pneurobio.2011.04.011
27. Dergham P, Ellezam B, Essagian C, Avedissian H, Lubell WD, McKerracher L. Rho signaling pathway targeted to promote spinal cord repair. *J Neurosci*. 2002;22(15):6570-6577. doi:10.1523/jneurosci.22-15-06570.2002
28. Gross RE, Mei Q, Gutekunst CA, Torre E. The pivotal role of RhoA GTPase in the molecular signaling of axon growth inhibition after CNS injury and targeted therapeutic strategies. *Cell Transplant*. 2007;16(3):245-62. doi:10.3727/000000007783464740
29. de Curtis I. Functions of Rac GTPases during neuronal development. *Dev Neurosci*. 2008;30(1-3):47-58. doi:10.1159/000109851
30. Fujita Y, Yamashita T. Axon growth inhibition by RhoA/ROCK in the central nervous system. *Front Neurosci*. 2014;8:338. doi:10.3389/fnins.2014.00338
31. Meyer G, Feldman EL. Signaling mechanisms that regulate actin-based motility processes in the nervous system. *J Neurochem*. 2002;83(3):490-503. doi:10.1046/j.1471-4159.2002.01185.x
32. Suetsugu S, Hattori M, Miki H, et al. Sustained activation of N-WASP through phosphorylation is essential for neurite extension. *Dev Cell*. 2002;3(5):645-658. doi:10.1016/S1534-5807(02)00324-6
33. Stern S, Hilton BJ, Burnside ER, et al. RhoA drives actin compaction to restrict axon regeneration and astrocyte reactivity after CNS injury. *Neuron*. 2021;109(21):3436-3455. doi:10.1016/j.neuron.2021.08.014
34. Madura T, Yamashita T, Kubo T, Fujitani M, Hosokawa K, Tohyama M. Activation of Rho in the injured axons following spinal cord injury. *EMBO Rep*. 2004;5(4):412-7. doi:10.1038/sj.embor.7400117

35. Mulherkar S, Tolias KF. RhoA-ROCK signaling as a therapeutic target in traumatic brain injury. *Cells*. 18 2020;9(1). doi:10.3390/cells9010245
36. Gungabissoon RA, Bamburg JR. Regulation of growth cone actin dynamics by ADF/cofilin. *J Histochem Cytochem*. 2003;51(4):411-20. doi:10.1177/002215540305100402
37. Boomkamp SD, Riehle MO, Wood J, Olson MF, Barnett SC. The development of a rat *in-vitro* model of spinal cord injury demonstrating the additive effects of Rho and ROCK inhibitors on neurite outgrowth and myelination. *Glia*. 2012;60(3):441-56. doi:10.1002/glia.22278
38. Boato F, Hendrix S, Huelsenbeck SC, et al. C3 peptide enhances recovery from spinal cord injury by improved regenerative growth of descending fiber tracts. *J Cell Sci*. 2010;123(10):1652-1662. doi:10.1242/jcs.066050
39. Hanada S, Fujioka K, Inoue Y, Kanaya F, Manome Y, Yamamoto K. Cell-based *in-vitro* blood–brain barrier model can rapidly evaluate nanoparticles' brain permeability in association with particle size and surface modification. *Int J Mol Sci*. 2014;15(2):1812-1825. doi:10.3390/ijms15021812
40. Holtje M, Just I, Ahnert-Hilger G. Clostridial C3 proteins: recent approaches to improve neuronal growth and regeneration. *Ann Anat*. 2011;193(4):314-20. doi:10.1016/j.aanat.2011.01.008
41. Lehmann M, Fournier A, Selles-Navarro I, et al. Inactivation of Rho signaling pathway promotes CNS axon regeneration. *J Neurosci*. 1999;19(17):7537-7547. doi:10.1523/jneurosci.19-17-07537.1999
42. Gutekunst CA, Tung JK, McDougal ME, Gross RE. C3 transferase gene therapy for continuous conditional RhoA inhibition. *Neurosci*. 2016;339:308-318. doi:10.1016/j.neuroscience.2016.10.022
43. Huelsenbeck SC, Rohrbeck A, Handreck A, et al. C3 peptide promotes axonal regeneration and functional motor recovery after peripheral nerve injury. *Neurotherapeutics*. 2012;9(1):185-98. doi:10.1007/s13311-011-0072-y
44. Bertrand J, Di Polo A, McKerracher L. Enhanced survival and regeneration of axotomized retinal neurons by repeated delivery of cell-permeable C3-like Rho antagonists. *Neurobiol Dis*. 2007;25(1):65-72. doi:10.1016/j.nbd.2006.08.008
45. Lord-Fontaine S, Yang F, Diep Q, et al. Local inhibition of rho signaling by cell-permeable recombinant protein BA-210 prevents secondary damage and promotes functional recovery following acute spinal cord injury. *J Neurotrauma*. 2008;25(11):1309-1322. doi:10.1089/neu.2008.0613
46. Fehlings MG, Chen Y, Aarabi B, et al. A randomized controlled trial of local delivery of a Rho inhibitor (VX-210) in patients with acute traumatic cervical spinal cord injury. *J Neurotrauma*. 2021;38(15):2065-2072. doi:10.1089/neu.2020.7096
47. Li N, Leung GK. Oligodendrocyte precursor cells in spinal cord injury: a review and update. *Biomed Res Int*. 2015:235195. doi:10.1155/2015/235195
48. Kim J, Ahn SI, Kim Y. Nanotherapeutics engineered to cross the blood–brain barrier for advanced drug delivery to the central nervous system. *J Ind Eng Chem*. 2019;73:8-18. doi:10.1016/j.jiec.2019.01.021
49. Duck KA, Simpson IA, Connor JR. Regulatory mechanisms for iron transport across the blood–brain barrier. *Biochem Biophys Res Commun*. 2017;494(1-2):70-75. doi:10.1016/j.bbrc.2017.10.083

50. Gabathuler R. Approaches to transport therapeutic drugs across the blood–brain barrier to treat brain diseases. *Neurobiol Dis*. 2010;37(1):48-57. doi:10.1016/j.nbd.2009.07.028
51. Bellettato CM, Scarpa M. Possible strategies to cross the blood–brain barrier. *Ital J Pediatr*. 2018;44(2):131. doi:10.1186/s13052-018-0563-0
52. Tashima T. Smart strategies for therapeutic agent delivery into brain across the blood–brain barrier using receptor-mediated transcytosis. *Chem Pharm Bull (Tokyo)*. 2020;68(4):316-325. doi:10.1248/cpb.c19-00854
53. Ding S, Khan AI, Cai X, et al. Overcoming blood–brain barrier transport: advances in nanoparticle-based drug delivery strategies. *Mater Today*. 2020;37:112-125. doi:10.1016/j.mattod.2020.02.001
54. Ronn LC, Doherty P, Holm A, Berezin V, Bock E. Neurite outgrowth induced by a synthetic peptide ligand of neural cell adhesion molecule requires fibroblast growth factor receptor activation. *J Neurochem*. 2000;75(2):665-71. doi:10.1046/j.1471-4159.2000.0750665.x
55. Alam M, Najmi AK, Ahmad I, et al. Formulation and evaluation of nano lipid formulation containing CNS acting drug: molecular docking, *in-vitro* assessment and bioactivity detail in rats. *Artif Cells Nanomed Biotechnol*. 2018;46(2):46-57. doi:10.1080/21691401.2018.1451873
56. Sahu MP, Nikkila O, Lagas S, Kolehmainen S, Castren E. Culturing primary neurons from rat hippocampus and cortex. *Neuronal Signal*. 2019;3(2):NS20180207. doi:10.1042/NS20180207
57. Amoozgar Z, Yeo Y. Recent advances in stealth coating of nanoparticle drug delivery systems. *Wiley Interdiscip Rev Nanomed Nanobiotechnol*. 2012;4(2):219-33. doi:10.1002/wnan.1157
58. Wong HL, Wu XY, Bendayan R. Nanotechnological advances for the delivery of CNS therapeutics. *Adv Drug Deliv Rev*. 2012;64(7):686-700. doi:10.1016/j.addr.2011.10.007
59. Sharma G, Sharma AR, Lee SS, Bhattacharya M, Nam JS, Chakraborty C. Advances in nanocarriers enabled brain targeted drug delivery across blood–brain barrier. *Int J Pharm*. 2019;559:360-372. doi:10.1016/j.ijpharm.2019.01.056
60. Farokhzad OC, Langer R. Impact of nanotechnology on drug delivery. *ACS Nano*. 2009;3(1):16-20. doi:10.1021/nn900002m
61. Carton F, Malatesta M. Assessing the interactions between nanoparticles and biological barriers *in vitro*: a new challenge for microscopy techniques in nanomedicine. *Eur J Histochem*. 2022;66(4). doi:10.4081/ejh.2022.3603
62. Ghosh S, Ghoshmitra S, Cai T, Diercks DR, Mills NC, Hynds DL. Alternating magnetic field controlled, multifunctional nano-reservoirs: intracellular uptake and improved biocompatibility. *Nanoscale Res Lett*. 2009;5(1):195-204. doi:10.1007/s11671-009-9465-9
63. GhoshMitra S, Cai T, Diercks D, et al. Evaluation of the biological effects of externally tunable, hydrogel encapsulated quantum dot nanospheres in escherichia coli. *Polymers*. 2011;3(3):1243-1254. doi:10.3390/polym3031243
64. Singh R, Lillard JW, Jr. Nanoparticle-based targeted drug delivery. *Exp Mol Pathol*. 2009;86(3):215-23. doi:10.1016/j.yexmp.2008.12.004
65. GhoshMitra S, Diercks DR, Mills NC, Hynds DA, Ghosh S. Moderate level exposure to magnetic nanodots encased in tunable poly(ethylene glycol) analouge biopolymer shell

do not deleteriously affect neurite outgrowth. *J Nanosci Nanotechnol*. 2013;13(12):8290-7. doi:10.1166/jnn.2013.8015
66. Sung B, Kim MH, Abelmann L. Magnetic microgels and nanogels: physical mechanisms and biomedical applications. *Bioeng Transl Med*. 2021;6(1):e10190. doi:10.1002/btm2.10190
67. Canfarotta F, Piletsky SA. Engineered magnetic nanoparticles for biomedical applications. *Adv Healthc Mater*. 2014;3(2):160-175. doi:10.1002/adhm.201300141
68. Mukalel AJ, Riley RS, Zhang R, Mitchell MJ. Nanoparticles for nucleic acid delivery: applications in cancer immunotherapy. *Cancer Lett*. 2019;458:102-112. doi:10.1016/j.canlet.2019.04.040
69. Liu M, Fang X, Yang Y, Wang C. Peptide-enabled targeted delivery systems for therapeutic applications. *Front Bioeng Biotechnol*. 2021;9:701504. doi:10.3389/fbioe.2021.701504
70. Liu G, Men P, Kudo W, Perry G, Smith MA. Nanoparticle-chelator conjugates as inhibitors of amyloid-beta aggregation and neurotoxicity: a novel therapeutic approach for Alzheimer disease. *Neurosci Lett*. 2009;455(3):187-90. doi:10.1016/j.neulet.2009.03.064
71. Guo T, Zhang D, Zeng Y, Huang TY, Xu H, Zhao Y. Molecular and cellular mechanisms underlying the pathogenesis of Alzheimer's disease. *Mol Neurodegener*. 2020;15(1):40. doi:10.1186/s13024-020-00391-7
72. Veettil RA. *Polyethylene glycol copolymer nanocarriers: biocompatibility, uptake and intracellular trafficking in neurons.* Dissertation. Texas Woman's University; 2017.
73. Sebastian S. *Drug release kinetics and blood–brain barrier crossing efficacy of polymer encapsulated magnetic nanocarriers*. Dissertation. Texas Woman's University; 2019.
74. Oudega M, Perez MA. Corticospinal reorganization after spinal cord injury. *J Physiol*. 2012;590(16):3647-63. doi:10.1113/jphysiol.2012.233189
75. Bathina S, Das UN. Brain-derived neurotrophic factor and its clinical implications. *Arch Med Sci*. 2015;11(6):1164-78. doi:10.5114/aoms.2015.56342
76. Pradhan J, Noakes PG, Bellingham MC. The role of altered BDNF/TrkB signaling in amyotrophic lateral sclerosis. *Front Cell Neurosci*. 2019;13:368. doi:10.3389/fncel.2019.00368

Chapter II

Afzal O, Altamimi ASA, Nadeem MS, et al. Nanoparticles in drug delivery: from history to therapeutic applications. *Nanomaterials*. 2022;12(24):4494. doi:10.3390/nano12244494

Ahlawat J, Guillama Barroso G, Masoudi Asil S, et al. Nanocarriers as potential drug delivery candidates for overcoming the blood–brain barrier: challenges and possibilities. *ACS Omega*. 2020;5(22):12583-12595. doi:10.1021/acsomega.0c01592

Albanese A, Tang PS, Chan WCW. The Effect of nanoparticle size, shape, and surface chemistry on biological systems. *Annu Rev Biomed Eng*. 2012;14(1):1-16. doi:10.1146/annurev-bioeng-071811-150124

Anselmo AC, Mitragotri S. Nanoparticles in the clinic. *Bioeng Transl Med*. 2016;1(1):10-29. doi:10.1002/btm2.10003

Bellettato CM, Scarpa M. Possible strategies to cross the blood–brain barrier. *Ital J Pediatr*. 2018;44(2). doi:10.1186/s13052-018-0563-0

Biroudian S, Abbasi M, Kiani M. Theoretical and practical principles on nanoethics: a narrative review article. *Iran J Public Health*. 2019;48(10):1760-1767. https://pubmed.ncbi.nlm.nih.gov/31850252/
Duck KA, Simpson IA, Connor JR. Regulatory mechanisms for iron transport across the blood–brain barrier. *Biochem Biophys Res Commun*. 2017;494(1-2):70-75. doi:10.1016/j.bbrc.2017.10.083
Ghosh S, GhoshMitra S, Cai T, Diercks DR, Mills NC, Hynds DL. Alternating magnetic field controlled, multifunctional nano-reservoirs: intracellular uptake and improved biocompatibility. *Nanoscale Res Lett*. 2009;5(1). doi:10.1007/s11671-009-9465-9
GhoshMitra S, Cai T, Diercks D, et al. Evaluation of the biological effects of externally tunable, hydrogel encapsulated quantum dot nanospheres in escherichia coli. *Polymers*. 2011;3(3):1243-1254. doi:10.3390/polym3031243
Gil ES, Lowe TL. Invention of polysaccharide-base nanoparticles for enhancing drug permeability across the blood–brain barrier. *TechConnect Briefs*. 2008;2(2008):379-381. https://briefs.techconnect.org/papers/invention-of-polysaccharide-base-nanoparticles-for-enhancing-drug-permeability-across-the-blood–brain-barrier/
Hanada S, Fujioka K, Inoue Y, Kanaya F, Manome Y, Yamamoto K. Cell-based *in-vitro* blood–brain barrier model can rapidly evaluate nanoparticles' brain permeability in association with particle size and surface modification. *Inter J Mol Sci*. 2014;15(2):1812-1825. doi:10.3390/ijms15021812
Hurlbert RJ, Hadley MN, Walters BC, et al. pharmacological therapy for acute spinal cord injury. *Neurosurg*. 2013;72(2):93-105. doi:10.1227/neu.0b013e31827765c6
Jiang Y, Fay JM, Poon CD, et al. Nanoformulation of brain-derived neurotrophic factor with target receptor-triggered-release in the central nervous system. *Adv Funct Mater*. 2018;28(6):1703982. doi:10.1002/adfm.201703982
Khan I, Saeed K, Khan I. Nanoparticles: properties, applications and toxicities. *Arab J Chem*. 2017;12(7). doi:10.1016/j.arabjc.2017.05.011
Kim J, Ahn SI, Kim Y. Nanotherapeutics engineered to cross the blood–brain barrier for advanced drug delivery to the central nervous system. *J Industr Eng Chem*. 2019;73:8-18. doi:10.1016/j.jiec.2019.01.021
Lombardo SM, Schneider M, Türeli AE, Türeli NG. Key for crossing the bbb with nanoparticles: the rational design. *Beilstein J Nanotechnol*. 2020;11(1):866-883. doi:10.3762/bjnano.11.72
Martin JH. Neuroplasticity of spinal cord injury and repair. *Handb Clin Neurol*. 2022;184:317-330. doi:10.1016/b978-0-12-819410-2.00017-5
Mitusova K, Peltek OO, Karpov TE, Muslimov AR, Zyuzin MV, Timin AS. Overcoming the blood–brain barrier for the therapy of malignant brain tumor: current status and prospects of drug delivery approaches. *J Nanobiotechnol*. 2022;20(1):412. doi:10.1186/s12951-022-01610-7
National Spinal Cord Injury Statistical Center. Spinal cord injury facts and figures at a glance. Updated 2020. Accessed January 9, 2023. https://www.nscisc.uab.edu/Public/Facts%20and%20Figures%202020.pdf
Nguyen KT, Pham MN, Vo TV, Duan W, Tran PHL, Tran TTD. Strategies of engineering nanoparticles for treating neurodegenerative disorders. *Curr Drug Metab*. 2017;18(9). doi:10.2174/1389200218666170125114751
Pandey PK, Sharma AK, Gupta U. Blood–brain barrier: an overview on strategies in drug delivery, realistic *in-vitro* modeling and *in vivo* live tracking. *Tissue Barriers*. 2015;4(1):e1129476. doi:10.1080/21688370.2015.1129476

Patra JK, Das G, Fraceto LF, et al. Nano based drug delivery systems: recent developments and future prospects. *J Nanobiotechnol*. 2018;16(1). doi:10.1186/s12951-018-0392-8
Pilakka-Kanthikeel S, Atluri VSR, Sagar V, Saxena SK, Nair M. Targeted brain derived neurotropic factors (BDNF) delivery across the blood–brain barrier for neuro-protection using magnetic nano carriers: an *in-vitro* study. *PLoS ONE*. 2013;8(4):e62241. doi:10.1371/journal.pone.0062241
Sebastian S. *Drug release kinetics and blood–brain barrier crossing efficacy of polymer encapsulated magnetic nanocarriers*. Dissertation. Texas Woman's University; 2019.
Singh R, Lillard JW. Nanoparticle-based targeted drug delivery. *Exp Mol Path*. 2009;86(3):215-223. doi:10.1016/j.yexmp.2008.12.004
Sonavane G, Tomoda K, Makino K. Biodistribution of colloidal gold nanoparticles after intravenous administration: effect of particle size. *Biointerfaces*. 2008;66(2):274-280. doi:10.1016/j.colsurfb.2008.07.004
Tashima T. Smart strategies for therapeutic agent delivery into brain across the blood–brain barrier using receptor-mediated transcytosis. *Chem Pharm Bull (Tokyo)*. 2020;68(4):316-325. doi:10.1248/cpb.c19-00854
Tyler JY, Xu XM, Cheng JX. Nanomedicine for treating spinal cord injury. *Nanoscale*. 2013;5(19):8821-8836. doi:10.1039/c3nr00957b
Veettil RA. *Polyethylene glycol copolymer nanocarriers: biocompatibility, uptake and intracellular trafficking in neurons.* Dissertation. Texas Woman's University; 2017.
Yetisgin AA, Cetinel S, Zuvin M, Kosar A, Kutlu O. Therapeutic nanoparticles and their targeted delivery applications. *Molecules*. 2020;25(9):2193. doi:10.3390/molecules25092193
Zhang H, Liu Y, Zhou K, Wei W, Liu Y. Restoring sensorimotor function through neuromodulation after spinal cord injury: progress and remaining challenges. *Front Neurosci*. 2021;15. doi:10.3389/fnins.2021.749465
Zhou Y, Peng Z, Seven ES, Leblanc RM. Crossing the blood–brain barrier with nanoparticles. *J Control Release*. 2018;270:290-303. doi:10.1016/j.jconrel.2017.12.015
Chapter III
Begley DJ. Delivery of therapeutic agents to the central nervous system: the problems and the possibilities. *Pharmacol Ther*. 2004;104(1):29-45.
Chen TC, Mackic JB, Mackic JB, et al. Cellular uptake and transport of methylprednisolone at the blood–brain barrier. *Neurosurg*. 1996;38(2):348-354. doi:10.1097/00006123-199602000-00023
Georgieva JV, Brinkhuis RP, Stojanov K, et al. Peptide-mediated blood–brain barrier transport of polymersomes. *Angew Chem Int Ed Engl*. 2012;51(33):8339-8342. doi:10.1002/anie.201202001
Gilleron J, Querbes W, Zeigerer A, et al. Image-based analysis of lipid nanoparticle-mediated siRNA delivery, intracellular trafficking and endosomal escape. *Nat Biotechnol*. 2013;31(7):638-646. doi:10.1038/nbt.2612
Glueckert R, Pritz CO, Roy S, Dudas J, Schrott-Fischer A. Nanoparticle mediated drug delivery of rolipram to tyrosine kinase B positive cells in the inner ear with targeting peptides and agonistic antibodies. *Front Aging Neurosci*. 2015;7:71. doi:10.3389/fnagi.2015.00071
Hu J, Zhang G, Rodemer W, Jin LQ, Shifman M, Selzer ME. The role of RhoA in retrograde neuronal death and axon regeneration after spinal cord injury. *Neurobiol Dis*. 2017;98:25-35. doi:10.1016/j.nbd.2016.11.006

Jeong W, Bu J, Kubiatowicz LJ, Chen SS, Kim Y, Hong S. Peptide–nanoparticle conjugates: a next generation of diagnostic and therapeutic platforms? *Nano Converg*. 2018;5(1):38. doi:10.1186/s40580-018-0170-1
Jin. Regulation of BDNF-TrkB signaling and potential therapeutic strategies for parkinson's disease. *J Clin Med*. 2020;9(1):257. doi:10.3390/jcm9010257
Kim J, Ahn SI, Kim Y. Nanotherapeutics engineered to cross the blood–brain barrier for advanced drug delivery to the central nervous system. *J Ind Eng Chem.* 2019;73:8-18. doi:10.1016/j.jiec.2019.01.021
Li X, Qinfeng Wu, Caizhong Xie, et al. Blocking of BDNF-TrkB signaling inhibits the promotion effect of neurological function recovery after treadmill training in rats with spinal cord injury. *Spinal Cord*. 2019;57(1):65-74. doi:10.1038/s41393-018-0173-0
Liu M, Fang X, Yang Y, Wang C. Peptide-enabled targeted delivery systems for therapeutic applications. *Front Bioeng Biotechnol*. 2021;9:701504. doi:10.3389/fbioe.2021.701504
McNeil SE. Nanotechnology for the biologist. *J Leukoc Biol.* 2005;78(3):585-594. doi:10.1189/jlb.0205074
Mitusova K, Peltek OO, Karpov TE, Muslimov AR, Zyuzin MV, Timin AS. Overcoming the blood–brain barrier for the therapy of malignant brain tumor: current status and prospects of drug delivery approaches. *J Nanobiotechnol*. 2022;20(1):412. doi:10.1186/s12951-022-01610-7
Papa S, Rossi F, Vismara I, Forloni G, Veglianese P. Nanovector-mediated drug delivery in spinal cord injury: a multitarget approach. *ACS Chem Neurosci*. 2019;10(3):1173-1182. doi:10.1021/acschemneuro.8b00700
Persidsky Y. Rho-mediated regulation of tight junctions during monocyte migration across the blood–brain barrier in HIV-1 encephalitis (HIVE). *Blood*. 2006;107(12):4770-4780. doi:10.1182/blood-2005-11-4721
Ronn LC, Doherty P, Holm A, Berezin V, Bock E. Neurite outgrowth induced by a synthetic peptide ligand of neural cell adhesion molecule requires fibroblast growth factor receptor activation. *J Neurochem*. 2000;75(2):665-71. doi:10.1046/j.1471- 4159.2000.0750665.x
Sahoo SK, Labhasetwar V. Nanotech approaches to drug delivery and imaging. *Drug Discov Today*. 2003;8(24):1112-1120. doi:10.1016/s1359-6446(03)02903-9
Sahu M, Nikkilä O, Lågas S, Kolehmainen S, Castrén E. Culturing primary neurons from rat hippocampus and cortex. *Neuronal Signal*. 2019;3(2). doi:10.1042/ns20180207
Singh R, Lillard JW. Nanoparticle-based targeted drug delivery. *Exp Mol Pathol*. 2009;86(3):215-223. doi:10.1016/j.yexmp.2008.12.004
Tedeschi A, Bradke F. Spatial and temporal arrangement of neuronal intrinsic and extrinsic mechanisms controlling axon regeneration. *Curr Opin Neurobiol*. 2017;42:118-127. doi:10.1016/j.conb.2016.12.005
Veettil RA. *Polyethylene glycol copolymer nanocarriers: biocompatibility, uptake and intracellular trafficking in neurons.* Dissertation. Texas Woman's University; 2017.
Watson PMD, Paterson JC, Thom G, Ginman U, Lundquist S, Webster CI. Modelling the endothelial blood-CNS barriers: a method for the production of robust *in-vitro* models of the rat blood–brain barrier and blood-spinal cord barrier. *BMC Neurosci*. 2013;14(1). doi:10.1186/1471-2202-14-59
Wen H, Jung H, Li X. Drug Delivery Approaches in addressing clinical pharmacology-related issues: opportunities and challenges. *AAPS J*. 2015;17(6):1327-1340. doi:10.1208/s12248-015-9814-9
Chapter IV

Cooke P, Janowitz H, Dougherty SE. Neuronal redevelopment and the regeneration of neuromodulatory axons in the adult mammalian central nervous system. *Front Cell Neurosci.* 2022;16:872501. doi:10.3389/fncel.2022.872501
Huebner EA, Strittmatter SM. Axon regeneration in the peripheral and central nervous systems. *Results Probl Cell Differ*. 2009;48:305-360. doi:10.1007/400_2009_19
Fawcett JW. The struggle to make CNS axons regenerate: why has it been so difficult? *Neurochem Res*. 2019;45(1):144-158. doi:10.1007/s11064-019-02844-y
Houlton J, Abumaria N, Hinkley SFR, Clarkson AN. Therapeutic potential of neurotrophins for repair after brain injury: a helping hand from biomaterials. *Front Neurosci.* 2019;13:790. doi:10.3389/fnins.2019.00790
Shi J, Votruba AR, Farokhzad OC, Langer R. Nanotechnology in drug delivery and tissue engineering: from discovery to applications. *Nano Lett*. 2010;10(9):3223-3230. doi:10.1021/nl102184c
Huelsenbeck SC, Rohrbeck A, Handreck A, et al. C3 peptide promotes axonal regeneration and functional motor recovery after peripheral nerve injury. *Neurotherapeutics*. 2011;9(1):185-198. doi:10.1007/s13311-011-0072-y
Jin. Regulation of BDNF-TrkB signaling and potential therapeutic strategies for Parkinson's disease. *J Cli Med*. 2020;9(1):257. doi:10.3390/jcm9010257
Meltzer S, Santiago C, Sharma N, Ginty DD. The cellular and molecular basis of somatosensory neuron development. *Neuron*. 2021;109(23):3736-3757. doi:10.1016/j.neuron.2021.09.004
Mahar M, Cavalli V. Intrinsic mechanisms of neuronal axon regeneration. *Nat Rev Neurosci.* 2018;19(6):323-337. doi:10.1038/s41583-018-0001-8
Keefe K, Sheikh I, Smith G. Targeting neurotrophins to specific populations of neurons: ngf, bdnf, and nt-3 and their relevance for treatment of spinal cord injury. *Int J Mol Sci.* 2017;18(3):548. doi:10.3390/ijms18030548
Rizvi SAA, Saleh AM. Applications of nanoparticle systems in drug delivery technology. *Saudi Pharm J*. 2018;26(1):64-70. doi:10.1016/j.jsps.2017.10.012
Ning S, Jorfi M, Patel SR, Kim DY, Tanzi RE. Neurotechnological approaches to the diagnosis and treatment of Alzheimer's disease. *Front Neurosci*. 2022;16:854992. doi:10.3389/fnins.2022.854992
Tam RY, Fuehrmann T, Mitrousis N, Shoichet MS. Regenerative therapies for central nervous system diseases: a biomaterials approach. *Neuropsychopharmacol*. 2013;39(1):169-188. doi:10.1038/npp.2013.237
Naqvi S, Panghal A, Flora SJS. Nanotechnology: a promising approach for delivery of neuroprotective drugs. *Front Neurosci.* 2020;14:94. doi:10.3389/fnins.2020.00494
Jacobs WB, Fehlings MG. The molecular basis of neural regeneration. *Neurosurg*. 2003;53(4):943-950. doi:10.1227/01.neu.0000083592.74383.b1
Tsou YH, Zhang XQ, Zhu H, Syed S, Xu X. Drug delivery to the brain across the blood–brain barrier using nanomaterials. *Small*. 2017;13(43):1701921. doi:10.1002/smll.201701921
Patel T, Zhou J, Piepmeier JM, Saltzman WM. Polymeric nanoparticles for drug delivery to the central nervous system. *Adv Drug Deliv Reviews*. 2012;64(7):701-705. doi:10.1016/j.addr.2011.12.006
Kim YG, Kim JW, Pyeon HJ, et al. differential stimulation of neurotrophin release by the biocompatible nano-material (carbon nanotube) in primary cultured neurons. *J Biomater Appl.* 2013;28(5):790-797. doi:10.1177/0885328213481637

Kuhn DA, Vanhecke D, Michen B, et al. Different endocytotic uptake mechanisms for nanoparticles in epithelial cells and macrophages. *Beilstein J Nanotechnol*. 2014;5:1625-1636. doi:10.3762/bjnano.5.174
Reddy JM, Raut NGR, Seifert JL, Hynds DL. Regulation of small GTPase prenylation in the nervous system. *Mol Neurobiol*. 2020;57(5):2220-2231. doi:10.1007/s12035-020-01870-0
Hu J, Zhang G, Rodemer W, Jin LQ, Shifman M, Selzer ME. The role of RhoA in retrograde neuronal death and axon regeneration after spinal cord injury. *Neurobiol Dis*. 2017;98:25-35. doi:10.1016/j.nbd.2016.11.006
Zhang G, Hu J, Rodemer W, Li S, Selzer ME. RhoA activation in axotomy-induced neuronal death. *Exp Neurol*. 2018;306:76-91. doi:10.1016/j.expneurol.2018.04.015
Fournier AE, Takizawa BT, Strittmatter SM. Rho kinase inhibition enhances axonal regeneration in the injured CNS. *J Neurosci*. 2003;23(4):1416-1423. doi:10.1523/jneurosci.23-04-01416.2003
Kopp MA, Liebscher T, Watzlawick R, et al. SCISSOR—spinal cord injury study on small molecule-derived Rho inhibition: a clinical study protocol. *BMJ Open*. 2016;6(7). doi:10.1136/bmjopen-2015-010651
Stern S, Hilton BJ, Burnside ER, et al. RhoA drives actin compaction to restrict axon regeneration and astrocyte reactivity after cns injury. *Neuron*. 2021;109(21):3436-3455. doi:10.1016/j.neuron.2021.08.014
Mulherkar S, Tolias KF. RhoA-ROCK signaling as a therapeutic target in traumatic brain injury. *Cells*. 2020;9(1):245. doi:10.3390/cells9010245
Gutekunst CA, Tung JK, McDougal ME, Gross RE. C3 transferase gene therapy for continuous conditional RhoA inhibition. *NeuroSci*. 2016;339:308-318. doi:10.1016/j.neuroscience.2016.10.022
Forgione N, Fehlings MG. Rho-ROCK inhibition in the treatment of spinal cord injury. *World Neurosurg*. 2014;82(3-4):e535-e539. doi:10.1016/j.wneu.2013.01.009
Lehmann M, Fournier A, Selles-Navarro I, et al. Inactivation of Rho signaling pathway promotes CNS axon regeneration. *J Neurosci*. 1999;19(17):7537-7547. doi:10.1523/jneurosci.19-17-07537.1999
Wilde C, Aktories K. The Rho-ADP-ribosylating C3 exoenzyme from clostridium botulinum and related C3-like transferases. *Toxicon*. 2001;39(11):1647-1660. doi:10.1016/s0041-0101(01)00152-0
Santiago-Lopez AJ, Gutekunst CA, Gross RE. C3 Transferase gene therapy for continuous RhoA inhibition. *Methods Mol Biol*. 2018;1821:267-281. doi:10.1007/978-1-4939-8612-5_19
Vogelsgesang M, Pautsch A, Aktories K. C3 exoenzymes, Novel insights into structure and action of Rho-ADP-ribosylating toxins. *Naunyn-Schmiedeberg's Arch Pharmacol*. 2006;374(5-6):347-360. doi:10.1007/s00210-006-0113-y
Coumans JV, Lin TTS, Dai HN, et al. Axonal regeneration and functional recovery after complete spinal cord transection in rats by delayed treatment with transplants and neurotrophins. *J Neurosci*. 2001;21(23):9334-9344. doi:10.1523/jneurosci.21-23-09334.2001
Durán WN, Sánchez FA, Breslin JW. Microcirculatory exchange function. *Microcirculation*. 2008;2008:81-124. doi:10.1016/b978-0-12-374530-9.00004-8
Auer M, Allodi I, Barham M, et al. C3 exoenzyme lacks effects on peripheral axon regeneration *in vivo*. *J Peripher Nerv Syst*. 2013;18(1):30-36. doi:10.1111/jns5.12004

Chapter V

1. Boato F, Hendrix S, Huelsenbeck SC, et al. C3 peptide enhances recovery from spinal cord injury by improved regenerative growth of descending fiber tracts. *J Cell Sci*. 2010;123(Pt 10):1652-62. doi:10.1242/jcs.066050
2. Karimi M, Sahandi Zangabad P, Ghasemi A, et al. temperature-responsive smart nanocarriers for delivery of therapeutic agents: applications and recent advances. *ACS Appl Mater Interfaces*. 2016;8(33):21107-33. doi:10.1021/acsami.6b00371
3. Gutekunst CA, Tung JK, McDougal ME, Gross RE. C3 transferase gene therapy for continuous conditional RhoA inhibition. *Neuroscience*. 2016;339:308-318. doi:10.1016/j.neuroscience.2016.10.022
4. Bellettato CM, Scarpa M. Possible strategies to cross the blood–brain barrier. *Ital J Pediatr*. 2018;44(2):131. doi:10.1186/s13052-018-0563-0
5. Ding S, Khan AI, Cai X, et al. Overcoming blood–brain barrier transport: advances in nanoparticle-based drug delivery strategies. *Mater Today*. 2020;37:112-125. doi:10.1016/j.mattod.2020.02.001
6. Cui B, Cho SW. Blood–brain barrier-on-a-chip for brain disease modeling and drug testing. *BMB Rep*. 2022;55(5):213-219. doi:10.5483/BMBRep.2022.55.5.043
7. Ferro MP, Heilshorn SC, Owens RM. Materials for blood–brain barrier modeling *in vitro*. *Mater Sci Eng R Rep*. 2020;140:100522. doi: 10.1016/j.mser.2019.100522
8. Sakolish CM, Esch MB, Hickman JJ, Shuler ML, Mahler GJ. Modeling barrier tissues *in vitro*: methods, achievements, and challenges. *EBioMedicine*. 2016;5:30-9. doi:10.1016/j.ebiom.2016.02.023
9. Lippmann ES, Al-Ahmad A, Palecek SP, Shusta EV. Modeling the blood–brain barrier using stem cell sources. *Fluids Barriers CNS*. 2013;10(1):2. doi:10.1186/2045-8118-10-2
10. Paving the way toward complex blood–brain barrier models using pluripotent stem cells. *Stem Cells Dev*. 2017;26(12):857-874. doi:10.1089/scd.2017.0003
11. Abbott NJ, Patabendige AAK, Dolman DEM, Yusof SR, Begley DJ. Structure and function of the blood–brain barrier. *Neurobiol Dis*. 2010;37(1):13-25. doi: 10.1016/j.nbd.2009.07.030
12. Ye M, Sanchez HM, Hultz M, et al. Brain microvascular endothelial cells resist elongation due to curvature and shear stress. *Sci Rep*. 2014/04/15 2014;4(1):4681. doi:10.1038/srep04681
13. Suk JS, Xu Q, Kim N, Hanes J, Ensign LM. PEGylation as a strategy for improving nanoparticle-based drug and gene delivery. *Adv Drug Deliv Rev*. 2016;99(A):28-51. doi:10.1016/j.addr.2015.09.012
14. Chenthamara D, Subramaniam S, Ramakrishnan SG, et al. Therapeutic efficacy of nanoparticles and routes of administration. *Biomater Res*. 2019;23(1):20. doi:10.1186/s40824-019-0166-x
15. Xia W, Tao Z, Zhu B, et al. Targeted delivery of drugs and genes using polymer nanocarriers for cancer therapy. *Int J Mol Sci*. 2021;22(17). doi:10.3390/ijms22179118
16. Gaudet AD, Fonken LK. Glial cells shape pathology and repair after spinal cord injury. *Neurotherapeutics*. 2018;15(3):554-577. doi:10.1007/s13311-018-0630-7
17. Cao T, Matyas JJ, Renn CL, Faden AI, Dorsey SG, Wu J. Function and mechanisms of truncated BDNF receptor TrkB.T1 in neuropathic pain. *Cells*. 2020;9(5):1194.
18. Yajima Y, Narita M, Narita M, Matsumoto N, Suzuki T. Involvement of a spinal brain-derived neurotrophic factor/full-length TrkB pathway in the development of nerve injury-

induced thermal hyperalgesia in mice. *Brain Res*. 2002;958(2):338-346. doi:10.1016/S0006-8993(02)03666-1
19. Renn CL, Leitch CC, Dorsey SG. *In vivo* evidence that truncated Trkb.T1 participates in nociception. *Mol Pain*. 2009;5:1744-8069-5-61. doi:10.1186/1744-8069-5-61
20. Luberg K, Wong J, Weickert CS, Timmusk T. Human TrkB gene: novel alternative transcripts, protein isoforms and expression pattern in the prefrontal cerebral cortex during postnatal development. *J of Neurochem*. 2010;113(4):952-964. doi: 10.1111/j.1471-4159.2010.06662.x
21. Carim-Todd L, Bath KG, Fulgenzi G, et al. Endogenous truncated TrkB.T1 receptor regulates neuronal complexity and TrkB kinase receptor function *in vivo*. *J Neurosci*. 2009;29(3):678. doi:10.1523/JNEUROSCI.5060-08.2009
22. Zhou LJ, Yang T, Wei X, et al. Brain-derived neurotrophic factor contributes to spinal long-term potentiation and mechanical hypersensitivity by activation of spinal microglia in rat. *Brain Behav Immun*. 2011;25(2):322-334. doi:10.1016/j.bbi.2010.09.025
23. Tejeda GS, Díaz-Guerra M. Integral characterization of defective BDNF/TrkB signalling in neurological and psychiatric disorders leads the way to new therapies. *Int J Mol Sci*. 2017;18(2):268.
24. Ghosh S, Ghoshmitra S, Cai T, Diercks DR, Mills NC, Hynds DL. Alternating magnetic field controlled, multifunctional nano-reservoirs: intracellular uptake and improved biocompatibility. *Nanoscale Res Lett*. 2009;5(1):195-204. doi:10.1007/s11671-009-9465-9
25. Dausend J, Musyanovych A, Dass M, et al. Uptake mechanism of oppositely charged fluorescent nanoparticles in HeLa cells. *Macromol Biosci*. 2008;8(12):1135-1143. doi:10.1002/mabi.200800123
26. Harush-Frenkel O, Debotton N, Benita S, Altschuler Y. Targeting of nanoparticles to the clathrin-mediated endocytic pathway. *Biochem Biophys Res Commun*. 2007;353(1):26-32.
27. Hillaireau H, Couvreur P. Nanocarriers' entry into the cell: relevance to drug delivery. *Cell Mol Life Sci*. 2009;66(17):2873-96. doi:10.1007/s00018-009-0053-z
28. Rejman J, Oberle V, Zuhorn IS, Hoekstra D. Size-dependent internalization of particles via the pathways of clathrin- and caveolae-mediated endocytosis. *Biochem J*. 2004;377(1):159-69. doi:10.1042/bj20031253
29. Veettil RA. *Polyethylene glycol copolymer nanocarriers: biocompatibility, uptake and intracellular trafficking in neurons.* Dissertation. Texas Woman's University; 2017.
30. Satapathy MK, Yen TL, Jan JS, et al. Solid lipid nanoparticles (SLNs): an advanced drug delivery system targeting brain through BBB. *Pharmaceutics*. 2021;13(8). doi:10.3390/pharmaceutics13081183
31. Boyes WK, van Thriel C. Neurotoxicology of nanomaterials. *Chem Res Toxicol*. 2020;33(5):1121-1144. doi:10.1021/acs.chemrestox.0c00050
32. Masoudi Asil S, Ahlawat J, Guillama Barroso G, Narayan M. Nanomaterial based drug delivery systems for the treatment of neurodegenerative diseases. *Biomater Sci*. 2020;8(15):4109-4128. doi:10.1039/d0bm00809e
33. Blanco E, Shen H, Ferrari M. Principles of nanoparticle design for overcoming biological barriers to drug delivery. *Nat Biotechnol*. 2015;33(9):941-51. doi:10.1038/nbt.3330